



**Universitat de les
Illes Balears**

Doctoral Thesis

2019

**PHYSICAL AND ECONOMIC IMPACTS DUE TO
SEA LEVEL CHANGES AND WIND-WAVES
AROUND THE BALEARIC ISLANDS.**

Alejandra Rodríguez Enríquez



**Universitat de les
Illes Balears**

Doctoral Thesis

2019

Doctoral programme of Physics

**PHYSICAL AND ECONOMIC IMPACTS DUE TO
SEA LEVEL CHANGES AND WIND-WAVES
AROUND THE BALEARIC ISLANDS.**

Alejandra Rodríguez Enríquez

Thesis Supervisor: Marta Marcos Moreno

Thesis Supervisor: Angel Bujosa Bestard

Thesis Tutor: Damià Gomis Bosch

Doctor by the University of Balearic Islands



Universitat
de les Illes Balears

This thesis has been written by Alejandra Rodríguez Enríquez under the supervision of Dr. Marta Marcos Moreno and Dr. Angel Bujosa Bestard.

Palma de Mallorca, October 17, 2019

Supervisors:

Two handwritten signatures in blue ink. The first signature is on the left and the second is on the right, both enclosed in a large blue oval.

PhD student:

A handwritten signature in blue ink, consisting of a stylized, cursive script.

List of publications included in the Doctoral Thesis:

Enrriquez, A. R., Marcos, M., Álvarez-Ellacuría, A., Orfila, A., Gomis, D., 2017. Changes in beach shoreline due to sea level rise and waves under climate change scenarios application to the Balearic Islands. *Natural Hazards and Earth System Sciences*, 17, 1075-1089.

Enrriquez, A. R., Marcos, M., Falqués, A., Roelvink, D., 2019. Assessing beach and dune erosion and vulnerability under sea level rise: a case study in the Mediterranean Sea. *Frontiers in Marine Science*, 6:4.

Enrriquez, A. R., Bujosa, A., 2019. Measuring the economic impact of climate-induced environmental changes on sun-and-beach tourism. Under review in *Climatic change*.

The 2017 quality indexes of the journals where articles are published (or under review) are:

Journal	CiteScore	Category Name	Total Journals in Category	Journal Rank in Category	Percentile in Category
NHESS ¹	2.43	Earth and Planetary Sciences	182	22	88th
FMARS ²	2.89	Ocean Engineering	91	6	93rd
		Aquatic Science	199	20	90th
		Oceanography	115	15	87th
CC ³	4.06	Atmospheric Science	102	9	91st
		Global Planetary Change	65	13	80th

¹Natural Hazards and Earth System Sciences

²Frontiers in Marine Science

³Climatic Change



Universitat
de les Illes Balears

Dr. Marta Marcos Moreno, of University of Balearic Islands

I DECLARE:

That the thesis titled “Physical and economic impacts due to sea level changes and wind-waves around the Balearic Islands”, presented by Alejandra Rodríguez Enríquez to obtain a doctoral degree, has been completed under my supervision and meets the requirements to opt for an International Doctorate.

For all intents and purposes, I hereby sign this document.

Signature

Palma de Mallorca, October, 2019.



Universitat
de les Illes Balears

Dr. Angel Bujosa Bestard, of University of Balearic Islands

I DECLARE:

That the thesis titled “Physical and economic impacts due to sea level changes and wind-waves around the Balearic Islands”, presented by Alejandra Rodríguez Enríquez to obtain a doctoral degree, has been completed under my supervision and meets the requirements to opt for an International Doctorate.

For all intents and purposes, I hereby sign this document.

Signature

Palma de Mallorca, October, 2019.

A mi hermana Reyes, porque quisiste aprender qué
es “batimetría”, “Matlab” o “paper”.

Agradecimientos

Ahora, después de añadir el punto final a este documento, puedo afirmar que sé qué es y qué conlleva hacer una tesis. Puede parecerse a la idea de un camino que te han dicho que está ahí pero el cual tienes que descubrir haciéndote paso entre una vegetación amazónica que te impide ver por dónde vas. El camino normalmente se empieza con una caja de herramientas casi vacía, las pocas herramientas que hay están nuevas y el manual de instrucciones te lo has leído . . . en diagonal. Menos mal que a mi lado iba algo parecido a Indiana Jones, Willy Fog, James Bond o MacGyver (elige tu favorito) que hizo que pudiese disfrutar de la tesis a pesar de que apareciesen serpientes venenosas de la especie “*Validations horribilus*”, escorpiones “*Simulacionus erroneus*” o arañas “*Primeros papers*” (debo anotar que el nombre de la araña inicialmente iba en singular pero siendo fiel a la realidad . . . sigue siendo una amenaza). Aunque lo peor de todo es la humedad densa a tu alrededor que podemos bautizar como una “no tengo ni idea” o “yo no sirvo para esto” que a veces hace que te sientas muy pequeña. En mi caso, he tenido la suerte de tener una directora que me apoyó siempre y estas sensaciones no fueron recurrentes. Aunque por otro lado, a veces los directores te tiran a acantilados o cuevas en los que no sabes lo que hay, de los que sales desconcertada, con arañazos y un poco sucia, pero con muchos más conocimientos, haya salido bien o mal la aventura. Gracias Marta y gracias Angel, el camino ha sido mucho más fácil con vosotros. He aprendido mucho de ciencia, pero sobre todo, siento que he crecido como persona. Me siento afortunada de haberos conocido y de haber compartido un tiempo de mi vida con vosotros. Esta tesis es vuestra.

Siguiendo con la historia, Indiana Jones, Willy Fog, James Bond o MacGyver no van solos, siempre tienen a un colaborador o colaboradores a su lado que facilitan mucho la tarea del investigador y de sus estudiantes. Muchas gracias por toda vuestra ayuda a lo largo de mi tesis, hay mucho de vosotros en ella. Desde el principio y hasta el final, habéis estado a mi lado limpiando el camino, gracias Juanma y gracias Ángel

Amores. Y por supuestísimo gracias a todo el grupo que, de veras, admiro: Damià, Sebas, Biel, Javi y Miguel.

En los márgenes del camino y con las herramientas en el suelo, están otros pequeños pimpollos que descansan después de haber estado trabajando en sus propias tesis. Con ellos he pasado mi tiempo libre, desahogado penas en el despacho, debatiendo e incluso conviviendo. También hemos descubierto Palma por el día y por la noche, hemos hecho mil y una excursiones a la montaña, a la verbena, a la playa, etc. Si es que la vida del doctorando no está tan mal como dicen. Gracias a todas/os por estar ahí y hacer este viaje mucho más divertido y acogedor: Laura, Carlota, Xisca, Julia, Vero, Paula, Noe, Inma, Albert, Guille Lara, Dani Chaparro, Nuria y Miguel (sí, el mismo que el de arriba). Ahora entiendo la expresión “no puedo expresar con palabras lo que siento”, pero creo que vosotras/os lo sabéis. Y por supuesto, gracias a toda la gente del IMEDEA que crea un ambiente genial en el instituto, hasta te sientes bien cuando estás trabajando. Los mejores momentos son en el ágora comiendo, debatiendo, haciendo porras de política con Melo, Guille, Edu, Joan Pons, Esther, Angel, etc. Sé que me dejo a muchos pero ya sabéis, prisas y más prisas (o como se dice en ciencia “*deadlines*”).

Desde casa, ¡Ay que morriña!, he sentido el apoyo de mis amigas de toda la vida, unas verdaderas guerreras amazónicas que luchan por cumplir sus propios deseos ya sea en Galicia o desde diversos rincones del mundo. Os he echado de menos muchas veces: Carmela, Ana, Cris, Sofía, Reyes (se repite, ya veréis), Sara y Aida.

Y por supuesto a mi familia. Creo que me estoy volviendo un poco sentimental con el tiempo/espacio o a medida que escribo estos agradecimientos o quizás lo he sido siempre. Bueno, vosotros me conocéis mejor que nadie. Aquí el mensaje es sencillo. Os quiero (mucho) y siento no estar con vosotros (mucho), Urbano, María, abuela (María de los Ángeles, pero ni yo me acordaba de tu nombre, así que “abuela”) y Reyes. Gracias a vosotros tengo la caja de herramientas, las instrucciones que no leo y a mí misma. En definitiva, la base sin la cual no podría estar aquí hoy ni ser quién soy. También os quiero y me gustaría veros más, tíos, sobrinos, primos, etc. Y te quiero y siento no estar ahí, Galicia.

No se me olvida agradecerle su aguante (sí amigos, aguante) a mi lado, desde el principio y hasta el final y en todos los aspectos de mi vida (esta es su tercera mención en estos agradecimientos). Has estado abriendo conmigo mi camino al mismo tiempo

que el tuyo, me has apoyado y hemos descansado juntos. Incluso a veces nos hemos escapado al río. Gracias Miguel.

Todo esto no hubiese sido posible sin el apoyo económico del Ministerio de Economía de España, que ha financiado el proyecto CLIMPACT (CGL2014-54246-C2-1-R) en el que se engloba la presente tesis. Gracias también al IMEDEA (Instituto Mediterráneo de Estudios Avanzados), lugar en el que se ha desarrollado todo este periplo.

Abstract

This thesis investigates and quantifies the impacts caused by climate change in the coasts of Balearic Islands (western Mediterranean Sea) from both a physical and an economic perspective. Two physical mechanisms that generate coastal hazards are considered in this work: mean sea-level rise and wind-waves. Their impacts are assessed, separately and jointly, in three case studies that have been selected due to the amount of available observations of nearshore waves, shoreline position and topo-bathymetries; these are two urban beaches (located in Mallorca island) and one natural beach (in Menorca island). The relevance of sandy coasts in the Balearic Islands, and in general in the Mediterranean coastal communities, is evident in terms of coastal protection but also from an economic point of view since sun-and-beach tourism is the main economic activity of the region.

The physical impacts on the beaches are investigated using numerical modelling to simulate the shoreline retreat, the beach erosion and the beach vulnerability resulting from projected mean sea-level rise and wind-wave changes up to 2100. The methodology and the assumptions vary depending on the hydro- and morphodynamical processes required to study the coastal impacts in each case. In addition, numerical simulations are validated against observations whenever possible, prior to the application of the modelling setup under projected future conditions. Our results for urban beaches, highly anthropised and backed by infrastructures such as promenades and buildings, indicate a permanent loss of approximately half of the present-day beach area; in addition, the beach is expected to be almost completely flooded under storm conditions. In other words, urban beaches are unable to respond to long-term changes in the oceanic forces. In the case of the natural beach, our results anticipate that the beach will retreat at the expense of the dune area located behind it. A noteworthy finding is the importance of simulating the beach morphological features when assessing beach impacts, which play a key role in the beach erosion rates.

The economic impact on sun-and-beach tourism is measured by means of a choice experiment application. More precisely, the shoreline retreat projections obtained for the urban beach cases studies are used to estimate the welfare loss that tourists would experience in a future scenario characterized by a reduction of the beach size, in addition to two other climate-induced environmental changes. Data on the socioeconomic and the travel profile of tourists as well as their preferences for different policies aimed at reducing climate-induced environmental changes, was collected through a survey conducted in the high season of 2016 at the airport of Palma (Mallorca). Overall, results show that sun-and-beach tourists have a positive willingness-to-pay to reduce climate change impacts. At the same time, the mixed logit specification accounting for preference heterogeneity allows to find that the welfare loss varies across tourists depending on their socioeconomic and travel characteristics.

Resumen

Esta tesis investiga y cuantifica los impactos causados por el cambio climático en las costas de las Islas Baleares (Mediterráneo occidental) desde un punto de vista tanto físico como económico. Dos mecanismos físicos, los cuales suponen una amenaza para las zonas costeras, son considerados en este trabajo: el aumento del nivel medio del mar y el oleaje. Sus impactos se evalúan, tanto de forma separada como conjuntamente, en tres casos de estudio que han sido seleccionados debido a la disponibilidad de observaciones de oleaje costero, posición de línea de playa y topo-batimetrías: dos playas urbanas (ubicadas en la isla de Mallorca) y una playa natural (en la isla de Menorca). La relevancia de las costas arenosas en las Islas Baleares, y en general en las comunidades costeras del Mediterráneo, es evidente en términos de protección costera, pero también desde un punto de vista económico ya que el turismo de sol y playa es la principal actividad económica de la región.

Los impactos físicos en las playas se estudian mediante el uso de modelos numéricos con los que se simula el retroceso de la línea de costa, la erosión y la vulnerabilidad de las playas como resultado del esperado aumento del nivel medio del mar y los cambios en el oleaje hasta 2100. La metodología y las premisas aplicadas varían dependiendo de los procesos hidro- y morfodinámicos necesarios para estudiar los impactos costeros en cada caso. Además, antes de ejecutar los modelos numéricos bajo condiciones oceánicas futuras, las simulaciones numéricas son validadas con observaciones en los casos en los que es posible. Nuestros resultados para las playas urbanas, las cuales presentan paseos marítimos y edificios tras ellas y por lo tanto, un alto nivel de antropización, indican una pérdida permanente de la playa de aproximadamente la mitad de su área actual. Además, el área de playa afectada por la inundación aumenta hasta su casi totalidad en condiciones de tormenta. En otras palabras, las playas urbanas son incapaces de responder a cambios de largo plazo en las fuerzas oceánicas. En el caso de la playa natural, nuestros resultados anticipan un retroceso, pero no pérdida, que

conlleva la desaparición del área dunar localizada detrás. Un resultado destacable es la importancia de simular las características morfológicas de la playa cuando se evalúan impactos costeros, las cuales desempeñan un papel clave en las tasas de erosión de la playa.

El impacto económico en el turismo de sol y playa se mide mediante un experimento de elección. Más concretamente, los resultados de retroceso de línea de costa obtenidos en el estudio de las playas urbanas se utilizan para estimar la pérdida de bienestar que el turista experimentaría por la reducción del tamaño de playa, además de por otros dos cambios ambientales provocados por el cambio climático. El perfil socioeconómico y de viaje de los turistas, así como sus preferencias hacia distintas políticas orientadas a reducir los impactos del cambio climático, se obtuvieron mediante una encuesta realizada en la temporada alta de 2016 en el aeropuerto de Palma (isla de Mallorca). En general, los resultados muestran que los turistas de sol y playa tienen una disponibilidad a pagar positiva para reducir los impactos del cambio climático. Al mismo tiempo, el modelo logit mixto, que captura la heterogeneidad de preferencias entre los individuos, permite observar que la pérdida de bienestar de los turistas varía entre sus características socioeconómicas y de viaje .

Resum

Aquesta tesi investiga i quantifica els impactes causats pel canvi climàtic a les costes de Illes Balears (Mediterrània occidental) des d'un punt de vista tant físic com econòmic. Dos mecanismes físics, els quals suposen una amenaça per a les zones costaneres, són considerats en aquest treball: l'augment del nivell mitjà del mar i l'onatge. Els seus impactes s'avaluen, tant de forma separada com conjuntament, en tres casos d'estudi que han estat seleccionats per la disponibilitat d'observacions d'onatge costaner, posició de línia de platja i topo-batimetries: dues platges urbanes (ubicades a l'illa de Mallorca) i una platja natural (a l'illa de Menorca). La rellevància de les costes arenoses a les Illes Balears, i en general en les comunitats costaneres de la Mediterrània, és evident en termes de protecció costanera, però també des d'un punt de vista econòmic ja que el turisme de sol i platja és la principal activitat econòmica de la regió.

Els impactes físics a les platges s'estudien mitjançant l'ús de models numèrics amb els quals es simula el retrocés de la línia de costa, l'erosió i la vulnerabilitat de les platges com a resultat de l'augment esperat del nivell mitjà del mar i els canvis en l'onatge fins al 2100. La metodologia i les premisses aplicades varien depenent dels processos hidro- i morfodinàmics necessaris per estudiar els impactes costaners en cada cas. A més, abans d'executar els models numèrics sota condicions oceàniques futures, les simulacions numèriques són validades amb observacions en els casos en què és possible. Els nostres resultats per a les platges urbanes, les quals presenten passeigs marítims i edificis darrere d'elles i per tant, un alt nivell d'antropització, indiquen una pèrdua permanent de la platja d'aproximadament la meitat de la seva àrea actual. A més, l'àrea de platja afectada per la inundació augmenta fins gairebé la seva totalitat en condicions de tempesta. En altres paraules, les platges urbanes són incapaces de respondre a canvis de llarg termini en les forces oceàniques. En el cas de la platja natural, els nostres resultats anticipen un retrocés, però no pèrdua, que comporta la desaparició de l'àrea dunar localitzada darrere. Un resultat destacable és la importància

de simular les característiques morfològiques de la platja, les quals tenen un paper clau en les taxes d'erosió de la platja.

L'impacte econòmic del turisme de sol i platja es mesura mitjançant una aplicació d'experiments d'elecció. Més concretament, els resultats del retrocés de la línia de costa obtinguts a l'estudi de les platges urbanes s'utilitzen per estimar la pèrdua de benestar que els turistes experimentarien en un escenari futur caracteritzat per una reducció de la superfície de platja, a més i dos altres canvis ambientals provocats pel canvi climàtic. El perfil socioeconòmic i de viatge dels turistes, així com les preferències dels turistes per a diferents polítiques dirigides a reduir els impactes del canvi climàtic, es van obtenir mitjançant una enquesta realitzada a la temporada alta de 2016 a l'aeroport de Palma (Mallorca). En general, els resultats mostren que els turistes de sol i platja tenen una disposició a pagar positiva per reduir els impactes del canvi climàtic. Al mateix temps, el model logit mixt, que captura l'heterogeneïtat de preferències entre els individus, permet observar que la pèrdua de benestar dels turistes varia en funció de les seves característiques socioeconòmiques i de viatge.

Contents

1	General Introduction	1
1.1	Global climate change and sea-level rise	1
1.1.1	Present-day mean sea-level and future projections	2
1.1.2	Extreme sea-level changes	4
1.2	Coastal impacts	4
1.2.1	Physical impacts	5
1.2.2	Economic impacts	7
1.3	The case of the Mediterranean Sea	8
1.4	Objectives of this thesis: a case study in the Balearic Islands	9
1.5	Numerical simulation of physical impacts	11
1.6	Assessment of economic impacts	12
2	Changes in beach shoreline due to sea-level rise and waves under climate change scenarios: application to the Balearic Islands (Western Mediterranean).	15
2.1	Introduction	15
2.2	Data and Methods	17
2.2.1	Topo-bathymetric surveys	18
2.2.2	Hydrodynamic data	18
2.2.3	Video imagery data	19
2.2.4	Numerical approach	20
2.2.5	Forcing of numerical models	22
2.3	Evaluation of model setup under present-day climate conditions	25
2.3.1	Comparison with wave observations	25
2.3.2	Comparison with observed shoreline position	28
2.4	Shoreline changes under climate change scenarios	31

2.5	Summary and conclusions	37
3	Assessing beach and dune erosion and vulnerability under sea-level rise: a case study in the Mediterranean Sea.	39
3.1	Introduction	39
3.2	Data	42
3.2.1	Site Description	42
3.2.2	Wave Data	43
3.2.3	Mean Sea-Level Data	44
3.3	Material and methods	44
3.3.1	Numerical Models	45
3.3.2	Estimation of the Shoreline Retreat	47
3.3.3	Beach and Dune Vulnerability and Erosion	49
3.4	Results	50
3.4.1	Shoreline Retreat Under Mean Sea-Level Rise	50
3.4.2	Beach and Dune Vulnerability and Erosion	52
3.5	Conclusion	55
4	Measuring the economic impact of climate-induced environmental changes on sun-and-beach tourism.	57
4.1	Introduction	57
4.2	Application and survey design	59
4.2.1	Climate-induced environmental changes in the Mediterranean coast	59
4.2.2	The choice experiment	60
4.2.3	Survey and sample	62
4.3	Methods	64
4.3.1	The mixed logit model	64
4.3.2	Welfare measurement	67
4.4	Results	67
4.5	Conclusions	71
5	Summary and Conclusions.	73
6	Main findings.	77

List of Figures	99
List of Tables	103
List of Terms and Abbreviations	105

Chapter 1

General Introduction

1.1 Global climate change and sea-level rise

The Intergovernmental Panel on Climate Change (IPCC), the United Nations body for assessing the science related to climate change defined, more than a decade ago in its fourth assessment report (IPCC 2007*b*), climate change as “a change in the state of the climate that can be identified by changes in the mean and/or the variability of its properties (. . .) It refers to any change in climate over time, whether due to natural variability or as a result of human activity.” Since then, it has been established that human contribution to climate change ranges between 93-123% during the period 1951-2010 (Knutson et al. 2017) due to the emission of greenhouse gases (GHG) released to the atmosphere associated to the anthropogenic activities. Increasing GHG concentrations and the resulting changes in the climate system have produced a cascade of global consequences, from physical effects to impacts in biological and socioeconomic systems. Among them are rising of global air and ocean temperatures, melting of snow and ice, mean sea-level rise, changes in the intensity of North Atlantic tropical cyclone activity and variations in precipitation rates and patterns (IPCC 2013). Given the magnitude of the anthropogenic contribution to contemporaneous climate change, throughout this thesis, we will refer only to human-induced changes when quoting climate change.

Among the consequences of climate change, mean sea-level rise is one of the potentially most hazardous and costliest aspects, with important implications to the highly populated coastal zones. Globally averaged, mean sea-level rise results from two causes, namely thermal expansion of sea water (due to ocean warming) and fresh water mass input from land-based ice melting (IPCC 2013). Regionally, mean sea-level trends show significant departures from its global mean associated to patterns of differential heat uptake, ocean circulation and surface mass redistribution fingerprints. Locally, changes in mean sea-level exacerbate to a large extent the coastal impact of extreme sea-levels caused by wind-waves (waves hereafter) and storm surges, as it defines the baseline level upon which extreme events reach the coastlines (Marcos and Woodworth 2017, Vousdoukas et al. 2017).

In the present thesis, we present the assessment of physical and economic impacts

induced by climate change in three coastal case studies. In the following, we describe in more detail the state-of-the-art of mean and extreme sea-level changes and their physical and economic impacts along the coastal regions.

1.1.1 Present-day mean sea-level and future projections

Due to its importance to the coastal zones, much research has been focused on the assessment and quantification of mean sea-level changes at spatial scales from global to local. Very often this research uses sea-level observations that are obtained from in-situ tide gauges, satellite radar altimetry or a combination of both. These two complementary data sets differ, primarily, in the record length and the spatial and temporal resolution. On the one hand, tide gauges provide long sea-level time series (some of them started *circa* 1700) with high temporal sampling although limited to a set of coastal locations. In addition, the number of operating tide gauges has been changing over time with a different rate over the northern and southern hemispheres (Church and White 2011). On the other hand, remote sensing satellite altimetry data have a significantly shorter temporal coverage, with records starting in early 1990s. However, its near-global spatial coverage provides an improvement in the global scale sea-level observations.

An important difference between these two sea-level data sets is their reference system. Satellite altimetry measures sea-level with respect to the Earth's reference ellipsoid (termed as "absolute sea-level"), while tide gauges record the local sea-level relative to the land upon which they are grounded. In consequence, for the two data sources to be comparable, tide gauge records must be corrected for global and local vertical motions of the Earth's crust (Cazenave et al. 1999, Dangendorf et al. 2017, Wöppelmann and Marcos 2016). On the large scale, the vertical land movement is dominated by the Glacial Isostatic Adjustment (GIA) (Peltier 2004) signal, a response of the Earth's crust to the melting from the Late Pleistocene ice-sheets. Conversely, local, small-scale vertical land motions have a broader range of causes from anthropogenic (groundwater pumping, deforestation, drainage of wetlands, etc) to natural processes (earthquakes, volcanism and sediment compaction) (Gornitz 1995). While the GIA signal is routinely removed from sea-level observations using solid Earth model outputs, the local vertical land motions are far more difficult to address and, in general, impossible to model. Thus, whenever possible, local vertical land motions are estimated using precise measurements of ground motions provided by Global Navigation Satellite Systems (GNSS), the most extended of which is the Global Positioning System (GPS) (Wöppelmann and Marcos 2016).

Satellite altimetry observations have shown that mean sea-level changes are not globally uniform but exhibit significant regional variations. These variations are the

result of various factors, the most important of which is the variability in the steric (i.e. density-driven) contribution that, in turn, is dominated by temperature changes, while salinity plays a minor role (Antonov et al. 2002). Likewise, the spatial variability of the mean sea-level responds also to surface wind stress anomalies and, to a lesser extent, to buoyancy forcing anomalies and the intrinsic oceanic variability (Meysignac et al. 2017). In addition, surface mass load redistribution resulting from the melting of land-based ice-sheets (Antarctica and Greenland) and glaciers generates spatial footprints in the gravitational field and, in consequence, also in mean sea-level (Mitrovica et al. 2001).

The study of global mean sea-level (GMSL) rise remains a matter of interest for the scientific community, as it represents one of the metrics that measures the impact of climate change. A number of methods exist that have reconstructed GMSL during the last decades, using different datasets, corrections and with different assumptions. Based on these reconstructions, the resulting linear trends of GMSL during the 20th century range from 1.3 to 2 mm yr⁻¹ (Church and White 2011, Jevrejeva et al. 2014, Hay et al. 2015, Dangendorf et al. 2017, Marcos and Woodworth 2017). There is a growing consensus in pre-altimetry GMSL rise of 1.1 ± 0.3 mm yr⁻¹ before 1990, while GMSL has been rising by 3.4 ± 0.4 mm yr⁻¹ since 1993, according to altimetry observations. Kopp et al. (2016) demonstrated that contemporaneous GMSL rise since the early 20th century is the largest in, at least, the last 2700 years.

Future projections of GMSL changes have been obtained as the sum of the outputs of 21 Atmospheric-Ocean General Circulation Models (AOGCMs). The uncertainties derived of using these 21 AOGMs combined with the uncertainties in modelling the contributions to GMSL, have been used to provide future GMSL change estimations in terms of probability (IPCC 2013, Stammer et al. 2019). According to the last IPCC assessment report (IPCC 2013), the future GMSL will likely be in the range of 0.36-0.71 m (0.53 m) and 0.52-0.98 m (0.74 m) by 2100 (median values), under a moderate RCP4.5 and a pessimistic RCP8.5 climate change scenario, respectively. Following the IPCC nomenclature, the *likely range* refers to the interval 17-83% of a not symmetric probability density function obtained from the model set and contributions spread, while *likely* indicates the 66-100% probability. Regional deviations from the mean, resulting from the processes discussed above, can reach up to 50% of the global values (Slangen et al. 2014). In terms of coastal impacts, it is this regional/local value of mean sea-level projections that matters, since it will determine the level upon which marine extremes will reach the shorelines.

1.1.2 Extreme sea-level changes

Extreme sea levels are particularly important for coastal regions since they are responsible of the major flooding and erosion events. Extreme sea-levels arise from the combination of mean sea-level, tides, extreme waves and storm surges, although only mean sea-level and waves are considered in the present thesis. Among them, mean sea-level has been the largest contributor to the extreme water level during the last decades (Marcos and Woodworth 2017, Vousdoukas et al. 2018). In addition, in shallow water environments, non-linear interactions among these components may occur; for example, with mean sea-level producing changing waves, tides and storm surges (e.g. Arns et al. 2017). As occurs to mean sea-level, extreme storm surges and waves also vary spatially. Spatial patterns of storm surges have been described at the global and regional scales using the worldwide network of tide gauge observations (Menéndez and Woodworth 2010, Marcos and Woodworth 2017). Variations on waves, including extreme waves, are more difficult to assess due to the lack of an extensive network of in-situ observations although satellite radar altimetry and the longer term voluntary observing ships data have been used for this purpose (Gulev and Grigorieva 2004, Young 1999).

Projections of waves during the 21st century have been obtained using atmospheric pressure and wind fields from AOGCMs to force either dynamical or statistical models (e.g. Hemer et al. 2013, Mentaschi et al. 2017, Vousdoukas et al. 2016). Model projections indicate that, along most of the coasts worldwide changes in sea-level extremes are small in comparison with the projected mean sea-level rise and its associated uncertainties (Vousdoukas et al. 2018). In other words, the major source of uncertainty in extreme sea-level evolution during the present century is associated to projected mean sea-level rise. In addition, over large continental shelves of shallow depths, storm surges may be further modified by the changing bathymetry as mean sea-level rises. The same principle applies to tidal waves, which are also expected to be modified in all coastal points, sometimes with significant trends (Mawdsley et al. 2015).

1.2 Coastal impacts

The wide range of coastal hazards caused by mean sea-level rise (including flooding, submersion, saltwater intrusion, permanent shoreline retreat and erosion) constitute a major threat to coastal communities, not only for their effects on the ecosystem but also for their impacts on coastal infrastructures, economic activities and human health. Furthermore, these impacts can be exacerbated by short-term oceanic forces such as storm waves, as well as by human actions (Nicholls and Cazenave 2010). This section presents a short (and inevitably limited) review of the start-of-the-art research on these impacts focusing on sandy coasts, as it is the central topic of this PhD dissertation. For

the sake of clarity, the review is divided in two parts to introduce, first, the research on the physical impacts caused by mean sea-level rise and, second, the research devoted to quantify their economic impact.

1.2.1 Physical impacts

The variety of coastal hazards derived of sea-level rise is reflected into a wide range of studies dealing with climate change impacts on coasts, including, for example, flooding (Nicholls 2002), submersion of low-lying delta areas (Sayol and Marcos 2018), impacts in aquifers and groundwater reservoirs (Bobba et al. 2000, IPCC 2007a), erosion of cliffs and platforms (Naylor et al. 2010) and changes in intertidal ecosystems (Alongi 2008). For a revision of the potential impacts of sea-level rise on coasts, the reader is referred to Wong et al. (2014). Particular attention has been paid to the study of the responses of sandy beaches, owing to their relevance to coastal protection, coastal ecosystem, local economy and their high value for recreation and residences (Lee 2008, Ruggiero et al. 2013, Vitousek et al. 2017, Wong et al. 2014).

Among the typology of coastal landforms (e.g. barrier islands, sea cliffs, tidal flats, river deltas, ports, etc.), sandy coasts compose the 31% of the world's ice-free shoreline. Nowadays, 48% of beaches are stable, 24% are eroding at $\sim 0.5 \text{ m yr}^{-1}$ and 28% are accreting, according to a recent study (Luijendijk et al. 2018). However, mean sea-level rise threatens the current state of the natural beaches around the world (Vitousek et al. 2017). The anticipation of shoreline retreat and beach erosion in response to climate change is a challenging topic, with uncertainties arising from mean sea-level changes but also from the difficulty of modelling the erosive impact of changing sea-levels (Le Cozannet et al. 2019). One of the reasons is the highly dynamic character of sandy coasts: the beach morphology, composed by non-consolidated sediment, responds relatively quickly to changes in external forcing such as waves, sea-level, currents and river flows. Likewise, its morphology affects to the same external forcing, leading to a complex feedback system.

In addition to this complexity, the assessment of climate change impacts on beaches involves many forcing factors acting at different temporal scales: mean sea-level rise, storm waves, tides and currents, climate cycles, sandy supply from rivers and reefs, tectonic processes, etc (Vitousek et al. 2017). In the present thesis, only two of these forcing factors have been considered to assess the future changes in beaches: mean sea-level rise and storm waves. The former acts at long-term scales, producing submersion and permanent beach shoreline retreat. The latter cause temporal beach erosion and shoreline retreat, which can, in principle, be recovered during post-storm periods. However, since storm waves will reach the coastline on higher mean sea-levels and further landward, the area of activity will change over time and therefore, the current beach

states and their equilibrium, too.

The response of beaches to the oceanic forces differs from site to site, so local rather than global assessments are required to obtain accurate projections of the potential impacts of climate change on beaches (Le Cozannet et al. 2014). For instance, Revell et al. (2011) obtained 214 km² of land eroded by 2100 under a 1.4 m of sea-level rise scenario in California coastal region. However, the potential erosion changes with the type of coast: they projected a maximum of 400 m of erosion if shoreline is backed by cliffs and a maximum of 600 m if it is backed by dunes.

Different approaches can be found in the literature aimed at evaluating the impacts of climate drivers over beaches. The assumptions made to simplify the above-mentioned problems (hydro and morphodynamic feedback and time scales) vary depending on the methodology and the hydrodynamic forcing considered, as well as on the final aim. In short, the methodologies applied in coastal modelling can be sorted in “physics-based”, “process-based” and “empirical-based” models as well as a combination of different methods (an “hybrid approach”), aimed at obtaining accurate results in a computationally efficient way (Vitousek et al. 2017). Physics-based numerical models are a widespread tool used to simulate the responses of the beach morphology to different forcing actors. The numerical models that have been applied in this thesis are described in more detail in Section 1.5. Most numerical models have been designed to simulate the beach changes under short-term processes, such as storm events, mainly due to the high computational demand for long model runs (Le Cozannet et al. 2014, Ranasinghe 2016). Conversely, when numerical models are used in a climate change context, mean sea-level rise is generally the unique ocean forcing considered, allowing the study of long-term processes at beaches but neglecting the storm effects instead (Dasgupta et al. 2007, Purvis et al. 2008).

In addition to numerical modelling, the process-based Bruun rule (Bruun 1962) has been routinely applied for engineering purposes due to its simplicity. The Bruun rule predicts a landward and upward displacement of the cross-shore beach profile in response to mean sea-level rise, however, it does not consider the effect of waves on the beach and has proved to be less reliable if accurate estimations are required (Ranasinghe et al. 2012). In this sense, some attempts have been done to improve the Bruun rule, such as the addition of other sediment transport contributions to the formulation or by combining its principle with other techniques (Revell et al. 2011, Rosati et al. 2013).

Statistical techniques are another tool that allow combining mean sea-level rise and storm waves. Due to their easy implementation and their low computational cost, these methods can evaluate the projected changes under a wide range of ocean conditions. However, they neglect the cumulative effect and the long-term changes on beaches since they do not solve the physical processes involved (Ranasinghe et al. 2012, Revell et al.

2011, De Winter and Ruessink 2017).

1.2.2 Economic impacts

Inevitably, the physical impacts associated to mean sea-level rise will adversely affect human activities (Tseng et al. 2009). However, the research on the socio-economic effects of these impacts remains limited. One exception is the study by Hinkel et al. (2014) that, using a global perspective, analyse the effects of a scenario of 25-123 cm of mean sea-level rise. According to their results, without adaptation measures, 0.2-4.6% of global population is expected to experience a flood event annually in 2100, with an associated annual cost of 0.3-9.3% of global Gross Domestic Product (GDP). However, coastal flood damage and its associated costs will vary locally according to the actual state of each coast, the expected number of flood events and the expected level of adaptation.

Beyond the increasing vulnerability associated to coastal erosion and flooding events, climate change will also impact the economic activity of coastal communities closely linked to climate-sensitive resources (IPCC 2007c). The literature on this field has been dominated by a couple of economic sectors such as agriculture and industry (Ahn et al. 2000, Pongkijvorasin and Chotiyaputta 2013). In contrast, the research on the impacts of climate change on other sectors with a high dependency on climatic and natural resources, like tourism, remains limited.

In this sense, travel and tourism is one of the world's largest industries accounting for 10.40% of global GDP in 2017 (WTTC 2018) and it has become the most important economic activity in many coastal areas attracting hundreds of millions of people (Moreno and Amelung 2009, UNWTO 2018). However, given that most of the recreational activities undertaken in coastal environments are highly sensitive to climatic and environmental conditions (Scott et al. 2008), climate change impacts are expected to result in a decrease of attractiveness and therefore visitor numbers in many coastal destinations (Uyarra et al. 2005, Gössling et al. 2012, Perch-Nielsen 2010). Publications addressing climate change impacts on tourism can be grouped into two categories depending in whether they analyze the alteration of 1) the climatic suitability or 2) the provision of natural resources, both determining to a great extent the attractiveness of the destination.

In the first case, the Tourism Climatic Index (TCI) is one of the most extended methods to capture human comfort preferences. This index, first introduced by Mieczkowski (1985), combines air temperature, humidity, precipitation rates, hours of sunshine and wind speed in a mathematical equation to assess the level of climate comfortability of a certain destination. Different studies using the TCI have projected a regional and seasonal redistribution of tourism flows as a result of the changing climate conditions

(Amelung and Viner 2006, Bujosa and Rosselló 2013, Maddison 2001, Perch-Nielsen et al. 2010, Scott et al. 2004, Tol 2002). Most of these works have been identified the temperature as the main factor determining the climatic comfortability at the destination and therefore, one of the most important parameters in the destination choice process.

In the second case, the literature aimed at studying the impact of climate-induced environmental changes in tourism has mainly focused on winter sports (Landauer et al. 2012, Unbehaun et al. 2008), mountain (Pröbstl-Haider et al. 2015) and glacier tourism (Vander Naald 2019). In spite of the limited attention received by coastal tourism (Rosselló-Nadal et al. 2011, Becken 2013), some studies can be found addressing the potential effects and loss of water transparency (Gössling et al. 2012). For instance, in the context of a beach retreat scenario, a negative effect in the satisfaction of tourists has been found in Barbados and Bonaire (Uyarra et al. 2005) and Playcar, Mexico (Buzinde, Manuel-Navarrete, Yoo and Morais 2010). More specifically, Uyarra et al. (2005) finds that 77% of tourists would be unwilling to return if the beach is largely reduced. In order to integrate these climate-induced environmental impacts into decision-making processes, in addition to the more usually considered climatic suitability, Perch-Nielsen (2010) developed a vulnerability index to analyse the performance of beach tourism under a climate change context in 51 coastal countries. Results showed that developing countries and small islands are the most vulnerable areas in this context.

1.3 The case of the Mediterranean Sea

The potential impacts of mean sea-level rise and waves are particularly concerning along the Mediterranean coasts. While the average population density in coastal areas is globally 10%, it reaches 34% in the case of the Mediterranean region (Lionello et al. 2006). In addition, the Mediterranean region is one of the world's leading sun-and-beach tourism destination (UNWTO 2018), being one of the main economic contributors. After France, Spain is the second most visited country in Europe. About 17% of the Spanish GDP comes from the tourism activity, being the Balearic Islands the second most important tourist destination after Catalonia coastal regions, which highlights the relevance of the sun-and-beach tourist sector. The importance of tourism on the GDP is similar in other Mediterranean countries such as Croatia (~ 17%), Greece (~16%), Morocco (~16%) and Turkey (~11%) (Ehmer et al. 2008).

From a physical perspective, the Mediterranean Sea is a marginal, deep (average depth of 1500 m) and semi-enclosed sea. It is connected with the Atlantic Ocean through the narrow Strait of Gibraltar that plays a key role in the water mass circulation of the Mediterranean Sea. Despite its relatively small size (2.5 million km²) in comparison with the Atlantic, the ocean and atmospheric climate is not uniform in the Mediterranean. On the contrary, resulting from its complicated morphology and

its location, between a subtropical area at south and temperate at north, the Mediterranean climate shows strong spatial contrasts. In consequence, ocean parameters such as sea-surface temperature, salinity or sea-level, show a relatively large spatial variability (Lionello 2012).

The Mediterranean Sea boast some of the longest instrumental sea-level records. The longest tide gauges (located in Marseille, Genoa and Trieste), show that, on average, mean sea-level has been rising by 1.1-1.3 mm yr⁻¹ during the 20th century; this includes a period between 1960 and 1990 of steady mean sea-level explained by the local atmospheric pressure over the region (Marcos and Tsimplis 2008, Tsimplis et al. 2008). In the most recent decades, satellite altimetry reveals an average rate of mean sea-level rise of 2.6 ± 0.2 mm yr⁻¹ across the Mediterranean Sea during the period 1993-2015 (Marcos et al. 2016).

Given the complexity of the Mediterranean climate, high resolution numerical models are required to simulate atmospheric and oceanic processes in a realistic fashion. These are regional models that are forced at their boundaries by global, coarser resolution models, which limits their ability to simulate changes in mean sea-level as this contribution must be introduced through a boundary condition. Despite their coarse resolution (state-of-the-art models range between 1 and 2 degrees in the ocean), the outputs of AOGCMs have been regionalised to provide the spatial patterns of the different contributors to mean sea-level changes under climate change scenarios (see Section 1.1.1). The variability of the mean sea-level in the Mediterranean Sea is caused by basin-scale processes combined with remote processes, the latter being represented as changes in the near northeast Atlantic sea-level. Therefore, reliable projections of mean sea-level rise in the Mediterranean should consider these two processes (Marcos et al. 2016).

In this thesis, we have accounted for all contributors to projected mean sea-level, including, glaciers and ice sheet surface mass balance, global steric component, dynamic topography, atmospheric pressure loading, ice sheet dynamics, groundwater depletion and GIA, using the outputs of regionalised climate models from Slangen et al. (2014) (Chapters 2 and 3). When applied to the western Mediterranean region, regionalised projections from AOGCMs result in a mean sea-level rise of 23 and 26 cm (median values) under RCP4.5 and RCP8.5 scenario, respectively, by mid-21st century and 50 and 68 cm (median values) by the end of the century.

1.4 Objectives of this thesis: a case study in the Balearic Islands

The aim of the present thesis is to assess the physical and economic impacts of ocean climate change in the Balearic Islands. The thesis is framed within the research project “Environmental and economic impacts of climate change on Spanish shores and harbours” (CLIMPACT, reference number CGL2014-54246-C2-1-R), that run during

2015-2018, funded by the Spanish Ministry of Economy. It therefore follows the general overarching goal of the project and focuses on particular case studies to develop the required methodologies. Located in the western Mediterranean Sea, the Balearic Islands are an archipelago composed of four large islands: Mallorca, Menorca, Ibiza and Formentera, and minor islands such as Cabrera and Dragonera. The coast of the Balearic Islands is composed by rocky and sandy platforms as well as ocean cliffs. Among them, the sandy coasts are those receiving the higher human pressure, since beaches conform a leisure environment for locals and a tourist attraction for visitors. Here, we have chosen three beaches to study the physical and economic impacts of climate change. Two of them are located in Mallorca island (Playa de Palma and Cala Millor), while the third one is in Menorca (Son Bou). The first two cases are urban beaches, backed by promenades and buildings that limit their capacity of response to changes in the ocean climate forcings. In addition, the sand distribution, and therefore their aerial shapes, is conditioned by human activities driven to maximize the public comfort. On the other hand, Son Bou beach is a natural beach backed by a wide and vegetated dune area. In this case, the beach is able to change depending on the ocean conditions and the sediment distribution is not conditioned by human demands.

These three beaches were chosen as case studies because they have been extensively monitored by the Balearic Islands Coastal Observing and Forecasting System (SOCIB) since 2011 (Tintoré et al. 2013). The monitoring programmes include several measurements of topo-bathymetries, parameters of nearshore wave conditions, sediment features and shoreline measurements. All these observations have been used to feed numerical models and to compare the simulation results against observations when possible (Chapters 2 and 3). In addition, their distinctive characteristics allow the assessment of climate change impacts under both, urban (Chapter 2) and natural (Chapter 3) environments. Chapter 4 will focus on measuring the economic consequences of these impacts in Mallorca.

To achieve the main purpose, we first assessed the physical consequences of mean sea-level rise and waves on coasts, in terms of surface beach loss and dune erosion. Before the design of the work, we anticipated a difference in the beach response depending on its nature, either urban or natural, and we developed two methods accordingly. The results were used to estimate the economic value of beach reduction for the tourists, in addition to other two climate-induced environmental changes, namely beach closure due to jellyfish outbreaks and loss of *Posidonia oceanica* seagrass, both of them associated with seawater warming. The methodology focused on the analysis of the tourist's preferences and their willingness-to-pay (WTP) for the introduction of policies aimed at reducing these three climate-induced environmental changes. There is a wide variety of methods available in the current state-of-the-art to solve coastal processes and to mea-

sure economic values; in the next two sections of this Chapter, we provide an overview on those that have been applied in this thesis and that summarize and complement the information developed in more detail in the next three Chapters.

Chapters 2 and 3 have been published in indexed journals and the complete references are indicated in their corresponding sections. Chapter 4 is currently under review, also in an indexed journal. The contents of each Chapter are the same as in the published (or submitted) articles, including figures and references.

1.5 Numerical simulation of physical impacts

Coasts are shaped by a wide range of physical processes: aerial sediment transport, tides, currents, waves, river discharges, etc. However, in this thesis only the ocean hydro (waves and mean sea-level) and coastal morphodynamic forces are accounted for, as they are considered as the drivers that are most directly involved in the coastal response to climate change. The waves and mean sea-level rise effects have been studied both separately and in combination with sediment transport.

In cases where the coastal sediment transport is not accounted for, hydrodynamic models are used to solve the wave processes. In the present thesis, two hydrodynamic models have been used. The first one is a phase-average model, which represents the sea surface height as a function of the wave frequency and wavelength. In other words, it is a spectral model that provides the evolution of the wave spectrum in space and time (Roland and Ardhuin 2014). Among all available spectral wave equation models, SWAN model (Simulating WAVes Nearshore model) (Booij et al. 1999) has been chosen to simulate the wave propagation from deep water conditions up to the nearshore. On the other hand, a nonlinear shallow water equation with non-hydrostatic pressure model, has been used to simulate the wave phase and the surf zone dynamics such as nonlinear shoaling, breaking of waves and run-up. In this case, SWASH model (Simulating WAVes till SHore) (Zijlema et al. 2011) has been chosen to simulate these more complex wave processes. The application of SWASH is restricted to small areas due to its high computational cost in contrast to SWAN, which allows a computationally feasible simulation of waves in relatively large areas. These two models have been combined, in presence of projected mean sea-level rise, to assess the shoreline changes during the 21st century in two urban beaches, as will be developed in Chapter 2.

On the other hand, when the simulation of coastal sediment transport is required, SWAN is combined with morphological models. Several approaches have been applied by different authors to simulate the whole coastal system (waves and sediment transport), which differ in the assumptions taken to simplify the problem (Ranasinghe 2016). In the present thesis, two morphodynamic models have been used to simulate, separately, the morphological changes due to short-term (storm waves) and long-term

(mean sea-level rise) processes. The beach changes caused by storm waves have been assessed with the XBeach model (Roelvink et al. 2009). This model solves the depth-averaged coupled equations, resolving also the infragravity motions and wave groups through a time-varying wave action balance equation. In addition, XBeach model solves the sediment transport and bed level change caused by the wave groups.

For the long-term processes, Q2D-morfo (Falqués et al. 2007) has been used to simulate the beach changes caused by mean sea-level rise. This is a nonlinear morphodynamic model developed to solve large-scale shoreline dynamics. Despite it represents the wave field and sediment transport in two horizontal dimensions, the surf processes are not simulated, as waves are modelled through CERC parametrizations (Fredsoe and Deigaard 1992, Smith et al. 2003). Q2D-morfo model is two-dimensional with respect to the depth-averaged sediment flux and bed changes. As a result, this model is highly efficient in terms of computational demands, allowing the modelling of long-term processes. In Chapter 3, the XBeach and Q2D-morfo models have been combined with SWAN, in order to obtain a more efficient and accurate method to assess the sediment changes on a natural beach with sediment supply.

1.6 Assessment of economic impacts

The economic valuation of a good non existing in the market, as in the environmental or healthy-related cases, is conducted by measuring the wellbeing (also called utility) that individuals obtain from different changes of the good under valuation. In this context, the stated preferences method is the most used technique, which translate the individual's choices into a welfare measure and gives a monetary value of the environmental goods (Akter and Bennett 2011, Birol and Koundouri 2008, Brouwer and Schaafsma 2013, Nahuelhual et al. 2004, Remoundou et al. 2015). Among all existing stated preferences techniques, the choice experiment is the most applied method in environmental studies, since it allows to measure individual's wellbeing by studying their preferences under hypothetical markets where the goods are offered at different prices.

In the choice experiment, the individual's preferences are obtained through a survey where the respondents are asked to choose a particular option among set a of alternatives. From the theory of utility (Lancaster 1966), it is assumed that respondents will choose the alternative that increase their utility the most. The alternatives are described by a group of attributes (the goods under valuation) as well as by the levels that these attributes take. Usually, one of these attributes is the price, so that the individual's preferences for an specific attribute or scenario can be traduced into monetary terms.

By using the choices made in the survey and through econometric models, it can be elicited the individual's utility as well the utility function for the specific case study. In the present thesis, we use a mixed model to estimate the tourists' utilities under different

climate-induced environmental scenarios. The utility function obtained from this model can be decomposed in a deterministic and stochastic component. The stochastic component is defined by an error term that represents those factors affecting the individual's choices but unknown by the researcher. On the other hand, the deterministic component is formed by a vector of the attributes included in the survey. In addition, the deterministic component is expected to vary depending on some individual's socioeconomic and attitude characteristics and therefore, these are collected within the survey and some are included in the function. The welfare measure, and therefore, the monetary value, is obtained through the estimation of the WTP for the good under valuation.

In the present thesis, we apply a choice experiment and mixed model to elicit the tourists' utilities under different climate-induced environmental scenarios. The respondents were asked to choose among three alternatives containing three environmental impacts: shoreline retreat due to mean sea-level rise, beach closure due to jellyfish outbreak and loss of seagrass due to water temperature rise. In addition to the choices, their socioeconomic characteristics were recorded and included in the model. More details of methods and results are explained in Chapter 4.

Chapter 2

Changes in beach shoreline due to sea-level rise and waves under climate change scenarios: application to the Balearic Islands (Western Mediterranean).

This chapter has been published as:

Enríquez, A. R., Marcos, M., Álvarez-Ellacuría, A., Orfila, A., and Gomis, D. (2017). Changes in beach shoreline due to sea level rise and waves under climate change scenarios: application to the Balearic Islands (western Mediterranean). *Natural Hazards and Earth System Sciences*, 17(7), 1075-1089.

Abstract

This work assesses the impacts in reshaping coastlines as a result of mean sea-level rise and changes in wave climate. The methodology proposed combines the SWAN and SWASH wave models to resolve the wave processes from deep waters up to the swash zone in two micro-tidal sandy beaches in Mallorca island, western Mediterranean. In a first step, the modelling approach has been validated with observations from wave gauges and from the shoreline inferred from video monitoring stations, showing a good agreement between them. Afterwards, the modelling set-up has been applied to the 21st century mean sea-level and wave projections under two different climate scenarios, representative concentration pathways RCP4.5 and RCP8.5. Mean sea-level projections have been retrieved from state-of-the-art regional estimates, while wave projections were obtained from regional climate models. Changes in the shoreline position have been explored under mean and extreme wave conditions. Our results indicate that the studied beaches would suffer a coastal retreat between 7 and up to 50 m, equivalent to half of the present-day aerial beach surface, under the climate scenarios considered.

2.1 Introduction

Rising mean sea-levels represent one of the major threats for coastal regions, causing submersion, erosion and increased vulnerability to extreme marine events, among

other negative impacts (Nicholls and Cazenave 2010). It is expected that such effects will be aggravated in the coming decades as sea-level rise accelerates in response to global warming (Church et al. 2013) and coastal population and economic growth (Hanson et al. 2011).

Several studies have related coastline retreat during the last decades with mean sea-level rise (e.g. Feagin et al. 2005, FitzGerald et al. 2008), although other relevant processes have also been identified (Passeri et al. 2015). These include oceanic forcing by wave climate and storms, direct or indirect human actions (e.g. mining activities or fluid extraction), and local features such as coastal morphology (Cazenave and Le Cozannet 2014). Coastline retreat has important environmental impacts but also socio-economic implications as it affects population, infrastructures and assets. The impact of mean sea-level rise in the shoreline position has therefore become a subject of increasing concern, particularly in densely populated regions with high urban development. This is the case for many Mediterranean regions, whose economies, which constitute about 14% of the total gross domestic product of the EU (Eurostat 2011), largely rely on tourism based on beach and other seaside recreational activities. Thus, mean sea-level rise and its potential impacts are key factors that must be incorporated in coastal risk management and climate change adaptation measures.

In this paper, we investigate the shoreline changes in two anthropized micro-tidal sandy beaches located in Mallorca (Balearic Islands, western Mediterranean Sea). Here, the shoreline is defined as the water-land interface of the beach, i.e. the limit of the swash zone. The potential impacts of a shoreline retreat would increase the vulnerability of the nearshore infrastructures. In addition, both are typical tourism-oriented beaches in urban environments of the Mediterranean region, so their reduction or disappearance would be detrimental for the local economies.

The impact of mean sea-level rise along sandy coastlines consists of two processes, namely inundation and erosion. Increased mean sea-levels allow waves and surges to act at higher levels landward in the beach profile, increasing erosion rates (Zhang et al. 2004). However, in this study the beach erosion has not been considered, which means that our estimates of landward migration of the coastline could be biased low if erosion rates increase and sediments are carried offshore; in other words, what is assessed here is the minimum impact in beach shoreline retreat. This assumption is further discussed later. Some earlier studies have explored the potential impact of future mean sea-level rise on shoreline changes, although without taking into account changes in the wave climate (see e.g. Wu et al. 2002, Stive 2004, Poulter and Halpin 2008, Le Cozannet et al. 2014). Others have addressed the impact of waves, including extreme events, erosion rates, morphological changes, flooding, and vulnerability of infrastructures but sometimes without including changes in mean sea-level (see e.g. Ruju et al. 2014, Guimarães

et al. 2015, Medellín et al. 2016). Here, in line with works in Villatoro et al. (2014), we address both effects. Furthermore, our study goes beyond the “bathtub” approach and takes into consideration the wave dynamic forces (as in, for example, Passeri et al. 2015, Plant et al. 2016, Gutierrez et al. 2011). To do so, we have used regional mean sea-level changes retrieved from global sea-level projections, with all the different contributions, in combination with regional wave projections over the western Mediterranean Sea up to the year 2100 under two different climate change scenarios. The paper is organized as follows. Section 2.2 is devoted to the description of the study areas, the characteristics of the wave climate, the data available and the numerical approach. The validation of the methodology, which includes the comparison between modelled and observed shallow water waves and coastline positions, is presented in Section 2.3. Section 2.4 describes the shoreline changes obtained under different climate change scenarios. Finally, a summary and some conclusions are presented in Section 2.5.

2.2 Data and Methods

Cala Millor and Playa de Palma are two micro-tidal sandy beaches located in Mallorca island (Balearic Islands, western Mediterranean Sea; Figure 2.1). Cala Millor is 1.7 km alongshore by 35–40 m cross-shore, with a rock bed and a small cliff at the southernmost sector of the beach, and it is exposed to offshore waves from the NE to ESE. Both beaches are reflective, with the Playa de Palma slope being slightly steeper than Cala Millor.

The wave regime in deep waters has a significant wave height (H_s) of 1 m and a peak period (T_p) of 4 s. Playa de Palma is 4 km alongshore by 30–50 m cross-shore and is exposed to offshore wave conditions from the SE to SW, with an H_s of 0.7 m and a T_p of 4.8 s. Figure 2.2 characterizes the mean wave regime offshore at both sites using self-organizing maps (SOMs) that have been built with a 58-year wave hindcast (see Section 2.2.5 for more details). SOMs graphically display the distribution of H_s , T_p and wave direction (in arrows). The results evidence that low-energy states are dominant at both sites and that, overall, Cala Millor is more energetic than Playa de Palma.

These two beaches are considered urban beaches since they are backed by promenades and buildings; therefore, the beach responses to hydrodynamic changes are restricted by these features. Also, their aerial shape depends on the distribution of the sand that is carried out by the council workers according to the tourist comfortability. Playa de Palma and Cala Millor beaches have been part of the beach monitoring programme of the Balearic Islands Coastal Observing and Forecasting System (SOCIB) since 2011 (Tintoré et al. 2013). This programme includes periodic topography and bathymetry surveys, continuous video monitoring of the shoreline position and in situ measurements of nearshore waves and currents, among others. In addition, a dedicated

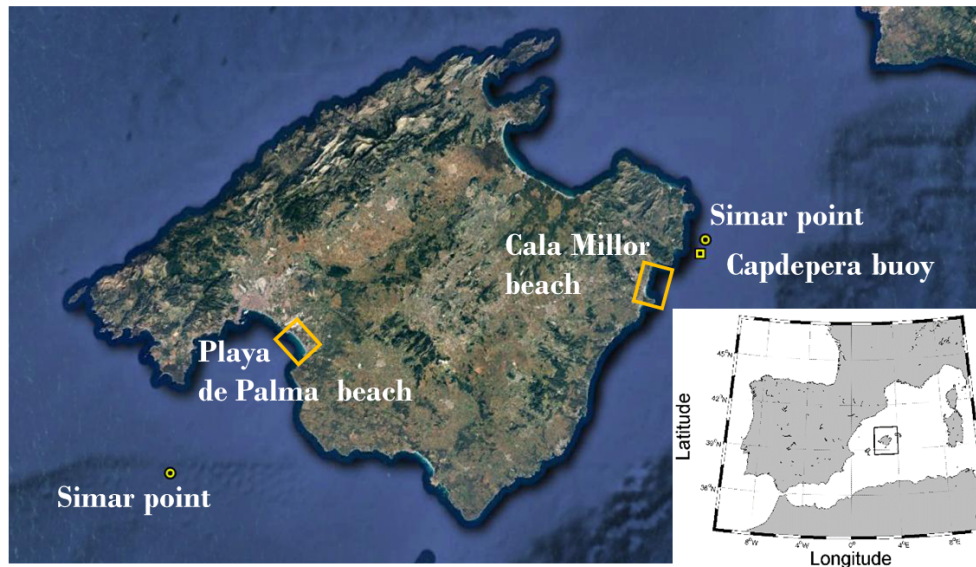


Figure 2.1 Mallorca island with Cala Millor and Playa de Palma beaches marked with yellow squares. SIMAR grid points used to characterize the offshore wave climate and the Capdepera wave buoy are also marked. The inset map represents the western Mediterranean basin.

field survey (RISKBEACH) was undertaken in Cala Millor in March-April 2014, during which higher resolution observations were obtained (Morales-Márquez et al. 2017). Specific data used in the present work are described in the following.

2.2.1 Topo-bathymetric surveys

Bathymetry surveys were conducted using a single-beam echo sounder, BioSonics DT/DE Series Digital Echosounder, in the Cala Millor beach and a multi-beam echo sounder, R2Sonic2020, in Playa de Palma. The final spatial resolution is 1 m cross-shore and 2 m alongshore in Cala Millor and 0.5 m x 0.5 m in Playa de Palma. These measurements were complemented with topographies of the aerial beach obtained using a survey-grade RTK-GPS (Real Time Kinematic Global Position System) mounted in a backpack carried by a human walker. These detailed beach topo-bathymetries were surveyed under calm conditions.

2.2.2 Hydrodynamic data

In Cala Millor, nearshore hydrodynamic data were obtained from three directional Acoustic Waves and Currents (AWACs) sensors located at 8, 12 and 25 m water depths; the AWACs were deployed as part of the RISKBEACH field survey, which covered 12 March to 14 April 2014. Offshore hourly hydrodynamic data have been recovered from Capdepera buoy, located 36.45 km northeast of Cala Millor at 48 m depth (see Figure

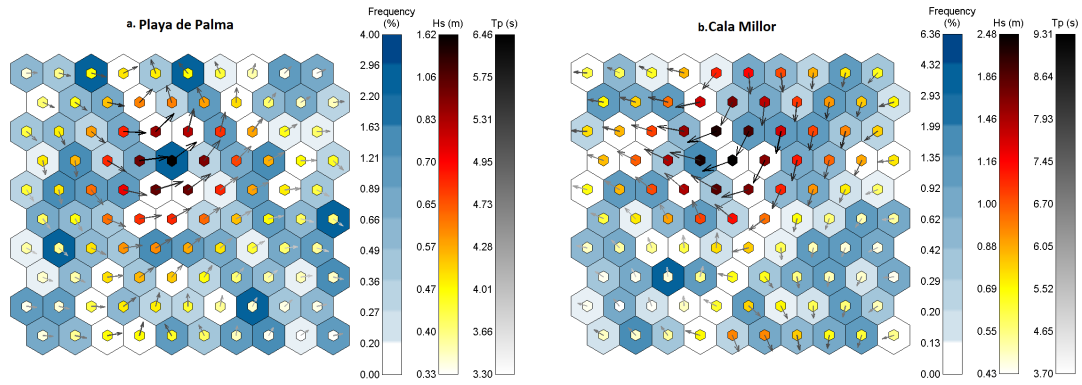


Figure 2.2 *Playa de Palma and Cala Millor self-organizing maps (SOMs). SIMAR databases are shown in 100 cells displaying the more representative deep water sea conditions at the Playa de Palma (a) and Cala Millor (b) beaches. The blue colour illustrates the frequency of the sea states, together with the Hs in metres (yellow to red), the period in seconds (white to black) and the direction in arrows. It can be seen that the more energetic conditions come from the SW in Playa de Palma and from the NE in Cala Millor, the higher frequency waves are also low-energy at both sites.*

2.1 for location). The buoy has been operative during the period 1989-2014 as part of Puertos del Estado (the Spanish holding of harbours) buoys network. On the other hand, in Playa de Palma, wave data came from a coastal buoy located at 23 m depth and an acoustic Doppler current profiler (ADCP) deployed at 17 m depth, both operating since January 2012 as part of the SOCIB beach monitoring programme.

2.2.3 Video imagery data

Five and fourteen video cameras are used to measure the coastline position along Cala Millor and Playa de Palma beaches, respectively. These cameras are part of the video-based coastal zone monitoring system called SIRENA developed by SOCIB and IMEDEA (Mediterranean Institute of Advanced Studies). Departing from images taken at 7.5 Hz, the SIRENA system generates statistical products that provide quantitative information of hydrodynamics and morphodynamics after specific post-processing (Nieto et al. 2010). Specifically, the coastline is routinely obtained from the time image consisting of the addition of all images captured during 10 min (a total of 4500 images) and applying a post-processing of cluster classification. After applying different corrections to overcome the coarser resolution of the far-field camera images as well as rectifying the perspective projection, the coastline is georeferenced in a world coordinate system.

The processing of camera images involves two types of errors related to the intrinsic and extrinsic calibrations. After images have been optically corrected, the extrinsic calibration relates pixel position with real-world coordinates, and thus errors are associated with the georeferencing (Simarro et al. 2017). Typically, resolution ranges between 0.5 and 2 pixels for Cala Millor and from 0.5 to 5 pixels for Playa de Palma. Conversely,

pixel resolution decreases with distance, but higher resolution (~ 0.2 m) is obtained at the shore since cameras are oriented to measure this part at the centre of the image. Only pixels where errors are less than 3 m have been considered in this study. Exemplarily, the pixel resolution is added to Figure 2.15 in one area with the lowest radial resolution in Playa de Palma.

2.2.4 Numerical approach

With the aim of simulating the shoreline changes under given offshore conditions, the SWAN (Booij et al. 1999) and SWASH (Zijlema et al. 2011) models have been combined to resolve the wave processes from deep waters up to the swash zone. SWAN is a third-generation wave model that solves the spectral action balance equation for the propagation of wave spectra (<http://swanmodel.sourceforge.net/>). This model allows an accurate and computationally feasible simulation of waves in relatively large areas. On the other hand, SWASH is a phase-resolving non-hydrostatic model governed by the nonlinear shallow water equations with the addition of a vertical momentum equation and non-hydrostatic pressure in horizontal momentum equations (<http://swash.sourceforge.net/>). Due to its computational cost, the application of SWASH is restricted to small areas. The combination of both models allows for high-resolution and accurate results with less computational cost.

For the present study, SWAN simulations have been performed in a stationary mode over two regular nested grids. In Cala Millor, the coarser grid covers a domain of 21 km x 21 km, with its lowest left vertex at 39.53° N, 3.38° E (Figure 2.3) and a resolution of 149 m x 119 m in the x and y directions, respectively. The size of the finer grid is 9.5 km x 9.5 km, with its lowest left vertex at 39.6° N, 3.38° E and a resolution of 60 m. The coarse grid in Playa de Palma covers a domain of 21.5 km x 27.7 km, with its lowest left vertex at 39.31° N, 2.5° E (Figure 2.4) and a resolution of 100 m x 100 m in x and y directions. The domain of the finer grid is 13 km x 10.8 km starting at 39.47° N, 2.58° E, with a resolution of 50 m x 50 m. In all cases, the SWAN output consisted of the 2-D variance energy density spectrum and the spectral parameters of propagated wave conditions. Each output SWAN spectra corresponded to 1 h of simulation and were used as the input wave conditions of SWASH.

SWASH simulations in Cala Millor have been performed on a 1.5 km x 3.2 km rectangular grid, with its lowest left vertex at 39.57° N, 3.38° E, a resolution of 3 m x 3 m (Figure 2.3) and a maximum depth at 17 m. A larger SWASH domain was required in Playa de Palma, so a 3 m x 3 m grid covering a domain of 3 km x 7 km starting at 39.47° N, 2.75° E and tilted 45° in order to orient the wave maker boundary parallel to the beach, at 15 m depth, was used. The SWASH simulations lasted for 30 min, with a time step of 0.05 s to keep the Courant number between 0.01 and 0.5.

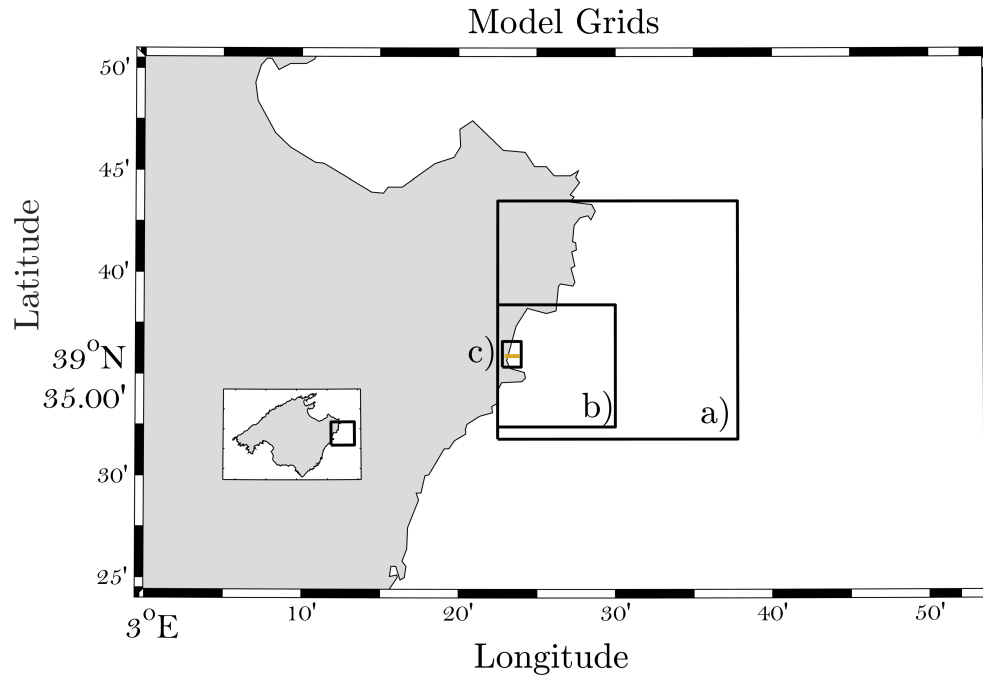


Figure 2.3 SWAN coarse (a) and fine (b) grids and SWASH (c) computational domains for the Cala Millor beach. Yellow line indicates the sector where the three ADCPs are located.

The initial wave conditions imposed at the eastern boundary in Cala Millor and at the southwestern boundary in Playa de Palma corresponded to the 2-D variance energy density spectrum field provided by the corresponding SWAN simulations.

The simulations of SWAN and SWASH were performed with the same over-land extent as the width of the beaches, that is, 35-40 m in Cala Millor and 30-50 m in Playa de Palma. The SWASH model requires a rectangular computational grid, so dummy values were used behind the measured topography in order to complete the computational grid, given that the beach width is not uniform. The final output of the model combination consists of instantaneous water level elevations in the whole domain and the position of the coastline at each time step. The shoreline simulated is obtained as a mask of wet-dry points on the computational grid, providing the limit of flooding at each time step and mesh position. More precisely, the SWASH model obtains the moving shoreline ensuring non-negative water depths for a one-dimensional case $(|u|\Delta t)/(\Delta x) \leq 1$. Flooding never happens faster than one grid size per time step, which is physically correct. Thus, the calculation of the dry areas does not need any special feature.

Finally, the PETRA model is used to evaluate the changes in the beach profile un-

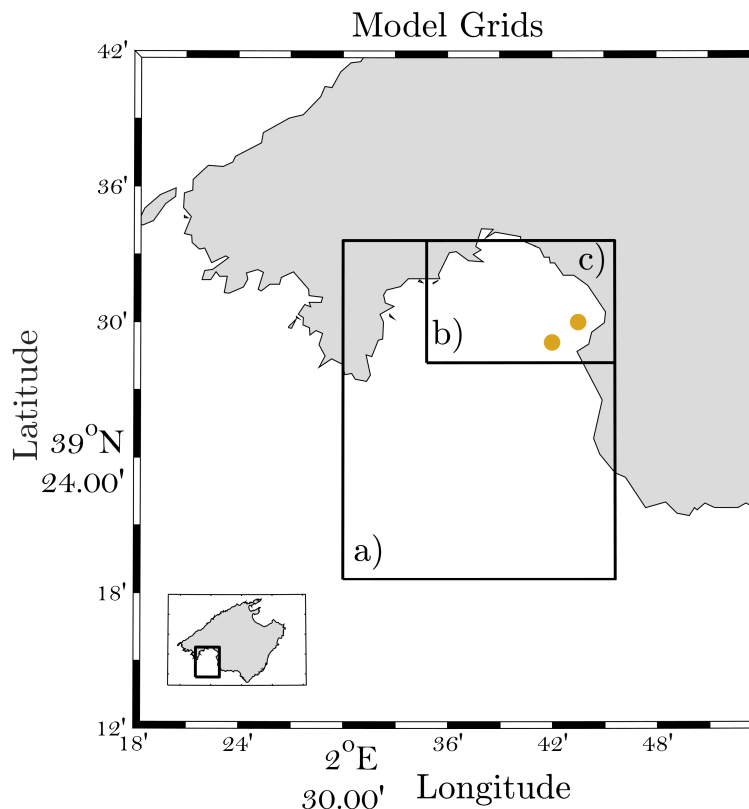


Figure 2.4 SWAN coarse (a) and fine (b) grids and SWASH (c) computational domains for Playa de Palma. Yellow dots indicate the locations of the shallow water wave buoy and ADCP.

der the different sea-level and wave conditions, in order to assess the limitations of the assumption of the unchanged profile. PETRA is a cross-shore beach model that simulates the sediment transport along a single beach profile. It takes into account both the hydrodynamic conditions and the conservation of sand to study the response in 1-D shape. The wave conditions are computed as a phase-averaged model and the sediment transport is calculated using different formulations. The reader is referred to González et al. (2007) for detailed information of this model.

2.2.5 Forcing of numerical models

The SWAN-SWASH model set-up described in Section 2.2.4 has been run under present-day and future climate conditions in both domains. The first step aims at validating the model performance, for which the present-day runs, forced with realistic offshore waves, have been compared against measured nearshore wave parameters. In the present-day runs deep water conditions were retrieved from the SIMAR database (Pilar et al. 2008), which is a 58-year wave reanalysis generated with the WAM model (WAMDI Group 1988). The reanalysis, which is freely distributed by Puertos del Estado, covers the western Mediterranean and provides 3-hourly wave data up to 2011

and hourly data since then. The two closest SIMAR grid points to each of the domains were selected to force the SWAN model for the periods of validation (as detailed later). Although this data set has already been evaluated against observations (Pilar et al. 2008, Martínez-Asensio et al. 2013, 2016), we have further compared the output with the offshore waves observed at Capdepera buoy in order to ensure the reliability of the forcing in the particular periods and locations studied here (Section 2.3.1). The mean sea-level rise is included simply by indicating the still water-level corresponding to the mean sea-level in the projections by 2100.

Once validated, the model set-up has been forced under future climate conditions. To do so, projected mean sea-level rise together with changes in the wave climate have been run. A summary of the values used for mean sea-level and waves is presented in Table 2.1. Regarding mean sea-level, projections by 2100 have been estimated following (Slangen et al. 2014), who provided the regional distribution of the different contributors to sea-level change under two climate change scenarios, namely representative concentration pathway (RCP)4.5 and RCP8.5 (Moss et al. 2010). These are representative of moderate and large emission scenarios, respectively. Slangen et al. (2014) used an ensemble of 21 atmosphere-ocean coupled general circulation models (AOGCMs) from the Coupled Model Intercomparison Project Phase 5 (CMIP5) archive to estimate changes in ocean circulation and heat uptake contribution, atmospheric loading, land ice contribution (including all glaciers, ice caps and ice sheets on Greenland and Antarctica), groundwater depletion and mass load redistribution worldwide, together with the associated uncertainties for each term. As the regional distribution of each component was provided, we selected the Mediterranean region and averaged the sum of the components as the input for projected mean sea-level rise. The results lead to a regional mean sea-level rise of 48 ± 23 cm and 67 ± 31 cm by 2100 for RCP4.5 and RCP8.5, respectively. Uncertainties quoted correspond to 1σ deviation from the ensemble mean (Slangen et al. 2014). Such values are thus consistent with the widely adopted values of sea-level rise and the definition of the future climate scenarios (Brunel and Sabatier 2009, Tamisiea and Mitrovica 2011, Church and White 2011, IPCC 2013).

Changes in the wave climate during the 21st century have been obtained from regional wave projections over the western Mediterranean (Aznar et al. 2016). These projections were carried out using the WAM model with a spatial resolution of $1/6^\circ$ (over the same grid as the SIMAR database) and forced with a set of dynamically-downscaled surface wind fields from AOGCMs. A total of six simulations were used, five corresponding to the A1B scenario and one to the A2 scenarios (IPCC 2000). Each projection was accompanied by a control simulation representing the climate of the last four decades of the 20th century, as it is usual practice. As the regional wave projections were computed before the adoption of the new set of RCP scenarios, for the

	Climate scenario	Cala Millor	Playa de Palma
Sea level rise (mean	RCP4.5	48±23	
±1σ, in cm)	RCP8.5	67±31	
Hs (in m)	A1B	1.1	0.64
	A2		
Hs 10-year return	A1B	4.5	4.4
period, (in m)	A2		

Table 2.1 *Input condition of the model set-up under climate change scenarios for the two beaches. See the text for details on their computation.*

purposes of the work, it is assumed here that the A1B (A2) scenario is equivalent to RCP4.5 (RCP8.5). One of these simulations is exemplarily represented in Figure 2.5, in which the evolution of Hs under the A2 scenario is depicted for the mean regimen (Figure 2.5a) and for the extremes (Figure 2.5b). Changes in the mean and extreme wave regimes have been assessed by computing the differences between the values averaged over the period 2080-2100 (from the future projections, in blue in Figure 2.5) and those averaged over 1980-2000 (from the control simulations, in black in Figure 2.5). These differences reach 0.2 m under calm conditions and up to 0.3 during an extreme event. The obtained differences were then added to the hindcasted values from the reanalysis, which represent the best approach to the actual present-day climate (in red in Figure 2.5). For each beach, the closest grid points (the same location as for the SIMAR database) were selected to simulate the future wave climate. At the point representative of the deep water wave regime of Cala Millor, the resulting values for mean Hs were 1.20 and 0.95 m for the A2 and A1B scenarios, respectively, while in Playa de Palma the values were 0.63 m and 0.65, respectively. The storm events have been assessed computing the 10-year return periods by fitting a generalized Pareto distribution to each time series. The values obtained were 4.5 and 4.2 m under the A2 and A1B climate change scenarios in Cala Millor and 4.3 and 4.4 m in Playa de Palma. Given the similarities between the two wave climate change scenarios, a single (average) value for the simulations has been used (see Table 2.1). Regarding the wave direction, the changes are negligible and remain unchanged in the future simulations.

In summary, six wave simulations have been carried out for each site to predict the shoreline changes under mean conditions: one for each of the two mean sea-level rise scenarios (RCP4.5 and RCP8.5) and one for their respective upper and lower uncertainty limits (i.e. plus 1σ and minus 1σ). Please note that, for the sake of simplicity, hereinafter we will refer to $1\pm\sigma$ as our upper and lower uncertainty limits, respectively. In addition, four simulations have been performed for extreme conditions; due

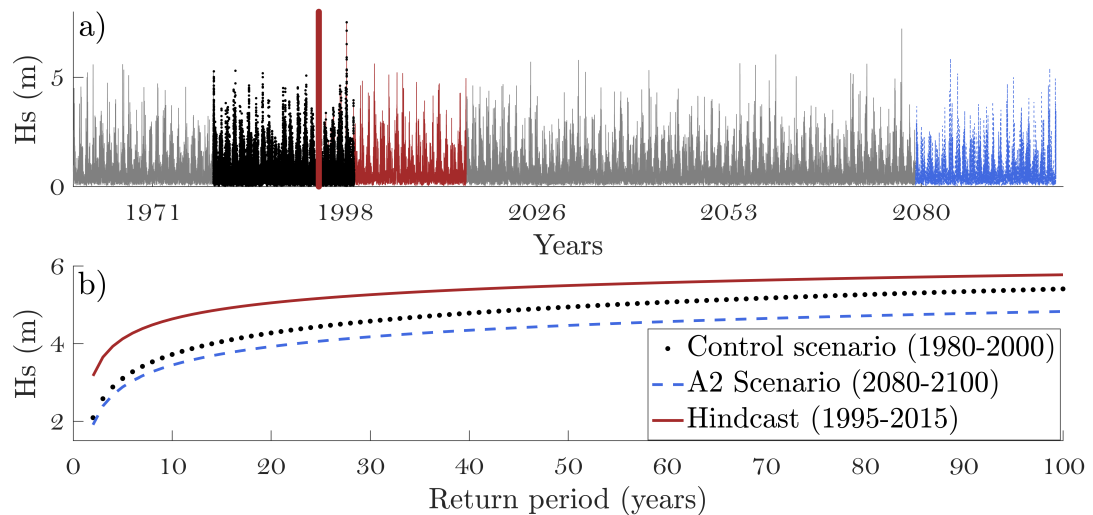


Figure 2.5 Return periods in the A2 scenario for future projections (blue dashed line), control simulation (black dotted line) and hindcast (red line). Note that there are different time periods for the series as well as the overlapping of hindcast and control scenarios. The red line indicates the 1st day of hindcast time series.

to computational constraints, we focused on the two highest mean sea-levels for each scenario, that is, the occurrence of the 10-year return level storm occurring over the two mean sea-level scenarios and their upper limit (i.e. for the mean value and the mean value $+1\sigma$).

2.3 Evaluation of model setup under present-day climate conditions

2.3.1 Comparison with wave observations

As described above, the SIMAR wave reanalysis has been taken as representative of the offshore wave conditions and used to force the numerical model set-up. To illustrate its reliability, the time series at the closest grid point in Cala Millor has been compared against observations from the nearby Capdepera buoy. The time series and scatter plots of the measured and modelled statistical wave parameters (H_s , T_p , θ) are shown in Figures 2.6 and 2.7 for a 3-month period (January- March 2014). The root mean square error (RMSE) and the correlation coefficient (ρ) between observed and modelled parameters are quoted in the figures. Results show that the hindcast agrees well with the observed H_s and T_p with correlations over 0.8 and a small RMSE. For wave direction, however, the correlation decreases down to 0.5, mostly due to the fact that the WAM resolution cannot properly resolve the coastal topography near the SIMAR location. A closer look at Figure 2.6 (bottom panel) reveals that SIMAR contains waves from the NW (315°) which are not recorded by the buoy. However, waves from the dominant directions (i.e. from N, 0° , to SE, 135°) are not affected, and, therefore, H_s and T_p have

enough accuracy to represent the wave climate of this offshore area.

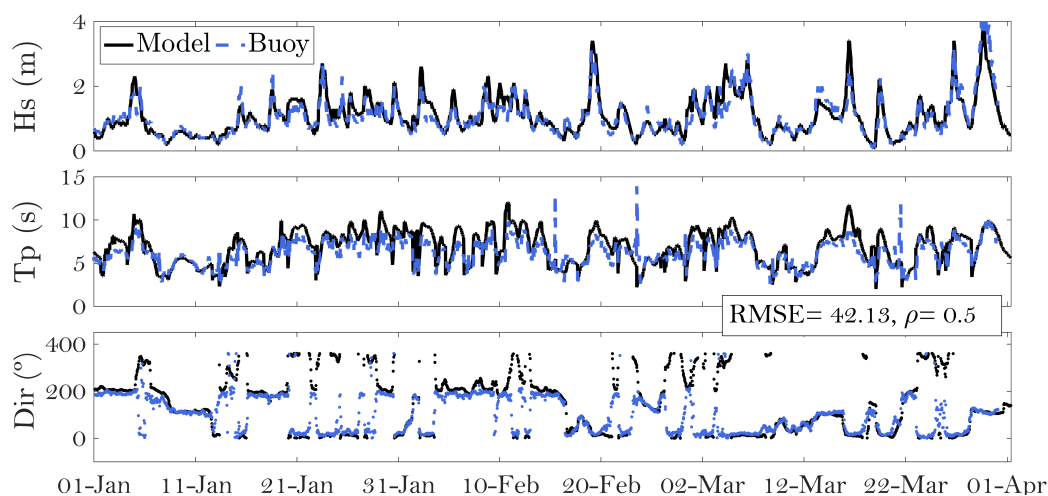


Figure 2.6 Capdepera buoy observations (blue) and hindcasted SIMAR (black) time series of H_s , T_p and wave direction. RMSE and correlation are quoted for the wave direction.

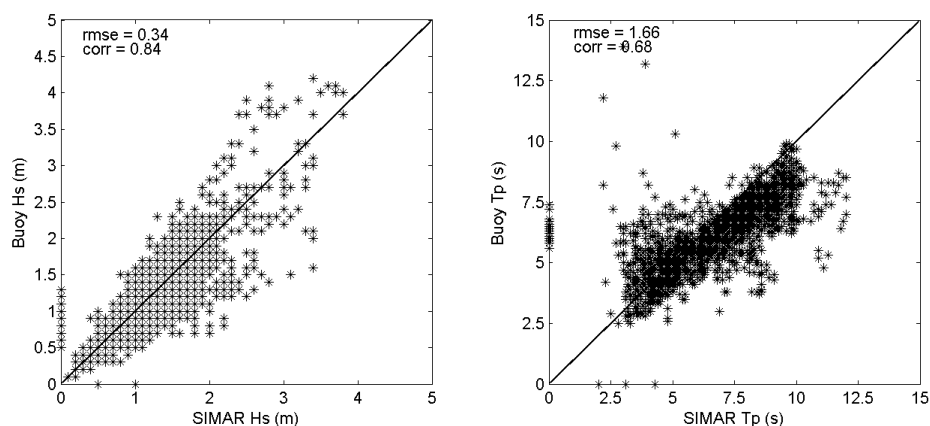


Figure 2.7 Scatter plots of buoy observations vs. SIMAR hindcast for H_s (a) and T_p (b). RMSE and correlation are quoted in each figure.

Despite the differences found in the wave direction, the advantages of using reanalysed data instead of observations for the input wave in SWAN are evident: first, the modelled time series are complete, while observations are often gappy; and second, the deep water waves can be propagated over large domains, thus providing values close to our two areas of study. Although the validation of the numerical hindcast is limited to a single grid point close to Cala Millor, previous assessments (e.g. Martínez-Asensio et al. 2013) also validated this hindcast, and it is therefore assumed that the reanalysis is equally valid for Playa de Palma.

The output of the SWAN model has been validated against observations in the two beaches. In Cala Millor the results of SWAN forced with SIMAR data were compared with nearshore wave observations during the period from 14 March to 14 April 2014

	ADCP 8 m			ADCP 12 m			ADCP 25 m		
	RMSE	BIAS	Corr.	RMSE	BIAS	Corr.	RMSE	BIAS	Corr.
Hs (m)	0.13	0.01	0.97	0.18	0.03	0.95	0.23	0.11	0.95
Tp (s)	1.21	0.02	0.94	1.24	0.01	0.94	1.22	-0.22	0.93
θ (°)	25.60	6.30	0.74	29.20	3.65	0.80	40.43	14.20	0.72

Table 2.2 Comparison between SWAN results and nearshore wave observations in the Cala Millor beach. The period spanned by the series is from 14 March to 14 April 2014.

(i.e. a total of 755 h of simulation). The closest grid points of the SWAN model to each of the three directional wave ADCPs were selected. Resulting correlations, RMSEs and biases are listed in Table 2.2 for the three ADCPs and for the three wave parameters. Overall, the statistical parameters show good agreement between measurements and the model output, with correlations over 0.9 for Hs and Tp and over 0.7 for the wave direction. To further illustrate the model performance, observed and modelled time series are plotted in Figures 2.8 and 2.9. Both reflect the ability of the model to capture the magnitude and variability of nearshore waves. Nevertheless, during the storm events recorded (as in 28 March), the model underestimates the observed Hs by up to 30 cm.

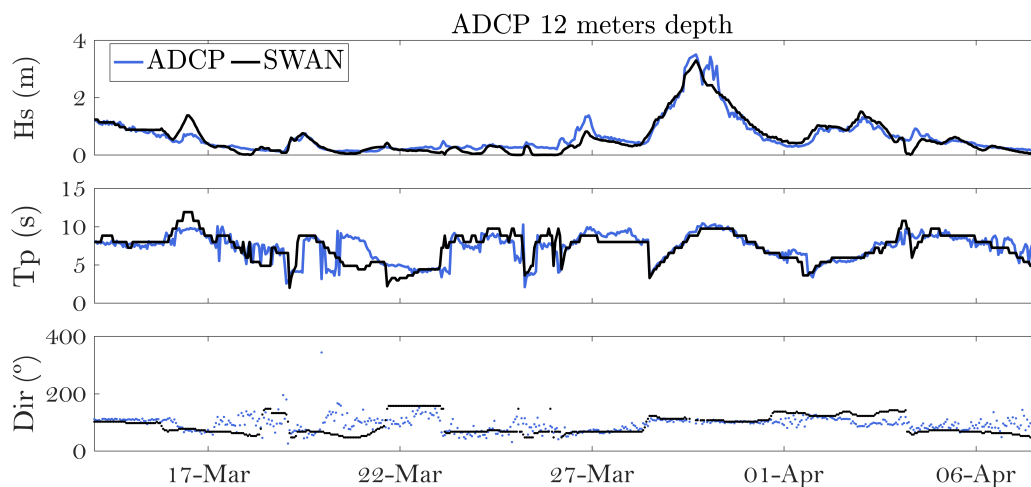


Figure 2.8 Hs, Tp and wave direction as modelled by SWAN and observed at the ADCP deployed at 12 m depth in the Cala Millor beach.

In Playa de Palma, the simulated waves have been compared with the observations from a buoy moored at 23 m depth and with an ADCP at 17 m depth for the period from 1 to 30 September 2015 (i.e. a total of 720 h of simulation). The results are summarized in Table 2.3 and the time series are plotted in Figures 2.10 and 2.11. Like in Cala Millor, there is a good agreement in Hs with correlations over 0.9. For Tp, however, observations display higher variability than modelled data, which makes the correlations drop to 0.32–0.34 and the bias reach 0.4–0.6 s for the buoy ADCP, respectively (see Figure

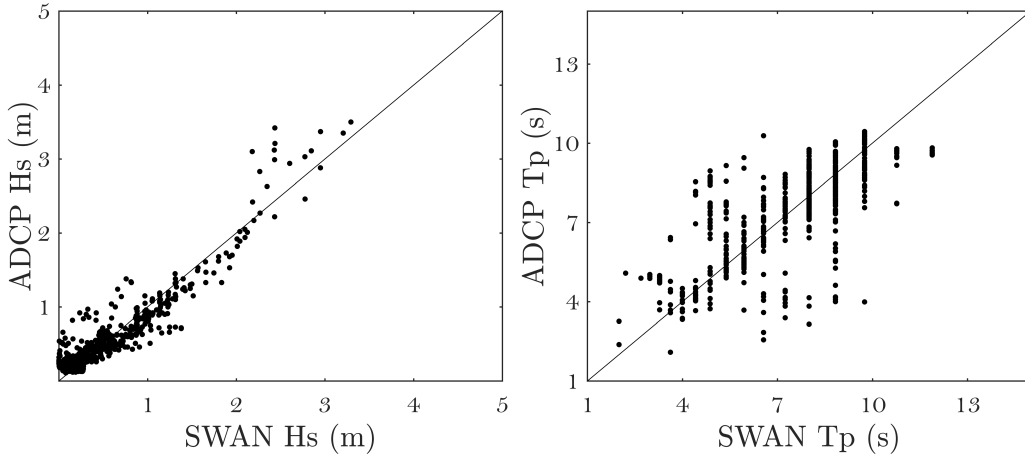


Figure 2.9 SWAN vs. ADCP scatter plots of H_s (a) and T_p (b) in Cala Millor.

2.11). Possible reasons for this discrepancy are the instrumental noise in measurements and/or the influence of local wind within the SWAN domain. The differences between observed and modelled wave directions are also larger than in Cala Millor, with non-significant correlations. The reason for the discrepancies in wave direction is probably the inability of the model to accurately represent the wave diffraction occurring at the SE of the bay of the Playa de Palma, where the buoy and the ADCP are located. This area is protected by a headland (see Figure 2.4) that may cause worse results in wave direction.

	Buoy 23 m			ADCP 17 m		
	RMSE	BIAS	Corr.	RMSE	BIAS	Corr.
H_s (m)	0.19	0.12	0.95	0.17	0.09	0.95
T_p (s)	0.56	0.40	0.32	1.74	0.60	0.34
θ ($^\circ$)	46.19	18.5	0.29	49.4	30.9	NS

Table 2.3 Comparison between SWAN results and nearshore wave observations in Playa de Palma. The period spanned by the series is from 1 to 30 September 2015.

2.3.2 Comparison with observed shoreline position

A total of four and three simulations have been carried out with the SWASH model for the Cala Millor and Playa de Palma beaches, respectively, in order to validate the model results with measurements of shoreline positions. The dates chosen for the validation correspond to dates in which the video monitoring provided good quality images, with them being also close to the dates when the bathymetry surveys were performed (they are listed in Tables 2.4 and 2.5). Wave makers were defined at the eastern boundary of the SWASH model domain in Cala Millor and at the southwestern boundary in

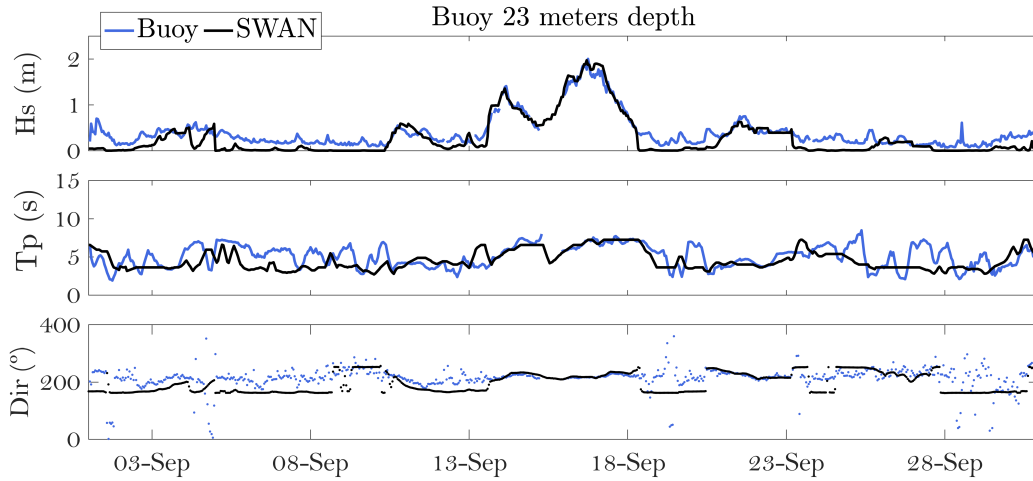


Figure 2.10 *Hs*, *Tp* and wave direction as modelled by the SWAN model and observed at the buoy deployed at 23 m depth in Playa de Palma.

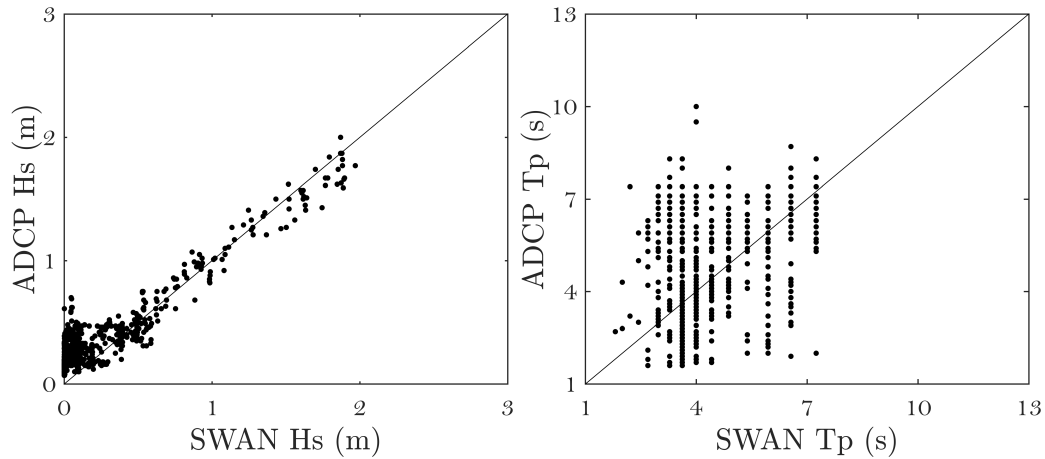


Figure 2.11 . SWAN vs. ADCP scatter plots of *Hs* (a) and *Tp* (b) in Playa de Palma.

Playa de Palma, in both cases with the SWAN wave conditions. These input wave conditions for the validation process are specified in Tables 2.4 and 2.5 for the indicated dates.

Observed and modelled shoreline changes for each case study have been compared in Figures 2.12 and 2.13 along the two beaches. Results show that the modelled shorelines line up with observations in all cases. In Cala Millor the agreement is better in the central part of the beach, while some differences are found in the northern and southernmost sector. It is important to remark that images obtained from the beach cameras are increasingly uncertain with the distance from the cameras (Section 2.2.3 for details). Therefore, part of the difference between the measured and simulated shoreline at the ends may come from this error in measurements. In Playa de Palma only the area between 39.51 and 39.53° N is used for the comparison as this is the stretch of the shoreline where the video system has the requested quality. We will also restrict the

discussion on future projections to this sector.

The RMSEs and biases between observations and model results have been calculated for each case and are listed in Tables 2.4 and 2.5. These statistics must be set in a proper context in order to evaluate how good the model performance is. To do so, the temporal variability of the shoreline position has been estimated as the standard deviation (cross-shore) at each alongshore position for which 10 coastlines measured from video monitoring have been used. In Cala Millor, higher variability is observed, calculated between April and May 2014, in the central part of the beach (mean value of 8.4 m) and lower towards the ends, with a mean value along the entire beach of 5.5 m. Figure 2.14 shows the shorelines simulated for the case studies (red lines), the corresponding measured shorelines (blue lines) and the variability of the shoreline (grey area), zoomed in around an area at the centre of the beach. In the case of Playa de Palma, the shoreline displays a cross-shore variability of 6 m in the area around the centre of the beach and lower at the extremes, with a mean value of 3 m, as calculated with observations between August and October 2014. The results are plotted in Figure 2.15 in which again the central area has been zoomed in, in order to highlight the differences. Notably, the modelled shorelines are very similar to each other, because the forcing is also similar in the three case studies.

	Hs (m)	Tp (s)	θ (°)	RMSE (m)	BIAS (m)
27 March	1.6	8.3	13	5.7	3.2
28 March	0.8	7.9	28	2.7	-0.6
1 April	0.5	5.5	137	6.5	-3.2
2 April	1.1	5.7	134	5.4	-3.2

Table 2.4 *Dates and forcing conditions of the SWASH simulations and results of the validation against observed shoreline position in the Cala Millor beach.*

	Hs (m)	Tp (s)	θ (°)	RMSE (m)	BIAS (m)
03 Sept.	0.4	3.7	154	6.1	1.5
15 Sept.	0.6	6.7	223	5.9	1.7
28 Sept.	0.4	2.7	47	5.8	1.4

Table 2.5 *Dates and forcing conditions of the SWASH simulations and results of the validation against observed shoreline position in Playa de Palma.*

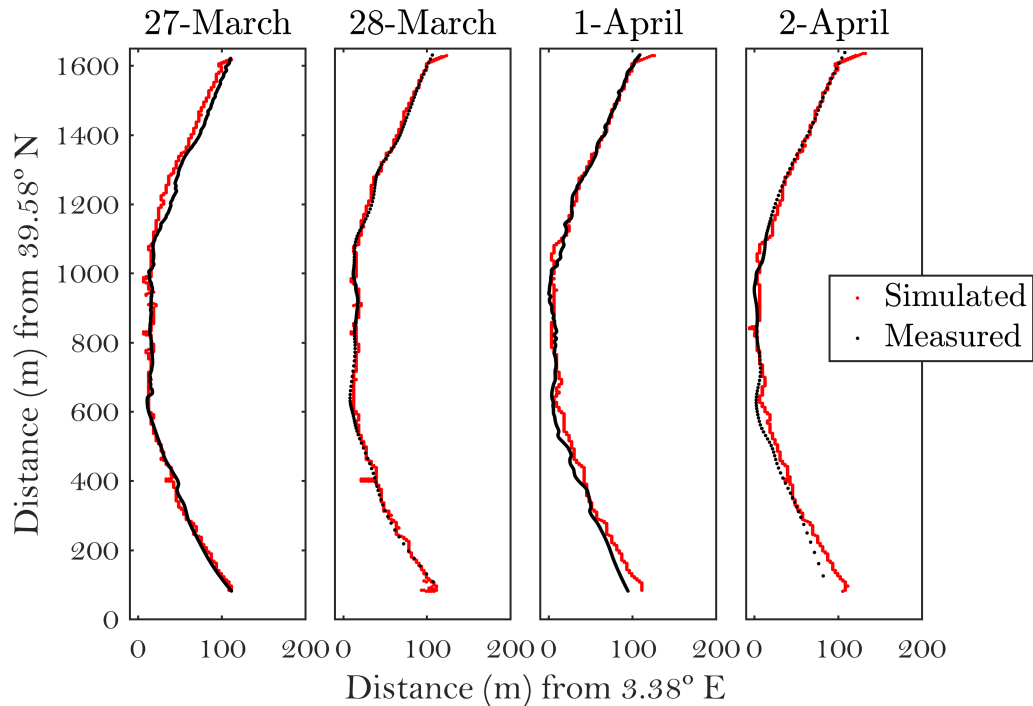


Figure 2.12 Observed (black) and modelled by SWASH (red) shoreline positions in Cala Millor.

2.4 Shoreline changes under climate change scenarios

Since the model performance for present-day climate conditions is considered to be satisfactory, the same model set-up has been used to assess the response of the shoreline under future climate change scenarios. Shoreline changes were simulated for both mean conditions and extreme waves (the latter being defined here as H_s corresponding to the 10-year return level) for the RCP4.5 and RCP8.5 climate change scenarios.

Future projected changes in shoreline have been evaluated assuming that the present-day beach profile remains constant. In order to check the limitations of this assumption, we have run a numerical one-dimensional model capable of estimating profile changes under different mean sea-level conditions. The model used here is PETRA (González et al. 2007), and it has been run for the central profile of each beach under the conditions of no sea-level rise and 0.5 and 0.9 m of sea-level rise and wave mean regime. The results of the model are plotted in Figure 2.16 for both beaches, zoomed in to the nearshore sector where the largest changes are expected. Profile changes are, at most, 20 cm under the highest sea level rise of 0.9 m; that is, in these environments profile changes due to mean sea-level rise are of the order of sandbar formation and mostly eroding the berm. We therefore have considered the variations in the beach profile to be negligible and the assumption of constant beach profile to be reasonable in this context.

A second assumption in our climate change simulations is that the beach shape

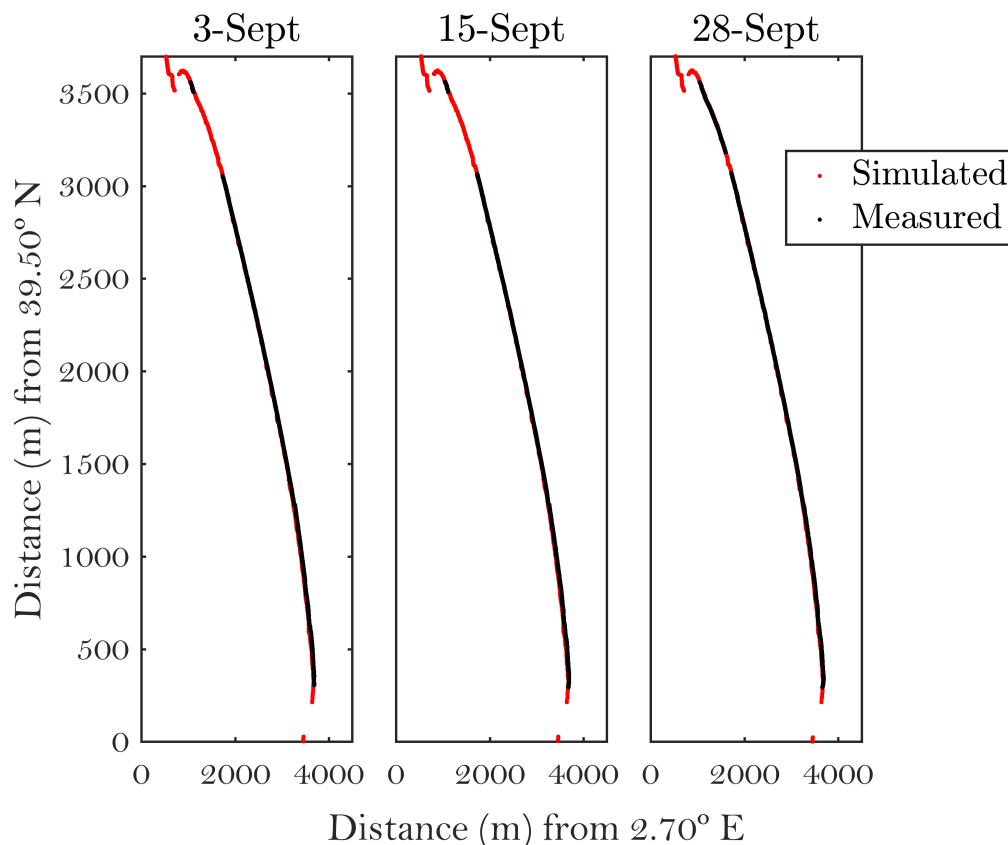


Figure 2.13 Observed (black) and modelled by SWASH (red) shoreline positions in Playa de Palma.

remains unchanged under future conditions. This means that we consider a constant direction in the mean wave energy flux. Thus, any redistribution in the alongshore sediments is neglected in front of the hydrodynamic response to increased mean sea-level. The present-day modelled coastline has been used as a reference to assess the changes under climate change scenarios. The loss of aerial beach, defined here as the landward migration averaged over the entire beach, is indicated in Tables 2.6 and 2.7 for each simulation and for the mean and extreme conditions expected under climate change scenarios. For the extreme conditions, the maximum loss is also listed. In addition, Figures 2.17 and 2.18 illustrate the maximum change in the shoreline position obtained for Cala Millor and Playa de Palma (corresponding to extreme wave conditions under the RCP8.5 $1+\sigma$ scenario). Major changes are projected to occur in the central part of the Cala Millor beach, where the higher variability is shown in Figure 2.14. Larger relative impacts (loss of width), however, are projected towards the extremes of the beach, as these are the narrower sectors. In Playa de Palma, the projected changes in the shoreline are quite uniform along the beach.

Since projected changes in H_s by 2100 are small, their potentially hazardous effects depend primarily on the mean sea-level with which they are combined. In Cala Millor,

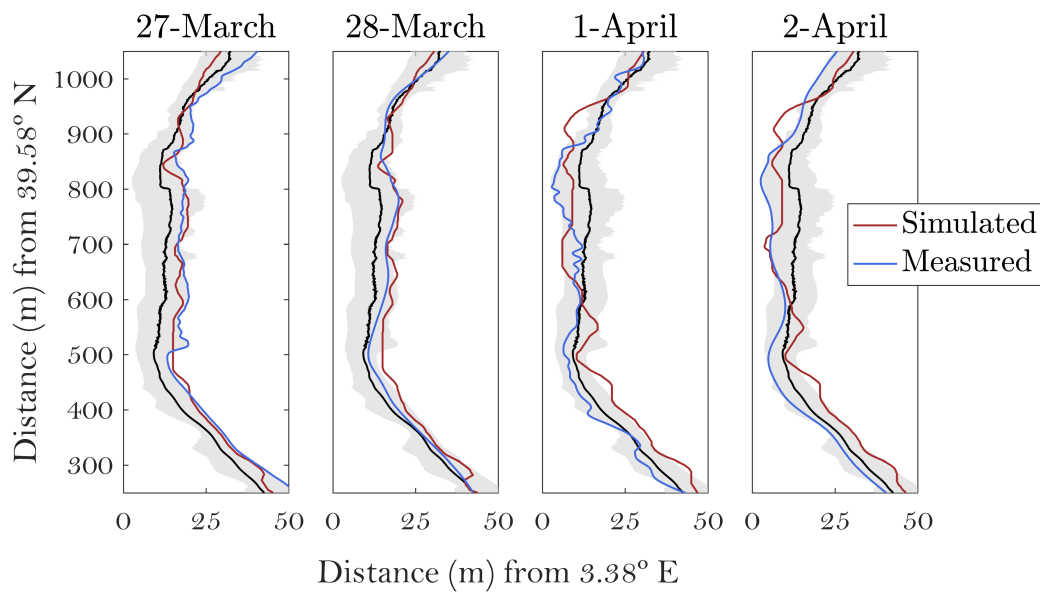


Figure 2.14 Modelled (red) and observed (blue) shorelines positions in Cala Millor with mean shoreline position (black line) and its standard deviation (grey shadow) zoomed in to the central sector:

the averaged coastline retreat ranges between 7 m under the moderate low scenarios and 24 m with the highest sea-level rise considered. During extreme wave conditions the shoreline would retreat up to 29 m on average and may reach 49 m at some parts of the beach. With such values the flooding would reach the urbanized area over the promenade. However, it must be pointed out that the topography does not include the height of the wall backing the beach and the simulations were stopped there, so the flooding extension could actually be underestimated. In Playa de Palma the average coastline retreat ranges from the 7 m obtained for the low scenario to the 21 m obtained for the upper limit considered here. Under extreme conditions, the loss of the beach in Playa de Palma increases with higher mean sea-level rise, and, in all the cases investigated, the water level reaches the promenade at least in part of the domain (Table 2.7).

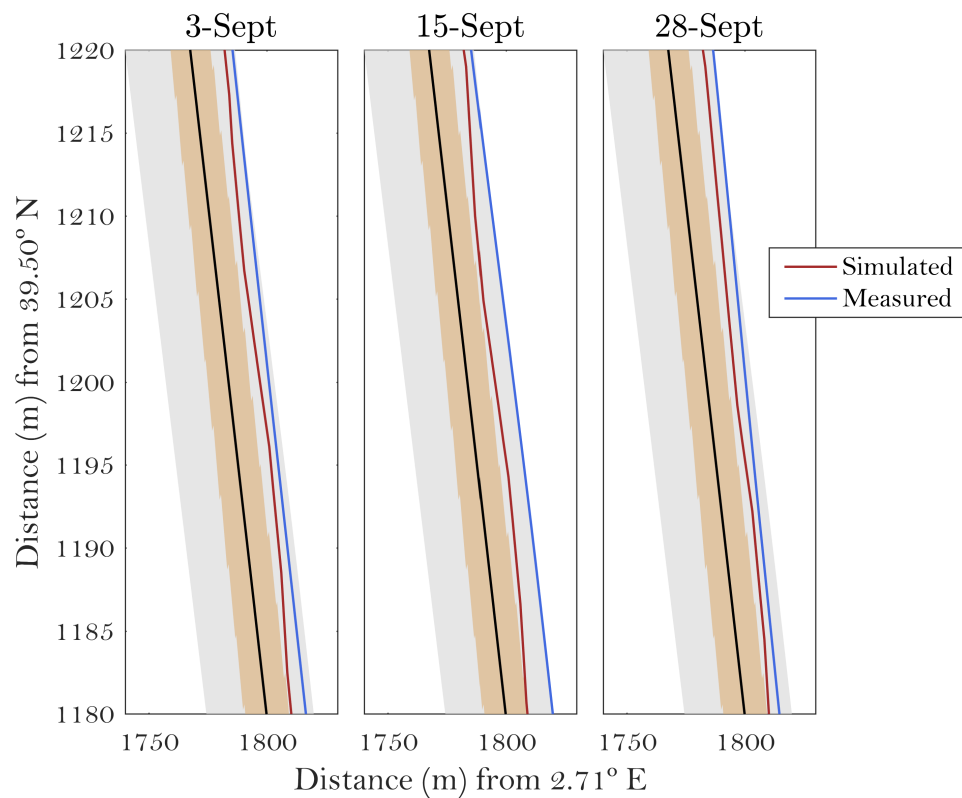


Figure 2.15 Modelled (red) and observed (blue) shorelines positions in Playa de Palma with mean shoreline position (black line), its standard deviation (grey shadow) and the resolution of the pixels of the cameras (orange shadow).

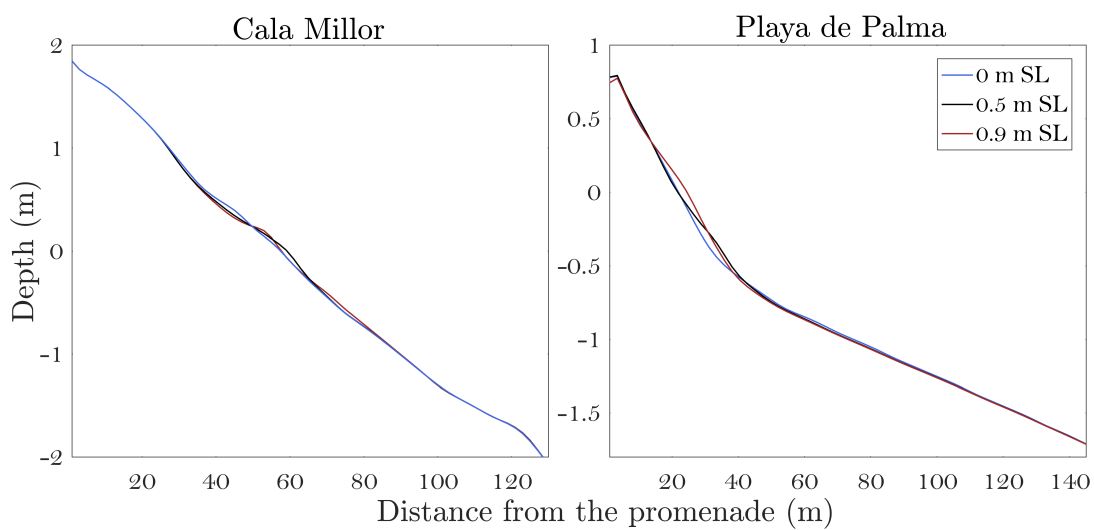


Figure 2.16 Changes in the cross profile in Cala Millor (a) and Playa de Palma (b) in the nearshore area under different sea levels.

Sea Level Rise (climate scenario \pm uncertainty, in cm)	Mean conditions	Extreme conditions	
	Mean loss (m)	Mean loss (m)	Max loss (m)
0.25 (RCP4.5 -1 σ)	7.2	-	-
0.36 (RCP8.5 -1 σ)	10.7	-	-
0.48 (RCP4.5)	11.7	18.5	29.4
0.67 (RCP8.5)	17.5	21.8	38.0
0.71 (RCP4.5 +1 σ)	17.5	24.6	39.5
0.98 (RCP8.5 +1 σ)	24.2	29.0	49.3

Table 2.6 Loss of aerial beach (defined here as the landward migration of the shoreline averaged over the entire beach) for both the mean and extreme conditions expected under climate change scenarios in Cala Millor (in m). For the extreme conditions, the maximum loss is also quoted.

Sea Level Rise (climate scenario \pm uncertainty, in cm)	Mean conditions	Extreme conditions	
	Mean loss (m)	Mean loss (m)	Max loss (m)
0.25 (RCP4.5 -1 σ)	7	-	-
0.36 (RCP8.5 -1 σ)	8.2	-	-
0.48 (RCP4.5)	11.3	17	30
0.67 (RCP8.5)	14.8	20.5	30
0.71 (RCP4.5 +1 σ)	15.7	23.4	30
0.98 (RCP8.5 +1 σ)	21.4	27.9	30

Table 2.7 Loss of aerial beach (defined here as the landward migration of the shoreline averaged over the entire beach) for both the mean and extreme conditions expected under climate change scenarios in Playa de Palma (in m). For the extreme conditions, the maximum loss is also quoted.



Figure 2.17 Present-day shoreline position (in black) and landward migration (in red) in the worst case scenario (mean sea-level rise under RCP8.5 and extreme wave conditions) by the end of the 21st century in the Cala Millor beach.



Figure 2.18 Present-day shoreline position (in black) and landward migration (in red) in the worst case scenario (mean sea-level rise under RCP8.5 and extreme wave conditions) by the end of the 21st century in Playa de Palma.

2.5 Summary and conclusions

This paper has investigated the capabilities of state-of-the-art numerical models to reproduce the changes in the shoreline position in the Cala Millor and Playa de Palma beaches. These two case studies were selected for two main reasons. First, they are representative of many other anthropized beaches in the Balearic Islands (and of many other beaches of the Mediterranean Sea): they are beaches located in urbanized areas, backed by walls, and therefore with limited possible landward migration of the shoreline. Second, these two sites are part of the beach monitoring programme carried out by SOCIB, and, consequently, a wide and complete set of observations are available, allowing the validation of the numerical models against measurements. Furthermore, the two beaches are exposed to offshore wave conditions from different directions and different wave heights, with Playa de Palma being located inside a bay and Cala Millor facing the open sea.

Much effort has been devoted to the validation of the model set-up to ensure that the chosen combination of SWAN-SWASH models is able to reproduce the shoreline variability within a reasonable accuracy. In both cases, modelled and observed H_s from nearshore instruments were in very good agreement, with correlations over 0.9. This increases our confidence in the forcing of the SWASH model. In turn, a satisfactory correspondence between the observed and modelled shoreline position has been found. The agreement between modelled and observed shorelines was better in the central sector of the beaches. This is because the observations derived from the video monitoring system are more reliable close to the location of the cameras and also because the SWASH model configuration requires a smooth bathymetry which can misrepresent some parts of the shore, as is the case of the southernmost sector of Cala Millor where a rock bed and a small cliff distort the wave field.

Regarding the projections of the shoreline changes under climate scenarios of mean sea-level and wave climate, a major assumption of our study is that the morphology of the beach will not change in the future. That is, both the beach shape and the profile will be the same under the climate conditions at the end of the century. It is well known that beach profile evolves in response to storms, moderate wave conditions and mean sea-level rise causing changes in the beach morphology (e.g. erosion followed by recovery episodes, see Short 1996, Simeone et al. 2014, Smallegan et al. 2016, Davidson-Arnott et al. 2002). It has also been demonstrated that the changes in the beach profile play a smaller role in the shoreline retreat due to mean sea-level rise and waves. On top of the above reasons, numerical approaches reproducing the long-term morphological response of the beach are still very limited (e.g. Ranasinghe et al. 2012).

Under the assumptions outlined above, we have found that the retreat in the future shoreline at both sites, Cala Millor and Playa de Palma, are primarily a consequence of

waves acting onto a higher mean sea-level. It must be mentioned that changes in the wave climate are small and the impact of extreme waves increases mostly because they are projected to occur concurrently with higher sea-levels. The results indicate that the beach regression varies between 7 and 24 m along Cala Millor and between 7 and 21 m in Playa de Palma, depending on the climate change scenario considered. This loss is further exacerbated under moderate (return period of 10 years) storm conditions, which may induce a temporary flooding reaching over 49 m in Cala Millor and 30 m in Playa de Palma, thus likely overtopping the walls of the promenade. The Playa de Palma coastal retreat is lower than in Cala Millor due to the steeper slope of the beach profile. As pointed out above in the introduction, the approach proposed here does not consider beach erosion, which means that the above estimates are conservative and could be biased low if erosion acts by removing beach sediments and accelerating aerial beach loss (Brunel and Sabatier 2009).

Playa de Palma and Cala Millor, like many other typical urban Mediterranean beaches, are subject to high touristic pressure, especially during the summer season, and thus concentrate valuable assets and infrastructures. Since tourism constitutes the main economic activity of a large fraction of the region, the social, environmental and economic impacts of future mean sea-level rise are anticipated if no adaptation measures are implemented.

Acknowledgements

This work is supported by the CLIMPACT (CGL2014-54246-C2-1-R) funded by the Spanish Ministry of Economy) and MORFINTRA (CTM2015-66225-C2-2-P). A. R. Enríquez acknowledges an FPI grant associated with the CLIMPACT project. M. Marcos acknowledges a “Ramón y Cajal” contract funded by the Spanish Government. We thank Puertos del Estado for providing deep-water wave data from the SIMAR database. Topo-bathymetries and video-monitoring observations are part of the beach monitoring facility of SOCIB. The authors are grateful to Dr. A. Slangen for providing the data for the regional sea level rise scenarios.

Chapter 3

Assessing beach and dune erosion and vulnerability under sea-level rise: a case study in the Mediterranean Sea.

This chapter has been published as:

Enríquez, A. R., Marcos, M., Falqués, A., and Roelvink, D. (2019). Assessing beach and dune erosion and vulnerability under sea level rise: a case study in the Mediterranean Sea. *Frontiers in Marine Science*, 6, 4.

Abstract

In this study, we estimate the shoreline retreat, the vulnerability and the erosion rates of an open beach-dune system under projected mean sea-level rise and the action of wind-waves (separately and in combination). The methodology is based on the combination of two state-of-the-art numerical models (XBeach and Q2D-morfo) applied in a probabilistic framework and it is implemented in an open sandy beach in Menorca Island (Western Mediterranean). We compute the shoreline response to mean sea-level rise during the 21st century and we assess the changing impacts of storm waves on the aerial beach-dune system. Results demonstrate the relevant role that the beach back-shore features, such as the berm, play as coastal defence, reducing the shoreline retreat and dune vulnerability rates in the near-term (a few decades ahead) and highlighting the importance of simulating the beach morphodynamic processes in coastal impacts assessments. Our findings point at mean sea-level rise as the major driver of the projected impacts over the beach-dune system, leading to an increase of $\sim 25\%$ of the volume eroded due to storm waves by the end of the century with respect to present-day conditions.

3.1 Introduction

Projected mean sea-level rise in response to increased greenhouse gasses concentrations and its combination with land subsidence and other oceanic forces such as wind-waves and storm surges affect the coastal zone, increasing coastal vulnerability, erosion

rates and shoreline retreat among other potential impacts (Nicholls 2002, Idier et al. 2013, Ranasinghe 2016). These coastal damages are expected to have numerous negative social consequences since the littoral is the most populated zone worldwide (Small et al. 2003). As a consequence, the economy of the littoral areas will be also affected because of its strong dependence on the coastal environmental resources (Gössling et al. 2012, Bujosa 2014).

Given the threats that climate change and the associated mean sea-level rise pose to the coastal regions, the assessments of future coastal vulnerability have become topic research issues in the last years (Nicholls 2002, Revell et al. 2011, Idier et al. 2013, Le Cozannet et al. 2014, Ranasinghe 2016, Luijendijk et al. 2018, Sayol and Marcos 2018) as well as their socio-economic consequences (Small et al. 2003, Dasgupta et al. 2007, Gössling et al. 2012). Among these, studies focused on sandy shores, mostly beaches, are very common because this type of coasts is subject to a very high level of human utilization (Gössling et al. 2012). One major challenge in predicting the response of beaches to increased mean sea-level is their highly dynamic character. This is due to the fact that their morphology responds relatively quickly to changes in the hydrodynamic forces in action (including sea-level but also waves, currents and river flows) in many ways. In addition, the morphological state of the beach itself affects the hydrodynamic conditions, leading to a complex feedback between coastal morphology and these forces.

To address these challenges, different approaches have been applied in the literature to assess the beach alterations under projected climate change scenarios. Depending on the hydrodynamic forcing considered and on the tools that are used, several assumptions are necessary in order to simplify the problem. For example, available numerical models are generally able to simulate processes occurring at a single spatio-temporal scale (e.g., one storm event). Thus, their application is limited in the context of climate change (Le Cozannet et al. 2014, Ranasinghe 2016). When these are used to investigate the continuous long-term beach response, estimations have mostly considered mean sea-level rise as the unique hydrodynamic forcing, ignoring the contribution of waves (Purvis et al. 2008, Dasgupta et al. 2007). On the contrary, those estimations that consider the marine extreme events (associated to storminess) combined with mean sea-level changes and sediment transport processes, have commonly been performed using statistical methods. In these cases, their main aim is to assess the coastal changes in specific time lapses and neglecting the cumulative effects over time, such as the continuous long-term mean sea-level rise (Revell et al. 2011, Ranasinghe et al. 2012, De Winter and Ruessink 2017). When coastal changes are concerned, the estimation of the shoreline retreat is widely used as a proxy of the long-term impact of mean sea-level rise. One simplified way to assess shoreline changes is the application of the Bruun Rule

(Bruun 1962) that predicts an upward and landward movement of the beach profile, controlled by the beach slope, in response to mean sea-level rise. The Bruun Rule has proved to be a useful tool for rough coastal retreat assessments, but it is less reliable if more accurate estimations are required (Ranasinghe et al. 2012). In addition, the Bruun Rule highly simplifies the cross-shore sediment transport and neglects some morphological processes such as dune erosion. In consequence, there have been some attempts to improve this simplified approach. In this respect, Rosati et al. (2013) proposed a modified form of the Bruun Rule that included, not only the cross-shore sediment transport, but also the aerial sand transport. Other studies have combined mean sea-level rise with short-term impacts of storm waves and surges, which have been considered in several ways. For instance, Revell et al. (2011) developed a new equation adding the run-up contribution to the Bruun Rule in order to estimate the erosion rates at dunes and cliff areas along the coast of California. They calculated the dune erosion based on the recession associated with a 100-year storm event that takes place at the end of the century using different shore slopes. Another example is found in Wahl et al. (2016) who assessed the erosion and flooding risk in the Gulf of Mexico using a probabilistic model that considered the run-up of wind-waves and the long-term mean sea-level changes. On the other hand, several approaches have focused on the use of numerical models to resolve the local wave propagation and the sediment transport. For instance, De Winter and Ruessink (2017) used XBeach numerical model combined with three climate change mean sea-level rise projections and three time horizons (years 2050, 2085, and 2200) to assess the dune erosion. They investigated the beach-dune system effects caused by changes in wave direction on the Dutch coasts. Ranasinghe et al. (2012) developed a simplified process-based model to estimate the coastal recession and the volume of dune erosion due to mean sea-level rise and single storm events in Narrabeen Beach, Australia. They performed a simulation of the combined mean sea-level and storm wave effects and the sediment transport. Similarly, Idier et al. (2013) investigated the vulnerability of sandy coasts in the near term at four beaches in France in a short-term simulation using three different numerical models.

Overall, coastal impact assessments on sandy coasts usually compute erosion volume and/or shoreline retreat resulting from a single storm event and for a mean sea-level change in a time lapse. However, they generally neglect the effect of long-term continuous processes that may significantly modify the beach morphology. In this paper, we consider long-term changes due to mean sea-level rise in a beach environment and we infer the beach-dune vulnerability, the shoreline retreats and the dune erosion rates resulting from the wave action. The assessment is performed under both, mean and extreme wave conditions during the 21st century and under two climate change scenarios. To address our purposes, we apply a combination of two numerical models and,

additionally, the Bruun Rule is used to compare the numerical results with this widely used formulation.

Our case study is Son Bou beach, located in Menorca Island (Balearic Islands, Western Mediterranean). This beach-dune system is a well preserved environmental area that has been extensively monitored during the last years. The beach has special relevance since it constitutes a touristic point in the island and, therefore, a regional economic source.

3.2 Data

3.2.1 Site Description

Son Bou beach is a micro-tidal (tidal components lower than 10 cm, Tsimplis et al. 1995) sandy beach located in Menorca Island (Balearic Islands, Western Mediterranean Sea). The beach is 2.4 km alongshore, 20-30 m cross-shore and it presents a wide dune area behind it (70 m wide, approximately) (see Figure 3.1 for location). Its shoreline is oriented NW-SE direction and it is bounded by two rock capes. This area is part of the beach monitoring program of the Balearic Islands Coastal Observing and Forecasting System (SOCIB, Tintoré et al. 2013) since 2011. The program includes periodic topography and bathymetry surveys and in situ measurements of nearshore waves, among others coastal features. The observed average wave conditions are characterized by waves of medium to low energy with average significant wave height (H_s) of 0.52 m, peak period (T_p) of 5.84 s and mean wave direction (θ) of 200° . Higher waves associated to extreme events exceeding 95th and 99th quantiles, are represented by H_s of 1.37 and 2 m, which are associated with T_p of 7.9 and 8.5 s, respectively, and θ of 209° in both cases. As expected, higher mean H_s (0.6 m), as well as larger directional spread, are found at offshore conditions. Directional distributions of H_s at offshore location and coastal buoy are shown in the right panel of Figure 3.1.

Son Bou topo-bathymetry survey was conducted in October 2011. The bathymetry data was recorded using a single-beam echo sounder while the aerial beach was monitored using a survey-grad RTK-GPS (Real Time Kinematic Global Position System) with a spatial resolution of 5 m in both cases. Moreover, the topography of the dune area was retrieved from the Geoportal data base, a Spanish national geographic information service¹. This topo-bathymetry data was complemented with twelve beach profiles measured during three field surveys carried out in 10/May/2012, 08/May/2013, and 14/April/2014. The observed beach profiles have been used to quantify the intra-model variability depending on the imposed equilibrium profile, while the bathymetry data have been used as bottom input of the models.

¹<https://sig.mapama.gob.es/geoportal/>

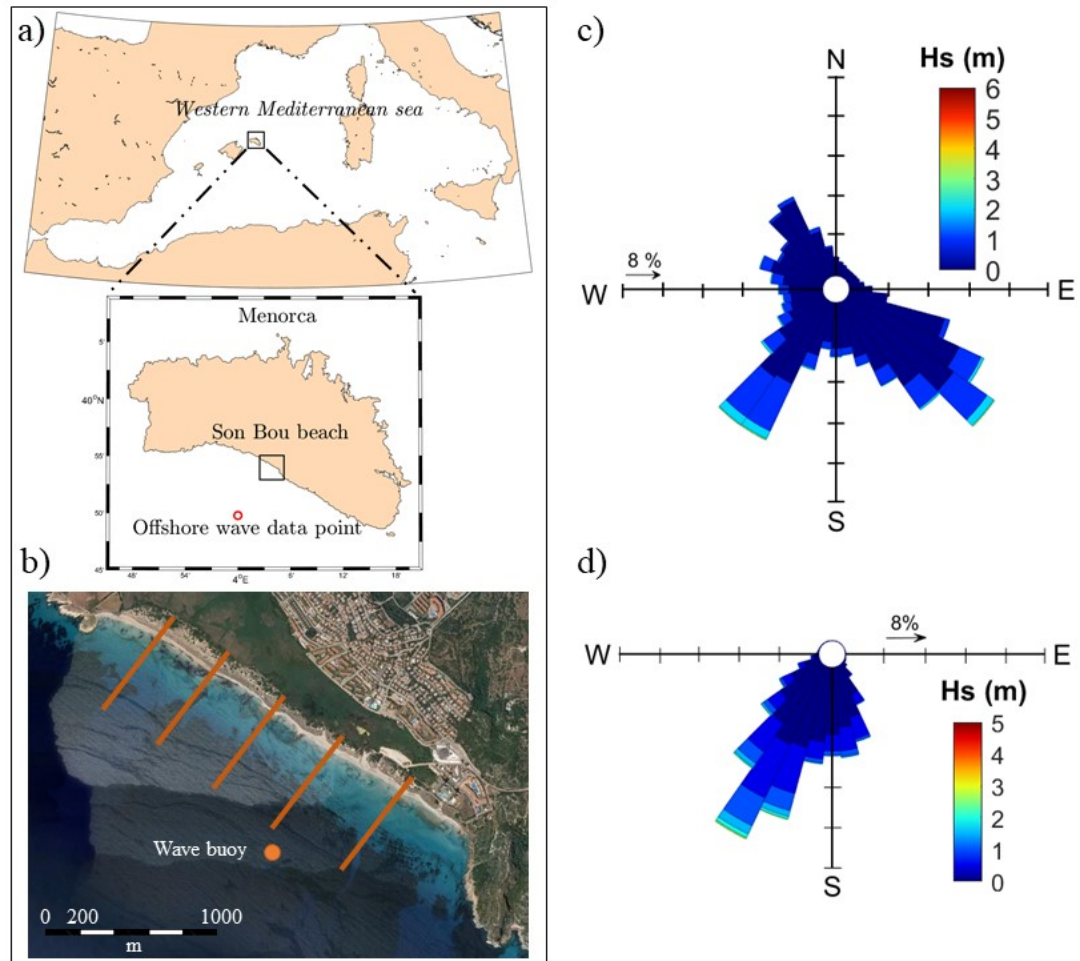


Figure 3.1 Left panel: (a) location map of Son Bou beach, Menorca Island, Western Mediterranean and the offshore wave data point. The buoy location and the location of the beach profile transects are shown in (b). Right panel; directional distributions of Hs at (c) offshore conditions and at (d) the coastal wave buoy.

3.2.2 Wave Data

Nearshore wave parameters in Son Bou (Hs, Tp, and θ) have been measured using a directional Acoustic Waves and Currents (AWAC) sensor located at 22 m depth in the southern part of the beach (see Figure 3.1 for location). The AWAC records consist of hourly wave parameters spanning the period from October 2011 to September 2016.

Wave parameters in offshore conditions are retrieved from the SIMAR database (Pilar et al. 2008), which is available upon request². The dataset consists of a 58-year (1958-2016) wave reanalysis over the Western Mediterranean basin generated with the WAM model (WAMDI Group 1988) with a spatial resolution of 12.5 km. The temporal resolution is 3-hourly from 1958 to 2011 and hourly since then. The SIMAR dataset has been evaluated against observations in several locations showing good performance

²<http://www.puertos.es/es-es/oceanografia/Paginas/portus.aspx>

when compared to in situ and remote observations (Pilar et al. 2008, Martínez-Asensio et al. 2013, 2016). For our purposes, the closest grid point to Son Bou, situated at 152 m depth, has been used as representative of the offshore wave climate in the beach (see Figure 3.1 for location).

3.2.3 Mean Sea-Level Data

Yearly mean sea-level rise projections up to 2100 for the Western Mediterranean are obtained from the last global IPCC projections (Church et al. 2013), available through the Integrated Climate Data Centre website hosted at the University of Hamburg³. We consider two climate change scenarios, namely a moderate Representative Concentration Pathway (RCP4.5) and the business-as-usual RCP8.5. These projections consist of gridded $1^\circ \times 1^\circ$ sea surface height fields that include the contributions of ocean dynamic changes, global ocean thermal expansion, inverted barometer effect, melting land ice from Greenland, Antarctica and glaciers, changes in land water storage and glacial isostatic adjustment. Following Sayol and Marcos (2018), local mean sea-level rise has been computed using the values at the closest grid point to our area of study for all contributors, except for the ocean dynamics, for which we have used a value in the nearby Atlantic Ocean. We have followed this approach because the Atmosphere-Ocean General Circulation Models (AOGCMs) used to provide global projections of climate variables have too coarse resolution as to resolve properly the water exchanges and ocean dynamics through the narrow Strait of Gibraltar. They can properly simulate the sea surface height variations in the neighbouring region, though. Since mean sea-level in the Mediterranean Sea does not differ, in the long-term, from that observed in its vicinity, we have thus used the ocean dynamical changes in the nearby Atlantic Ocean as representative of the whole basin. The outputs are provided as the ensemble average of 21 AOGCMs, from the Coupled Model Intercomparison Project Phase 5 plus the corresponding uncertainties given by the 5 and 95% confidence intervals (Slangen et al. 2014). We have neglected land subsidence as it has not been reported in this region.

3.3 Material and methods

We recall here that we aim at estimating the shoreline retreat and the potential losses of the beach-dune area and volume in Son Bou that are consequence of mean sea-level rise and the action of waves during the 21st century. To do so, we perform our analyses in two stages. First, we compute the shoreline changes under mean sea-level rise and low energy wave conditions, considering sediment transport and the morphological

³<http://icdc.cen.uni-hamburg.de/1/daten/ocean/ar5-slr.html>

shifts of the beach; we also estimate the variability around the projected mean state (see Section 3.3.2). Secondly, we use the temporal evolution of the beach profiles driven by mean sea-level rise to assess the vulnerability of the aerial beach-dune system, defined here as the risk of erosion due to the number of wave events reaching the dune toe as well as the eroding capacity of these events. To achieve this, we base our approach on a probabilistic tool (see Section 3.3.3).

3.3.1 Numerical Models

The shoreline changes in response to projected mean sea-level rise have been calculated using the Q2D-morfo numerical model, a non-linear morphodynamic model for large-scale shoreline dynamics (Falqués et al. 2007). It considers sediment transport in two horizontal dimensions and computes the wave field over the whole domain. However, the nearshore hydrodynamics is not considered because the sediment transport is computed directly from the wave field through parametrizations. The longshore transport is computed from the CERC formula, which assumes that the sediment transport mainly depends on the incoming waves (Fredsoe and Deigaard 1992, Smith et al. 2003). The cross-shore transport is proportional to the difference between the bed slope and the slope of the equilibrium profile for each water depth so that it causes a relaxation of the profile to the equilibrium profile. The relaxation time at each location depends on the wave energy dissipation. Therefore, the model ignores the surf zone processes like bar dynamics or rip currents. In summary, the model is 2DH regarding depth-averaged sediment flux and bed updating, but not fully as it does not resolve the hydrodynamics and is therefore called quasi two dimensional (Q2D) model. The Q2D-morfo is computationally effective both in time and in computing resources, allowing the modeling of long-term simulations.

Although it is not an open-source model yet, Q2D-morfo model has already been successfully applied to assess shoreline changes under different wave conditions. The first version of the model was tested by (Falqués et al. 2007) at La Barceloneta beach (Barcelona, North-Western Mediterranean) during the period from October to November 2003, when two consecutive storms occurred. The results were compared against beach bathymetry measurements allowing the model calibration. Van den Berg et al. (2011, 2012) used the model to investigate the long-term evolution of a rectilinear coast dominated by waves with high incidence angle, testing the model under high variability conditions. More recently, Arriaga et al. (2017) have validated Q2D-morfo with 3 year-data from the Zandmotor mega-nourishment (Dutch coast). They have applied the model to predict the nourishment evolution for the next 30 years using the corresponding wave data projection.

So far, this model has not been used under long-term changing sea-levels. Thus, we

assess the model capability to simulate the beach adaptation to different mean sea-level rise scenarios and predict the evolution of the shoreline. In order to account for the model uncertainty, it has been run using five equilibrium profiles that were obtained from observations at the five locations indicated in Figure 3.1. Each equilibrium profile was calculated as the average of the twelve observations for each location. In addition, the depth closure was obtained from the wave height buoy measurements. The equilibrium profiles have been forced to not have positive slope due to Q2D-morfo model requirements. Imposing five equilibrium profiles, we can quantify the intra-model variability depending on this input parameter. Furthermore, we also compare the model results with the Bruun Rule approach.

The beach erosion caused by storm waves has been simulated with the XBeach model (Roelvink et al. 2009). XBeach is an open-source numerical model developed to simulate morphodynamic processes caused by high-energy wave conditions. The model solves phase-averaged coupled equations for cross-shore and longshore hydro and morphodynamics. XBeach has become a state-of-the-art numerical model and has therefore been widely validated. Among these works, Van Dongeren et al. (2009) compared XBeach model results with field measurements at eight European sites. They concluded that the model has skills in predicting the coastal profile, although it overestimates the erosion around the mean water line and the depositions at the lower beach face. Roelvink et al. (2009) tested the morphodynamics and hydrodynamics of the model in 1D and 2DH mode and contrasted the results with several lab and field cases. The model showed reasonable results regarding to the dune toe retreat (correlation of 0.83 and bias of 0.05) and the sediment/erosion rates (mean correlation of 0.91 and bias of 0.11). However, these authors also found a dune erosion overestimation of 10-15%. McCall et al. (2010) simulated the beach morphological response after a hurricane in Santa Rosa Island (FL, United States) in 2DH mode and compared the numerical results with the field measurements. The model resulted in a good capability to solve processes as over-swash, fore-dune erosion and deposition caused by a storm event. De Winter et al. (2015) calibrated the hydrodynamics and dune erosion modules comparing the model results with field observations at Egmond aan Zee (Netherlands) and concluded that XBeach model simulates the magnitude of erosion volumes satisfactorily (correlation coefficient up to 0.55) but overestimates the erosion volumes in regions with dune scarps. Nowadays, XBeach model is extensively applied to assess beach impacts and dune erosion (see for instance, Harley et al. 2011, Vousdoukas et al. 2012, Bugajny et al. 2013, Harley et al. 2016, Karunarathna et al. 2018).

Our approach to investigate the beach evolution combines both models' capabilities: we use of the Q2D-morfo model to simulate the beach changes due to mean sea-level rise and then apply the XBeach model to estimate the response to storm conditions

under the modified beach. Both models are used in 2D mode in order to account the cross-shore and long-shore sediment transport.

Offshore waves have been propagated toward the coast using the state-of-the-art SWAN model (Booij et al. 1999), a third-generation wave model that solves the spectral action balance equation for the propagation of wave spectra⁴. Despite SWAN model is not computational demanding, the simulation of the whole offshore wave time series (58 years of three sea state parameters) is unfeasible. To avoid this problem, the nearshore wave data is obtained by applying a combination of numerical modeling and statistical downscaling approaches as it is explained in the following. Before using SWAN, a Maximum Dissimilarity Algorithm (MDA) is applied to analyze trivariate (H_s , T_p , θ) hourly time series of offshore wave parameters (Camus, Mendez, Medina and Cofiño 2011). The MDA algorithm allows selecting a representative subset of the offshore wave climate diversity suitable to be implemented in a nearshore propagation methodology. The algorithm chooses the representative sea states (defined by its H_s , T_p , and θ) of the wave climate, basing on the maximum dissimilarity with respect to the whole wave dataset. This dissimilarity between one sea state and the others, is calculated from the Euclidean distance. Based on previous studies (Camus, Mendez, Medina and Cofiño 2011), 200 sea states of the offshore time series have been selected as representative of the wave climate. These sea states are the ones that have been propagated up to the coast using SWAN model. From the resulting modified wave parameters, it is possible to reconstruct the entire nearshore wave time series through an interpolation technique based in radial basis functions (RBF) (Camus, Mendez and Medina 2011). To do this reconstruction, the coefficients obtained from the RBF are applied to the complete offshore wave series transferring them from deep to shallow water.

3.3.2 Estimation of the Shoreline Retreat

Sandy beaches are adaptable to changes in short-term hydrodynamic conditions varying around a mean morphological state (Carter 2013, Muñoz-Perez and Medina 2010). Thus, persistent beach changes will be due to changes in long-term forces. Here, we assume that long-term changes in the beach morphology, including the position of the shoreline, are caused by mean sea-level rise. Therefore, we neglect the short-term changes such as those resulting from storm events and cumulative storm effects. In other words, we consider that the beach always recovers its equilibrium profile after every storm, which we anticipate will likely underestimate the shoreline retreat.

We use the Q2D-morfo model to solve the sediment transport and the morphological shifts of the beach caused by sea-level changes on a yearly basis and we impose low energy wave conditions. In order to cover the entire uncertainty range of mean sea-level

⁴<http://swanmodel.sourceforge.net/>

rise, we have considered four possible pathways, two of them corresponding to the ensemble average of RCP4.5 and RCP8.5. The other two correspond to the 5% confidence interval of the multi-model ensemble spread under the scenario RCP4.5 and to the 95% confident interval of the multi-model ensemble spread for the RCP8.5 scenarios. In this way, we account for the maximum (RCP8.5 95%) and minimum (RCP4.5 5%) limits of the model ensemble, taking into account the two scenarios jointly (Figure 3.2). In addition, constant low energy wave parameters, obtained from the more frequent low energy AWAC measurements, are used to force the model. Wave conditions are needed to run the model, but they are the same over the whole simulated period so that changes in shoreline retreat are not conditioned by wave effects. Thus, we obtain the yearly evolution of the shoreline position for each of the mean sea-level rise scenarios.

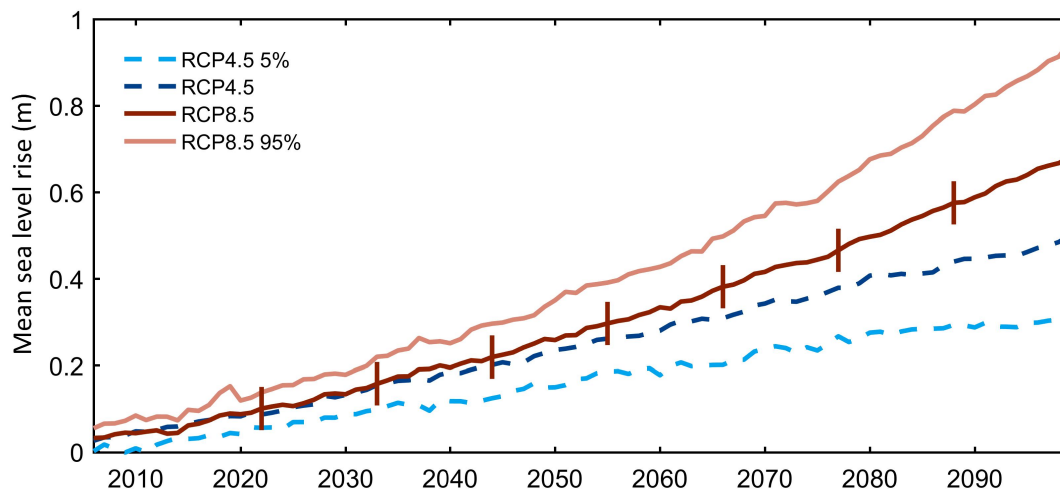


Figure 3.2 Projected sea level rise scenarios used in the present study. 5–95% refer to the uncertainties derived from the multi-model ensemble spread of each of the two scenarios. The vertical lines indicate the time lapses when the erosion volume is estimated (see Section 3.3.3).

In addition, we performed the same assessment using the Bruun Rule. The Bruun Rule predicts a landward and upward displacement of the cross-shore sea-bed profile in response to a mean sea-level rise as follows:

$$R = L * S / (B + h) \quad (3.1)$$

where h is the depth closure, B is the elevation of dune or berm above mean sea-level, S is the mean sea-level change and L is the distance from the berm crest to the h location. This formulation is based on the assumption of a balance system between the sediment budget of the nearshore and bottom profile (Bruun 1962). In this way, the shoreline retreat can be easily quantified from the landward displacement of the actual shoreline location but assuming the profile shape remains unchanged.

3.3.3 Beach and Dune Vulnerability and Erosion

We provide a measure of the dune vulnerability as the number of annual wave run-up ($R_{2\%}$, the vertical height exceeded by 2% of maxima water-level) events reaching the dune toe for each of the four mean sea-level rise scenarios. Based on the field measurements, the dune toe is determined as the topographic line of 1 m height above the current mean sea-level. We calculate the $R_{2\%}$ with the empirical formulation developed by Stockdon et al. (2006):

$$R_{2\%} = 1.1(0.35\beta_f + 0.5(0.563\beta_f^2 + 0.004)^{1/2})(H_0L_0)^{1/2} \quad (3.2)$$

where β_f is the foreshore beach slope, calculated from the topo-bathymetry measurements, and H_0 and L_0 are the wave height and wave length in deep-water conditions, respectively. Although the beach shoreline is shifted landward due to mean sea-level rise (as described in Section 3.3.2), the Bruun Rule assumes that the equilibrium state remains the same and, therefore, the foreshore beach slope (β_f) does not change over time.

In order to increase the number of offshore wave time series, we use SIMAR data to simulate, via Monte-Carlo, a set of 10000 time series of Hs and duration of extreme events spanning 100 years each that are statistically consistent with present-day wave climate, as described below. We expect mean sea-level rise to be the major driver controlling the collision of waves with the dune and therefore we will not consider changes in the wave fields during the 21st century. This assumption is supported by earlier analyses showing only slight changes of waves in the western Mediterranean area under climate change scenarios (Enrquez et al. 2017, Mentaschi et al. 2017, Sayol and Marcos 2018).

The steps to build this synthetic dataset are the following: first, we select the independent wave extreme events whose Hs exceeds the 90th percentile of Hs of the entire series from SIMAR, since we are interested in the largest waves that may reach the dune. We consider that these 10% highest waves are independent if they are separated by at least 72 h. We also compute the duration for each of them. Second, we fit univariate marginal probability distribution functions to the empirical Hs and to the duration distributions; we select the best fit among the Generalized Pareto Distribution (GPD), Weibull, Gamma, Log-normal and Exponential distributions, based on their minimum log-likelihood. The results indicate that the most suitable distribution is the GPD for both Hs and duration of the events. Third, we search the relationship between these marginal distributions of Hs and duration using Copula functions to fit their joint probability distribution. We fit the bivariate distribution based on the Clayton, Frank, Gumbel and Gaussian Copulas and select the one displaying smaller root mean square differences with the original values, which in our case is the Gaussian Copula. Fourth,

we compute the number of events each year from our initial time series and fit a Poisson distribution, resulting in λ around 24 (λ being the parameter of the distribution and corresponding to the average number of events per year), matching with previous results that suggest a λ value between 15 and 25 (Mazas and Hamm 2017). Finally, we use the obtained Poisson distribution to simulate the yearly distribution of wave events in 10000 time series of 100 years each; we then simulate H_s and duration of each of these events from the bivariate distribution obtained with the Copula function. Wave T_p is calculated for each simulated event using a linear relationship between H_s and T_p in the original time series. The resulting set of H_s , T_p and duration represents 10000 different realizations, each of them of 100-year long, of the highest 10% of waves, consistent with the present-day wave climate in the study region.

The synthetic wave time series have been superimposed onto the beach profiles modified by mean sea-level rise resulting from Q2D-morfo model and Bruun Rule simulations. Then, they are used to assess the probability of the wave run-up (computed as $R_{2\%}$ as indicated above, Equation 3.2) to reach the dune toe and induce dune erosion during the 21st century.

In addition, the erosion caused by the wave events can be calculated by the XBeach model. However, computational constraints limit our ability to provide estimates for each event in each of the 10000 synthetic time series. Instead, we have computed the H_s and duration corresponding to the 10-year and 100-year return periods from the bivariate distribution described above. The corresponding waves are propagated nearshore using the SWAN model and then, they are used to force the XBeach model at the coast for the selected years as representative of each decade (vertical lines in Figure 3.2). This has been carried out for a single mean sea-level rise scenario, namely RCP8.5. In order to reduce the number of simulations, the eroded volume was computed for 7 years equally spaced (vertical lines in Figure 3.2) and for moderate (10-year return period) and high (100-year return period) extreme waves. This makes 35 simulations for each return period (resulting from 7 time steps 5 input equilibrium profiles) with the XBeach model, which is computationally feasible.

3.4 Results

3.4.1 Shoreline Retreat Under Mean Sea-Level Rise

Figure 3.3 represents the yearly shoreline retreat obtained from the outputs of the Q2D-morfo model and the Bruun Rule. For the Q2D-morfo, a 20-year spin up has been applied under low energy wave conditions and no mean sea-level rise. The spin up has been needed to ensure that waves do not change the beach shoreline configuration so that we can quantify the shoreline retreat caused by mean sea-level rise only. Figure

3.3 represents the yearly alongshore average position of the shoreline for the period ranged from 2017 to 2099 and for the two RCP4.5 and RCP8.5 scenarios (in blue and red colours, respectively). The intramodel variability of the Q2D-morfo (shadowed areas around dashed lines in Figure 3.3) is calculated as the spread in the model results when the set of 5 equilibrium profiles are used. For the sake of consistency, the uncertainty in the Bruun Rule arising from the set of profile slopes is also plotted as the shadowed area around solid lines. The comparison between the two approaches shows that the Bruun Rule significantly overestimates the loss of aerial beach resulting from mean sea-level rise, in agreement with earlier assessments (Esteves et al. 2009, Ranasinghe et al. 2012, Deng et al. 2015). In our case, we find that, by 2100, the shoreline retreat obtained with Q2D-morfo is 12 m (9 m) on average while the Bruun Rule results in up to 28 m (19 m), under the RCP8.5 (RCP4.5) scenario. This overestimation is not constant and increases over time, since the Bruun Rule responds faster to mean sea-level rise. Another notable feature is that Q2D-morfo is strongly sensitive to the assumed equilibrium profile. This is reflected in the intramodel uncertainties overlapping for the two scenarios (Figure 3.3).

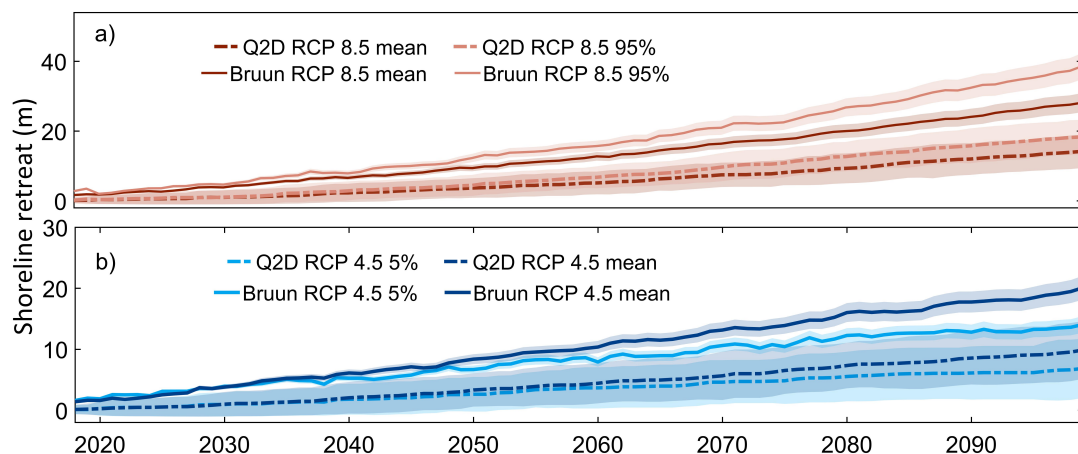


Figure 3.3 *Shoreline retreat comparison using Q2D-morfo model (dashed lines) and Bruun Rule (solid lines) under (a) RCP8.5 (red colour) and (b) RCP4.5 (blue colour) scenarios. The light colours represent the uncertainties of the two scenarios and the shadow areas represent the intra-model uncertainties.*

Whatever the model used, the shoreline retreat due to mean sea-level rise is smaller than the beach width (30 m approximately); this indicates that the dune area would not be affected if only projected mean sea-level rise and low energy wave conditions are taken into account. This picture may change under more energetic waves, however. In order to quantify the variability of the shoreline induced by storm waves around the time-variable mean response to mean sea-level rise, the shoreline position after the annual largest storm has been obtained from the XBeach model. Due to computational constraints, only three 100-year wave time series (generated as described in Section

3.3.3) have been evaluated for two scenarios. Figure 3.4 shows the shoreline retreat, averaged along-shore, with respect to the annual mean shoreline position from 2017 to 2099, under RCP4.5 and RCP8.5. Along-shore variations of the shoreline position are represented as shadowed areas. These curves thus represent the variability of the shoreline in addition to the retreat caused by mean sea-level rise. Changes around the mean shoreline position resulting from mean sea-level rise are on average 12-14 m during the 2020s, and then progressively reduce until an average value of 5-8 m during the 2090s. We speculate that this decreasing trend is the result of the larger slope on the fore-dune zone with respect to the beach-face slope. As it will be shown later, it does not imply that the eroding capacity of storm waves is reducing over time.

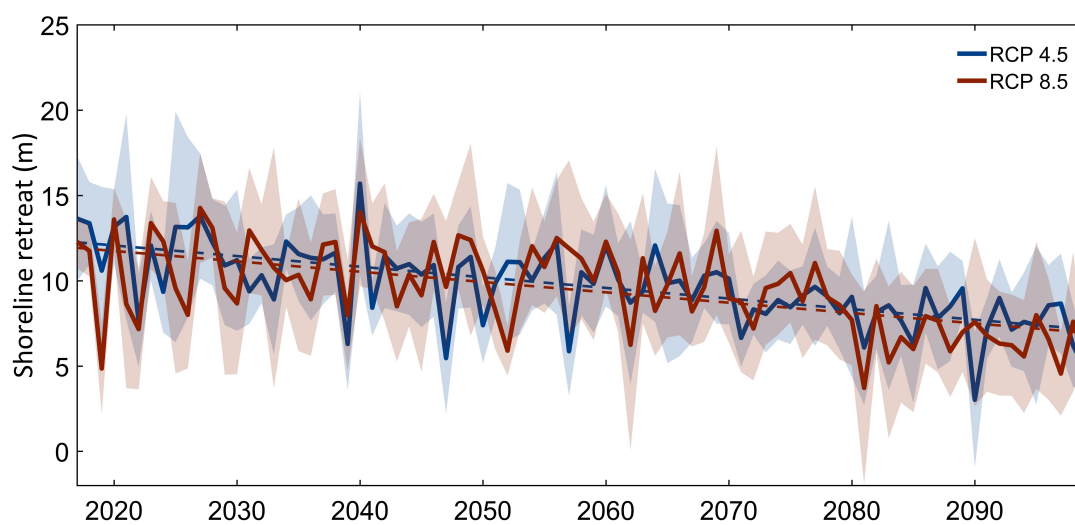


Figure 3.4 *Shoreline retreats derived from maximum annual storms and sea level rise under two scenarios with respect to the annual mean position. Red and blue solid lines represent shoreline retreats on average, under RCP8.5 and RCP4.5 mean sea-level rise scenarios, respectively. Shadow areas represent the variability of shoreline retreat along the beach and the dashed lines are the trends.*

3.4.2 Beach and Dune Vulnerability and Erosion

The vulnerability of the beach-dune system is represented as the number of events for which the associated wave run-up reaches the dune toe for every year and for each of the 10000 synthetic 100-year time series. The beach configurations for every year are those estimated by Q2D-morfo and the Bruun Rule under mean sea-level rise conditions from Section 3.3.2. The results for the RCP8.5 scenario are shown in Figure 3.5, as the annual evolution of the average number of events reaching the dune toe (bold lines). The shaded areas indicate the standard deviation of the number of run-up events reaching to the dune toe as a result of 10000 wave time series simulations performed.

When the shoreline evolution given by the Bruun Rule is used (Figure 3.5, green

line), the number of events that reach the dune toe increases steadily from present until 2068, ranging from 3 to 5 annual events in the near term to more than 20. Since then, all the events considered (that represent the top 10% of highest waves) reach the dune toe. We recall here that the annual average number of events that exceed the 90th percentile is 24; thus, the horizontal lines in Figure 3.5 indicate that this threshold has been reached and that all the modelled wave events arrive, at least, up to the dune toe. The evolution of the number of events the run-up reaches the dune toe is very different when the results of the Q2D-morfo model are used (Figure 3.5, red line). It shows a stable number ranging from one to two yearly events until approximately the year 2050. Since then to 2066, the average number rapidly increases until it reaches the maximum around the same year as with the Bruun Rule. The origin of these differences in the initial frequency between the two methods is twofold: first, they are consequence of the faster shoreline retreat obtained from Bruun Rule (see Figure 3.3). Second and most important, the Q2D-morfo model progressively reduces the berm located between the coastline and the dune, simulating its continuous erosion. Until this berm does not disappear in response to mean sea-level rise (around 2050), the wave run-up is unable to reach the dune because of its protective effect. When this happens, the potential for beach and dune erosion increases rapidly.

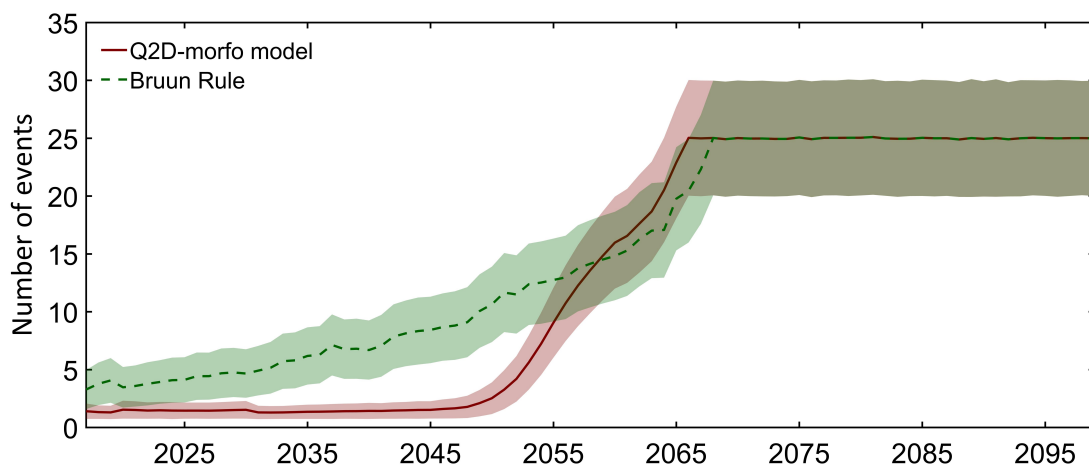


Figure 3.5 Number of events reaching the dune toe under RCP8.5 mean sea-level rise using the beach retreat obtained by Q2D-morfo model (solid red line) and Bruun Rule (dashed green line) results. Shaded areas represent the standard deviation derived from the of 10,000 wave time series simulations performed. Horizontal lines after late 2060s indicate that all the events considered (that represent the top 10% of highest waves) reach the dune toe.

The average number of wave run-up events that can reach the dune measures the potential of erosion due to wave forcing. So, in the next step, in order to quantify this erosion, we calculate the volume that is actually eroded under the action of moderate (10-year return level) and large (100-year return level) storms. We anticipate that the

impact of these events will strongly depend on the mean sea-level (and by extension on the shoreline position) at their arrival; thus, we explore the induced erosion during different decades, ranging from 2020s until 2090. The years for which the erosion volume has been calculated are those indicated by vertical lines in Figure 3.2.

The wave parameters for 10 and 100-year return periods (RP) are 2.9 m of H_s , 8.26 s of T_p and 91 h of duration and 3.96 m, 9.5 s, and 120.5 h, respectively. The total volume eroded, per linear m, is plotted in Figure 3.6 for the two RP and for each time horizon. The shadowed areas correspond to the standard deviation of the erosion rates obtained with the Q2D-model outputs fed with the five equilibrium profiles (i.e., intra-model uncertainty), while the bold lines indicate the averaged erosion rates. The results show that the volume of dune eroded generally increases as mean sea-level rises, even for small values of mean sea-level rise. Note that we are propagating always the same exact storm, whose eroding potential is, in most cases, larger with higher sea-levels. This is not surprising, as the dunes become closer to the shoreline with higher sea-levels. The increase is obtained for both the moderate and the large storms, but with different evolutions (note the different vertical scales in the figure). The eroded volume ranges from 34.1 m^3/m in 2022 to 42.8 m^3/m in 2088 using the 10-year RP storm (an increase of 25.5%), while it ranges from 61.2 m^3/m in 2022 to 77.7 m^3/m with the 100-year RP storm (increasing 27%).

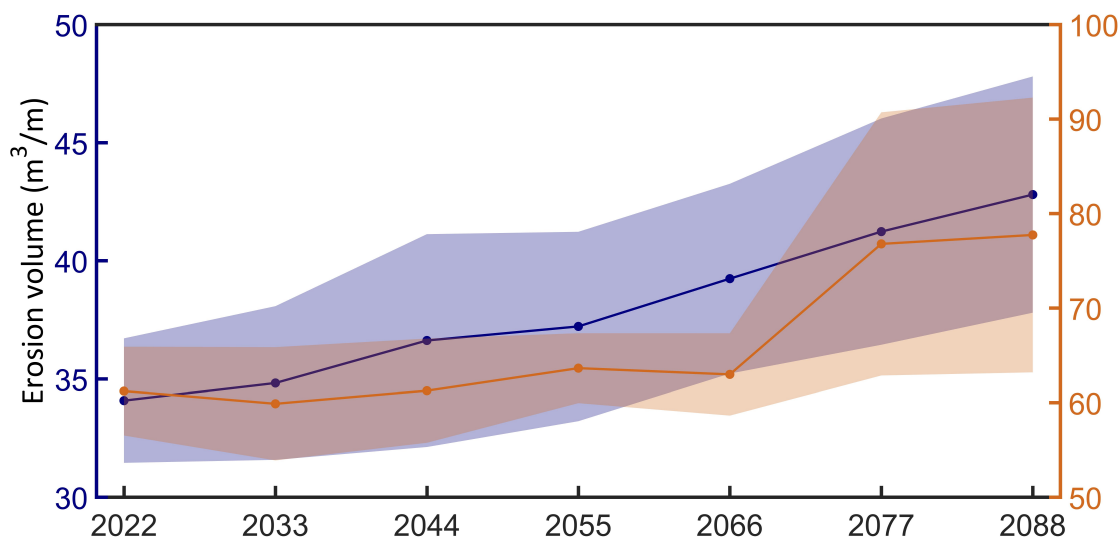


Figure 3.6 Dune-beach erosion volume taking into account the sea-level rise and the 10-year RP (dark blue line, left axis) and 100-year RP (orange line, right axis) under RCP8.5 scenario. The shadowed areas indicate the standard deviation based on the equilibrium profile used in the Q2D-morfo model simulations.

Figure 3.6 shows that the erosion volume increases significantly in the 2070s under 100-year RP storm. This finding highlights the relevance of the timing when the strongest storm takes place and the importance of the combined sea-level and wave effects; i.e., a storm hitting the coast without a protective berm has a stronger eroding

potential. Figure 3.6 also reveals the same erosion in 2055 and 2066 under this 100-year RP storm. This is indicating that, under similar mean sea-level conditions and similar beach configurations (with or without a berm), the effect of the largest storms is the most decisive factor in the erosion. The erosion volume of 10 years RP storms increases gradually from 2022 to 2088, which indicates that low-to-medium wave energy conditions have limited consequences for the dune area, under the assumption of neglecting the cumulative effect of several storms, and that the effect of mean sea-level has a stronger weight in the erosion for moderate storms.

3.5 Conclusion

We have evaluated the response of an open sandy beach in a microtidal environment to the impacts of mean sea-level rise and the action of wind-waves, under prescribed climate change scenarios for the 21st century. In agreement with earlier studies (e.g., Ranasinghe et al. 2012), our results indicate that the widely applied Bruun Rule overestimates the shoreline retreat in this type of coasts; therefore, impacts assessments of, for example, flood risks or vulnerability changes, must be considered with caution if they are based on this approach. On the contrary, using a numerical morphodynamic model, the shoreline retreat is slowed down due to the simulation of the berm erosion. This result highlights the relevance of the protection role of the beach and its berm, suggesting that there are tipping points after which the dune erosion may become irreversible.

Our findings indicate that, when the morphodynamic response of the beach to rising sea-levels is considered, its configuration, including the shoreline position, does not change steadily even if the forcing does. The consequence is that the impacts of climate change on the beach-dune system in Son Bou may be overlooked, especially if the shoreline position is used as a proxy, as it is often the case. In addition, our results suggest that the monitoring of the aerial beach, and whether it includes a protective berm or not, could be a better alternative measurement of the response of the system to the effects of climate change.

This study concludes that mean sea-level rise is the major driver of the projected changes in the shoreline position in Son Bou beach, inducing an average retreat between 12 and 23 m (2-15 m) under RCP8.5 (RCP4.5) by 2100. These numbers increase up to 25-42 m (13-22 m) under RCP8.5 (RCP4.5) when the Bruun Rule is used instead of the Q2D-morfo model. This average value is altered under storm conditions, which may temporarily displace the shoreline around ± 10 m in the near future and half of that value by the end of the century. In both cases, these values are obtained under the assumption of no cumulative storm effects. As sea-level increases so does the number of waves that reach the dune toe and therefore the potential dune erosion. The estimated erosion volume for the 1 in a 100 years event is ~ 60 m³/m until the 2060s, when the

berm has not yet disappeared. After that period, the potential erosion increases by 27% only within a decade.

It is important to note that this study relies on some assumptions. First, we have neglected changes in wave direction that may be relevant for the beach planform evolution even under fair weather conditions. Second, we have considered that the observed equilibrium beach profile in present-day conditions remains constant under future mean sea-level rise. This is a reasonable assumption since the main driver is mean sea-level rise and the wave climate is not expected to change significantly. Finally, we have neglected the cumulative storm effects on the beach configuration; in other words, we have considered that the beach is able to recover its equilibrium state after every storm episode. This assumption is necessary due to the inability of present-day numerical models to simulate both the storm effects and the beach recovery in a realistic way for long-term periods. But this is also a strong limitation since previous work has demonstrated that the impact of storm groups may significantly exceed from those caused by a single event (Ferreira 2005). Therefore, our estimates of beach-dune vulnerability and potential erosion should be taken as a lower bound.

Data availability statement

Publicly available datasets were analysed in this study. This data can be found here: <http://www.socib.eu/>.

Acknowledgments

AE acknowledges an FPI grant associated with the CLIMPACT project (CGL2014-54246-C2-1-R). We thank Puertos del Estado for providing deep water wave data from the SIMAR database. Topo-bathymetries and wave observations are part of the beach monitoring facility of SOCIB.

Chapter 4

Measuring the economic impact of climate-induced environmental changes on sun-and-beach tourism.

This chapter is under review as:

Enríquez, A. R. and Bujosa, A. (2019). Measuring the economic impact of climate-induced environmental changes on sun-and-beach tourism. *Climatic Change*.

Abstract

Despite the economic importance of the tourism sector and its close relationship to the environment and climate, substantial gaps remain in the investigation of climate change (CC) impacts on tourism. Unlike the increasing body of literature focusing on the alteration of the climatic suitability of tourism destinations, this paper focuses on the impacts of CC on the provision of natural resources affecting the attractiveness of destinations. More specifically, the paper provides an economic measurement of climate-induced environmental changes in the coast of Mallorca (Spain), one of the Mediterranean's leading sun-and-beach destinations. A choice experiment is used to elicit the willingness-to-pay (WTP) of tourists for the introduction of policies aimed at reducing three climate-induced environmental changes. Estimated results show the positive WTP of tourists to reduce CC impacts and find evidence of preference heterogeneity among individuals with different socioeconomic and travel characteristics.

Keywords: choice experiment, sun-and-beach tourism, climate-induced environmental changes, Mallorca.

4.1 Introduction

Tourism is one of the world's largest and fastest-growing industries (Amelung and Nicholls 2014). Indeed, travel and tourism accounted for 10.40% of global gross domestic product (GDP) and its direct contribution to GDP is expected to grow at an average of 3.8% per year over the next ten years according to the World Travel and Tourism Council (WTTC 2018). At the same time, with its close relationship to the

environment and climate, tourism is considered a highly climate-sensitive economic sector (Amelung and Viner 2006, Scott et al. 2009, Goh 2012). In fact, climate variability is expected to result in important impacts on tourism destinations and operators varying substantially by geographic region (Cabrini et al. 2009).

Regardless of the economic importance of the sector and its relative vulnerability to climate change (CC), the investigation of climate-induced impacts on tourism has not received sufficient attention and substantial knowledge gaps remain. In different reviews of studies addressing CC effects on tourism, Gössling et al. (2012), Becken (2013), Rosselló-Nadal (2014) show that the focus of current publications has been on the direct consequences of a changed climate, that is, the alteration of the climatic suitability of tourism destinations. In particular, the literature on climate as a resource for tourism builds on studies which seeks to identify comfortable conditions for tourists by means of different climate indices (e.g. Scott et al. 2004, Amelung and Viner 2006, Amelung et al. 2007, Moreno and Amelung 2009) or to develop demand models to estimate potential shifts in tourism flows or visitation patterns as a result of CC (e.g. Hamilton et al. 2005, Rosselló-Nadal et al. 2011, Goh 2012, Tol and Walsh 2012, Bujosa and Rosselló 2013).

However, beyond the alteration of climatic conditions (in terms of temperature, precipitation, etc.), CC will also affect the provision of natural resources that determine, to a great extent, the attractiveness of any tourism destination (Gössling and Hall 2006, Gössling et al. 2012). Unfortunately, the study of climate-induced environmental changes has received relatively less attention and, in addition, the body of this literature has focused mainly on the effects of CC on winter tourism (Becken 2013).

The literature on the physical changes caused by CC on coastal and marine ecosystems and their potential impact on tourism is still in its initial stage (Rosselló-Nadal 2014), despite the hundreds of millions of people visiting these areas (Moreno and Amelung 2009). In this context, while a number of studies have investigated the effects of environmental changes in coral reefs, beaches and water bodies on key tourism variables such as awareness (Ngazy et al. 2004, Buzinde, Manuel-Navarrete, Kerstetter and Redclift 2010), satisfaction (Roman et al. 2007, Zeppel 2012) or destination choice (Uyarra et al. 2005), there is a lack of research in assessing the long-term effect of these changes (Gössling et al. 2012) as well as in quantifying their economic impacts (Tol 2018).

In light of this gap, the purpose of the study presented here is to provide an economic measurement of climate-induced environmental changes in the coast of Mallorca (Spain), one of the Mediterranean's leading sun-and-beach destinations. The welfare impact on the wellbeing of tourists is measured in terms of their willingness-to-pay (WTP) for the introduction of policies aimed at reducing three climate-induced envi-

ronmental changes using a choice experiment (CE). The CE is a stated preference non-market valuation methodology where respondents are presented with different scenarios describing specific changes in the levels of the good under valuation and are asked to choose the scenario providing the highest level of wellbeing (see, for instance, Hanley et al. 1998, Birol and Koundouri 2008, Carson and Louviere 2011).

In last years, CE have become very popular to assess the economic impact of CC on many ecosystems such as forests and agricultural lands (Shoyama et al. 2013), river basins (Andreopoulos et al. 2015, Chaikaew et al. 2017), wetlands (Torres et al. 2017, Faccioli et al. 2019) as well as coastal and marine areas (Remoundou et al. 2015, Rodrigues et al. 2016). However, the growing literature on this field doesn't show a special interest for tourism and, in fact, the limited number of CE studies assessing the effects of CC on tourists have only considered the alteration of the climatic suitability of coastal destinations (Bujosa et al. 2018) and the impact of environmental changes on winter sports (Unbehauen et al. 2008, Landauer et al. 2012), mountain (Pröbstl-Haider et al. 2015) and glacier tourism (Vander Naald 2019). Consequently, this paper also aims to contribute to this limited literature by extending the use of CE to assess the WTP of sun-and-beach tourists for climate-induced environmental changes.

The remainder of this paper is organized as follows. The next section describes the most relevant characteristics of the application and the CE survey instrument. Section 4.3 introduces the mixed logit model used to analyze CE responses and to derive welfare estimates accounting for the heterogeneous preferences of tourists. The results of the model and the economic values estimated for the climate-induced environmental changes are presented in Section 4.4. Finally, Section 4.5 concludes the paper.

4.2 Application and survey design

4.2.1 Climate-induced environmental changes in the Mediterranean coast

The Mediterranean region is considered, at the same time, the world's leading tourism destination –attracting around one fifth of international tourism arrivals worldwide (UNWTO 2018)– and one of the most vulnerable areas to CC because of its morphologic and geographical characteristics (Lionello et al. 2006, Giorgi and Lionello 2008). In this context, it is not surprising that the Mediterranean has become one of the most studied tourism regions from the perspective of CC impacts (Scott and Hall 2012), not only due to the large number of publication analyzing the expected changes in climate variables (e.g. Giorgi 2006, Mariotti et al. 2008) and climate extremes (Baettig et al. 2007, Fowler et al. 2007), but also for the increasing number of studies focusing on different ecosystem changes caused by CC such as sea-level rise, ocean warming and acidification (e.g. Vargas-Yáñez and Salat 2007, Marcos and Tsimplis 2008, Lionello

2012, Ruti et al. 2016).

The application presented here focuses on three climate-induced environmental changes with a high potential to alter the attractiveness of sun-and-sand destinations in the Mediterranean. The first one is beach retreat caused by sea-level rise because beach access and wider beaches are among the most important determinants of beach recreation (Whitehead et al. 2000, 2008, Landry et al. 2003, Parsons et al. 2013, Remoundou et al. 2015). The second environmental change considered in the application is the loss of *Posidonia oceanica* meadows associated to seawater warming (Marbà and Duarte 2010, Jordà et al. 2012, Marbà et al. 2014). This seagrass is endemic to the Mediterranean Sea and provides significant ecosystem services by increasing, among others, water quality and transparency which are key attributes for beach users (Barbier et al. 2011, Hendriks et al. 2014, Marbà et al. 2014). Finally, the third environmental change under evaluation is the increase in jellyfish population associated to seawater warming (Attrill et al. 2007, Brotz et al. 2012). There is no doubt that the outbreaks of this unpleasant and harmful species will affect negatively tourists in coastal destinations, not only because they sting swimmers, but also because their proliferation will force local authorities to close the beach for recreational use (Purcell et al. 2007, Gössling et al. 2012, Purcell 2012, Remoundou et al. 2015).

4.2.2 The choice experiment

In order to evaluate the economic value of the above-mentioned climate-induced environmental changes, three attributes have been defined in the CE application. The selected attributes represent changes in the recreational potential of coastal ecosystems and, hence, are expected to be relevant not only to tourists but also to policy makers as they can alter the attractiveness of the destination. The attributes and their levels have been defined in a comprehensible way to respondents (i.e. tourists). In addition, the projections provided by different modelling studies (see description below) have been considered in the definition of the expected level of the attributes in a no-action scenario. The remaining levels of the attributes presented in Table 4.1 describe plausible situations under different scenarios of adaptation to CC impacts.

The first attribute (beach retreat) represents the loss of beach area caused by sea-level rise measured as the number of meters of landward shoreline retreat compared to the current state. According to the wave simulations developed by (Enríquez et al. 2017),¹ a shoreline retreat between 11.7 and 24.2 meters is expected in Mallorca by 2100 depending on the CC scenario under evaluation (RCP4.5 and RCP8.5). The same authors have estimated that the loss of beach by half century will be of 8.7 meters under

¹Enríquez et al. (2017) use SWAN and SWASH numerical models (Booij et al. 1999, Zijlema et al. 2011) to project the shoreline retreat in Mallorca.

the above-mentioned CC scenarios. The remaining levels of the attribute (0, 2.9 and 5.8 meters), describe situations where the administration acts to reduce, completely or partially, the expected beach retreat adopting a variety of measures.

The loss of seagrass is the second attribute in the CE described as the area of *Posidonia oceanica* meadows lost due to water temperature raise. Following the laboratory experiment of Jordà et al. (2012), CC-induced seawater warming and local anthropogenic pressures are increasing the seagrass mortality and predict that, by the middle of the century, the present density of *Posidonia oceanica* meadows will be reduced by 90%. The remaining levels of the attribute present a scenario where seagrass recovery techniques are implemented and the current area of the seagrass is reduced by 36%, 57% or 72%.

The third attribute is the number of days of beach closure due to jellyfish outbreaks. When faced with a large bloom, local authorities can take the decision to close the beach to avoid dangerous situations caused by jellyfish. Although the adoption of this measure avoids painful stings to beach users, it also causes the discomfort and annoying of tourists as they must move to a different beach to undertake their activities (Richardson et al. 2009, Fenner et al. 2010). In the light of the number of actual blooms in the area of study (see, for instance, the CIESM JellyWatch Program²) and the expected increase in jellyfish population in the Mediterranean (Purcell et al. 2007; Kogovšek et al. 2010; Brotz and Pauly 2012³), the no-action scenario assumes that the beach will be closed fifteen days per month by 2050. The number of days of beach closure can be reduced to 2, 5 or 10 per month in the high season if measures are adopted to reduce the effects on tourism of jellyfish outbreaks.

Finally, a monetary attribute has been included in the CE application to allow for the calculation of the WTP for the three previous attributes. More specifically, the cost attribute is defined as a tax that tourists would have to pay, per day of stay, to contribute to a public fund aimed to financing policies intended to reduce the above-mentioned climate-induced environmental changes. It was emphasized that residents would also contribute to sustain the fund through the payment of local taxes and that all funds raised would only be used to implement the presented measures. The levels of the attribute ranged from 0 to 6 euros, based on previous CE studies in the same area (see, for instance, Bujosa et al. 2018), the comments from focus groups and the results of a pilot study.

The four attributes and their levels were combined to create the choice sets included

²The CIESM JellyWatch Program is devoted to monitor jellyfish blooms along Mediterranean coasts and in the open sea and provides an interactive map of the blooms that can be consulted at <http://www.ciesm.org/gis/JW/build/JellyBlooms.php> (accessed on July 23th 2018).

³Changes in the frequency of jellyfish blooms have been studied by using temporal series of observed jellyfish densities, showing positive trends of blooms in native and invasive species in the Mediterranean. For more details see Purcell et al. (2007), Kogovšek et al. (2010), Brotz and Pauly (2012).

Attribute	Description	Levels
Beach retreat	Beach shoreline retreat due to sea level rise (meters)	0, 2.9, 5.8, 8.7 (BAU)
Loss of seagrass	Loss of seagrass area due to water temperature rise (%)	36, 54, 72, 90 (BAU)
Beach closure	Days of beach closure due to jellyfish outbreaks (days a month)	2, 5, 10, 15 (BAU)
Cost	Daily tax per person aimed to reduce the climate change impacts (euros)	0 (BAU), 1, 2, 3, 4, 5, 6

Table 4.1 *Attributes and their levels*

in the survey. These choice sets have been generated in ©Ngene software (version 1.1.1) using a Bayesian D-efficient design (Scarpa and Rose 2008) for a mixed logit model. Prior information on the parameter values was derived from a preliminary model estimated on data available from a pilot study. The experimental design has resulted in 24 profile combinations which were blocked into four different versions of six choice sets. Each choice set consisted of two improving alternatives and a business as usual (BAU) option. The improving alternatives presented a scenario where action was taken to reduce the climate-induced environmental changes based on a combination of attribute levels from Table 4.1. In contrast, the BAU described a no-cost alternative presenting the expected level of climate-induced environmental changes by the middle of the century if no action is taken. Figure 4.1 gives an example of a choice card.

4.2.3 Survey and sample

The questionnaire was organised in three parts. Beyond asking about the main characteristics of the trip and accommodation, the first part enquired about the importance of different environmental problems that could affect the tourism experience in the destination. The second part introduced a detailed description of the expected CC impacts on the destination, focusing on the likely environmental changes described in Section 4.2.1, and presented the attributes and levels of the CE defined above (see Section 4.2.2 for more details). This part of the questionnaire was designed to get respondents thinking about the subject of the study before presenting the six choice sets (see Figure 4.1). Finally, the third part of the questionnaire asked for socioeconomic information of respondents.

Prior to the launch of the survey, a large pilot study with 100 respondents was conducted to check the validity of the CE instrument, to perform preliminary statistical tests of hypotheses and to estimate the priors of the experimental design described above.

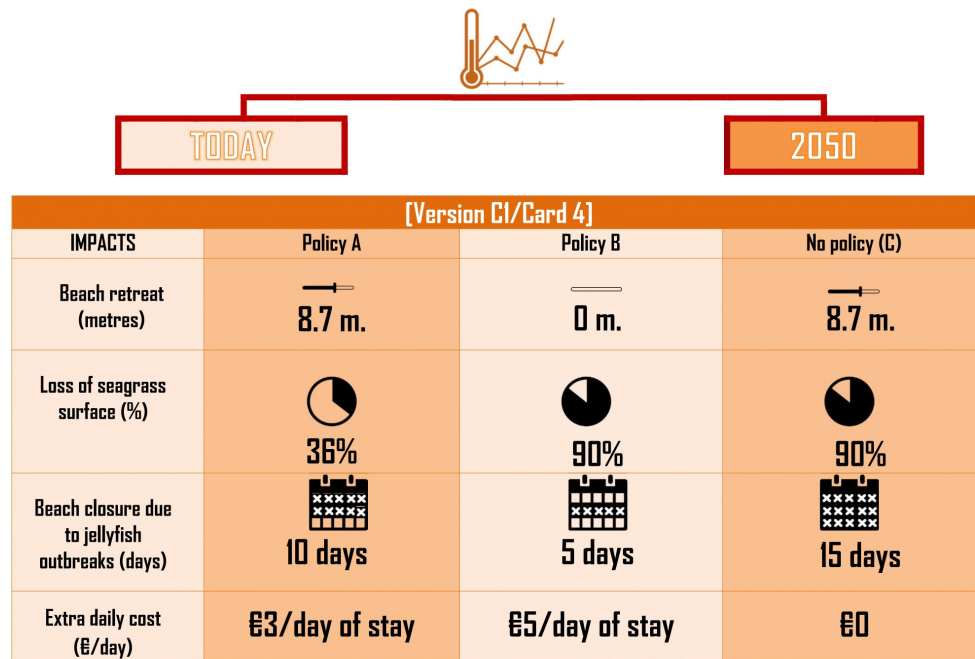


Figure 4.1 Example choice card.

The final survey was conducted in the departure terminal of the airport of Mallorca from July to September 2016, coinciding with the high season, and was administered in three languages (Spanish, English and German) by a professional surveying company. Tourists waiting at the boarding gates were randomly intercepted by trained interviewers and asked to participate in a face-to-face interview. 280 individuals accepted to participate in the survey achieving a response rate of 64.24% and an average interview length of 13 minutes. Incomplete questionnaires and respondents who declared having chosen the BAU alternative because they objected to a feature in the survey (e.g., the payment vehicle) were excluded from the sample following the common practice in the CE literature (see, for instance, the recent applications of Faccioli et al. 2015, Lundhede et al. 2015, Remoundou et al. 2015).

Table 4.2 reports the most relevant socioeconomic characteristics of the 231 individuals included in the final sample: 51.26% women and 48.74% men. Overall, the average respondent is 42.25 years old, has a university degree (50.18%) and a monthly personal income of 2,088 euros. The distribution of respondents by nationality is similar to the official records of tourists' arrivals: German (31.19%), British (24.73%), Spanish (11.11%) and others (32.97%). Concerning trip characteristics, Table 4.3 shows as individuals in the sample have taken, on average, 3.15 trips to Mallorca in the last five years. In their last trip, the average length of stay has been of 6.35 days and the average size of the group of individuals traveling together is 2.75. The good travel connectivity, the climate and the island's provision of beaches have been determinant in the choice of the destination for a large part of the sample (70.00%, 69.53% and 59.14%,

respectively). In contrast, other tourism supply attributes have only been relevant for a smaller group of individuals: the natural heritage (10.00%), the availability of leisure activities (7.88%), cultural and historic attractions (7.53%), price (6.81%), accommodation infrastructure (4.30%) and safety (4.30%). The survey also gathered data about the environmental problems experienced by individuals during their stay on Mallorcan beaches. The most commonly reported problems are dirty and garbage (27.96%), congestion (17.20%) and noise pollution (15.77%). Although less frequent, water turbidity (10.03%), water pollution (6.09%), jellyfish presence (3.58%) and other kinds of environmental degradation (3.58%) also affected a small part of sampled individuals.

Variable	Mean	Std. Dev.
Age (years)	42.25	14.85
Gender (percentage)		
- Female	51.26	
- Male	48.74	
Monthly income (in euros)	2,088	1,383.90
Houshold size	2.66	1.06
Nationality (percentage)		
- German	31.19	
- British	24.73	
- Spanish	11.11	
- Others	32.97	
Education (percentage)		
- Primary school level	12.27	
- Secondary school level	37.55	
- University level	50.18	
Number of respondents	231	

Table 4.2 *Socioeconomic characteristics of the sample.*

4.3 Methods

4.3.1 The mixed logit model

In a typical CE, the choice of the respondents' most preferred alternative is analysed using a discrete choice econometric model based on random utility maximization (RUM). RUM models assume that the level of utility U_{nj} that individual n derives from an alternative j can be decomposed into a deterministic and a stochastic component

Variable	Mean	Std. Dev
Number of trips to Mallorca in the last 5 years	3.15	1.67
Number of days spend in Mallorca in the current trip	6.35	1.23
Number of individuals traveling together	2.75	1.53
Percentage of individuals considering the following attributes as key determinant to choose Mallorca as holiday destination:		
- Connectivity	70.00	
- Climate	69.53	
- Beaches	59.14	
- Natural heritage	10.00	
- Leisure activities	7.88	
- Cultural and historic heritage	7.53	
- Price	6.81	
- Accommodation infraestructure	4.30	
- Safety	4.30	
- Global destination image	3.23	
Percentage of individuals experiencing the following environmental problems at beaches during their stay:		
- Dirt and garbage	27.96	
- Congestion	17.20	
- Noise pollution	15.77	
- Massive construction	10.39	
- Water turbidity	10.03	
- Water pollution	6.09	
- Jellyfish presence	3.58	
- Other kinds of environmental degradation	3.58	
Individuals planning to come back in the future (percentage)		
- Yes	86.74	
- No	13.26	
Number of respondents	231	

Table 4.3 *Trip characteristics if the sample.*

(McFadden 1973, Manski 1977). According to Lancaster's (1966) theory of value, the deterministic component of utility is usually defined as a function linear and additive in the vector of k observed attributes (x_{nj}) and the vector of k coefficients to be estimated (β). In contrast, the stochastic component captures the unobserved factors that determine the choice which are unknown to the researcher (ε_{nj}).

In addition, alternative specific constants (ASC) and error components (μ) can be included in the specification to accommodate the possibility that respondents may treat one or more alternatives systematically different to the others that they are presented with (Scarpa and Thiene 2005, Scarpa et al. 2007, Hess and Rose 2009, Marsh et al. 2011). This systematic difference may arise in this CE application as a result of the fact that the BAU alternative is held constant across choice tasks whereas the remaining (improving) alternatives are forced to vary by way of the experimental design. For this reason, an ASC equalled 1 for the BAU alternative and 0 for the improving alternatives has been included in the deterministic component of utility ($\beta' x_{nj}$). At the same time, an error component (μ_j) distributed $N(0, \sigma^2)$ has been added to account for different correlations patterns between the utility of the improving alternatives and the utility of the BAU (μ_j is equal to zero in the BAU alternative):

$$U_{nj} = \beta' x_{nj} + \mu_j + \varepsilon_{nj} \quad (4.1)$$

Assuming that the error term (ε_{nj}) is independent and identically distributed as Type I extreme value, the probability that individual n chooses alternative j from choice set J takes the familiar logit form (Hensher and Greene 2003):

$$P_{nj} = \frac{\exp(\beta' x_{nj} + \mu_j)}{\sum_{l=1}^J \exp(\beta' x_{nl} + \mu_l)} \quad (4.2)$$

In addition, the random parameter specification of the mixed logit model is applied to account for the heterogeneous preferences of respondents towards the attributes in the CE (Revelt and Train 1998, McFadden and Train 2000). For this reason, the vector of coefficients (β) is allowed to vary among individuals with values that depend on an underlying distribution $f(\cdot)$:

$$\beta_n = \beta^* + \sigma \nu_n \quad (4.3)$$

where ν_n is the individual-specific unknown heterogeneity and σ is the standard deviation of the distribution of β_n around the mean β^* . The model can also be used to explain preference heterogeneity based on the socioeconomic profile of respondents (Greene and Hensher 2010). In this case, a vector of socioeconomic characteristics (y_n) can be included as additional explanatory variables in the specification to model a shift of the mean β^* :

$$\beta^* = \beta + \delta y_n \quad (4.4)$$

where δ is the vector of estimated coefficients that capture the effect of the socioeconomic characteristics on the mean of the random parameter.

4.3.2 Welfare measurement

The economic interpretation of the estimated coefficients is not straightforward and requires the calculation of the marginal rates of substitution between each attribute under evaluation (*beach retreat*, *loss of seagrass* and *beach closure*) and the marginal utility of income represented by the coefficient of the monetary attribute (*cost*). In this way, the analysis of welfare measures follows the development of Hanemann (1984) and assumes that the marginal rates of substitution can be interpreted in terms of the marginal willingness-to-pay (MWTP) for a change in the level of provision of each attribute (Hensher et al. 2005, Brouwer and Schaafsma 2013, Veronesi et al. 2014, Remoundou et al. 2015). Consequently, the economic value for individual n of a unitary improvement in each attribute is measured by:

$$MWTP_n = \frac{\beta_n}{-\beta_{cost}} \quad (4.5)$$

where β_n is the value of the coefficient of each climate-induced environmental change for individual n and β_{cost} is the coefficient of the cost attribute. The distribution of the MWTP will be obtained using the Krinsky and Robb (1986) bootstrapping method to accommodate welfare effects among respondents with heterogeneous preferences towards the attributes in the CE.

4.4 Results

The statistical analysis was conducted in NLOGIT 6 (Econometric Software, 2016) using Halton draws with 1000 replications and accounting for the panel nature of the data. Several distributional assumptions (normal, log-normal, triangular, constrained triangular, etc.) and a range of socioeconomic variables accommodating heterogeneity in the mean of the distribution were investigated for the specification of the random parameters. The results of the preferred model, their standard errors and some goodness-of-fit measures are reported in Table 4.4. The ASC and all the attributes, except the cost, were included as random parameters following a constrained triangular distribution (Greene et al. 2006, Kragt and Bennett 2012). The coefficient of the cost attribute was specified as fixed to ease the estimation of the MWTP, as is done in common practice (e.g. Revelt and Train 1998, Hensher et al. 2005, Veronesi et al. 2014). In addition, two socioeconomic characteristics of respondents (age and level of education) and two

characteristics of the trip (the determinants to choose the destination and the environmental problems at beaches) turned to be statistically significant as shifters of the mean of the random parameter of the BAU alternative (see equation 4.4). Taking the above into account, the utility function of the estimated models is:

$$\begin{aligned}
 U_{nj} = & (\beta_n^{ASC} + \delta^1 AGE_n + \delta^2 LOW_SCHOOL_n + \delta^3 DEGRADATION_n \\
 & + \delta^4 ACCOMODATION_n) ASC_{nj} + \beta_n^1 BEACH_RETREAT_{nj} \\
 & + \beta_n^2 LOSS_SEAGRASS_{nj} + \beta_n^3 BEACH_CLOSURE_{nj} \\
 & + \beta_n^4 COST_{nj} + \mu_j + \varepsilon_{nj}
 \end{aligned} \tag{4.6}$$

As shown in Table 4.4, all attribute parameters (β) are statistically significant and have the expected sign. More specifically, the three attributes capturing the effect of climate-induced environmental changes (beach retreat, loss of seagrass and beach closure) have a negative parameter indicating a disutility from higher levels of CC impacts. That is, respondents are more likely to choose improving alternatives achieving a larger reduction of the analysed environmental changes. The cost attribute is also negative demonstrating that individuals preferred less costly alternatives. Finally, the ASC for the no-action scenario is also negative and significant showing the disutility of respondents in the BAU and, hence, a preference to implement measures to address climate-induced environmental changes. In the same line, the error component (μ) capturing the magnitude of the correlation between the improving alternatives is highly significant indicating that these alternatives have a substantial effect on the stochastic component of the utility. Therefore, the high degree of substitutability existent between the improving alternatives confirms that individuals treat these alternatives systematically different to the BAU.

Following equation 4.4, a vector of variables has been used to capture the effect of socioeconomic characteristics on the mean of the distribution of all random parameters. However, only the inclusion of these variables on the specification of the ASC parameter has led to significant estimates and to better model fit. As a result, although the BAU has a negative effect on the wellbeing of all respondents, the magnitude of this effect varies with four socioeconomic characteristics. In this way, the estimated coefficients of these variables (δ) accommodate heterogeneity in the mean of the distribution of the ASC parameter.

In particular, the negative parameter of the variable *age* shows that, the older the respondent is, the higher the disutility he will experience under the BAU scenario. At the same time, the positive coefficient of the variable *low school level* indicates that individuals with a primary level of education (as well as those with no education at all) will have a smaller disutility in the BAU compared to respondents with secondary or uni-

Variable	Coefficient	St. Er.
<i>Random parameters</i>		
Beach retreat	-0.0443***	0.012
Loss of seagrass	-0.1108***	0.024
Beach closure	-0.0331***	0.009
ASC	-2.2201***	0.832
<i>Random parameters spread</i>		
Beach retreat	0.0443***	0.012
Loss of seagrass	0.1108***	0.024
Beach closure	0.0331***	0.009
ASC	2.2201***	0.832
<i>Fixed coefficient</i>		
Cost	-0.0418**	0.019
<i>Heterogeneity in random parameter mean (δ)</i>		
Age	-0.0432*	0.023
Low school level	1.8024**	0.825
Environmental degradation	2.1938*	1.141
Accommodation infrastructure	1.7597**	0.836
<i>Error component (μ)</i>		
Sigma	1.2618**	0.593
Log-likelihood		-1071
Restricted log-likelihood		-1522.68
McFadden Pseudo R-squared		0.2966
Number of observations		1,386

Parameters denoted by ***, ** and * are significantly different from zero at the 1%, 5% and 10% significance levels, respectively.

Table 4.4 *Mixed logit model results.*

Attribute	Mean	95% confidence interval
Beach retreat	1.23	(0.18 to 3.74)
Loss of seagrass	0.31	(0.05 to 0.99)
Beach closure	0.90	(0.13 to 2.51)

Table 4.5 MWTP estimates: WTP per individual and day of stay, in euros. 95% confidence intervals based on the 2.5th and 97.5th percentile of the simulated MWTP distribution

versity levels of education. These results are in line with previous studies showing that older and higher-educated individuals have a greater awareness towards CC (Franzen and Vogl 2013, Lee et al. 2015, Beiser-McGrath and Huber 2018), tend to be more concerned about the sustainability of tourism and show a more environment-friendly behavior (Dolnicar 2004, Dolnicar et al. 2008).

The disutility faced in the BAU will be smaller also for individuals reporting *other kinds of environmental degradation* problems during their stay on the beach, compared with respondents facing other environmental problems (see Table 4.3 for the complete list). In a similar way, individuals choosing the destination for its provision of *accommodation infrastructure* (rather than other desirable destination attributes listed also in Table 4.3) will show a smaller disutility in the BAU. Note that, in this case, the attribute which has become determinant in choosing Mallorca as holiday destination, is not associated to its climatic and natural resources and, hence, it is not expected to be impacted by CC. Therefore, it is not surprising that individuals visiting the destination for its provision of *accommodation infrastructure* have smaller welfare impacts in a future hypothetical CC scenario.

The estimated parameters of the mixed logit model have been used to calculate the welfare impacts of the three climate-induced environmental changes under evaluation. Following equation 4.5, Krinsky and Robb (1986) parametric bootstrapping with 1,000 pseudo-random draws has been used to construct the simulated distribution for the MWTP per individual and day of stay. Table 4.5 presents the mean and the 95% confidence interval of the MWTP distribution for the beach retreat, loss of seagrass and beach closure attributes, respectively. According to these results, the beach retreat is the attribute generating the worst impact on tourists' wellbeing, as they are willing-to-pay 1.23 euros per day of stay to recover one meter of beach shoreline. Beach closure due to jellyfish outbreaks also generates a high impact on tourists, with a WTP to avoid a one-day closure of 0.9 euros, per day of stay. Finally, the WTP to recover a 1% of the affected seagrass area is 0.31 euros, per day of stay.

4.5 Conclusions

Estimated results show the support of tourists visiting the sun-and-beach destination of Mallorca, in Spain, to implement adaptation policies aimed at counteracting the three climate-induced environmental changes under evaluation: beach retreat caused by sea-level rise, the loss of *Posidonia oceanica* meadows and the increase in jellyfish outbreaks, both associated to seawater warming. These findings are consistent with previous studies. First, because they confirm that beach width (Uyarra et al. 2005, Buzinde, Manuel-Navarrete, Kerstetter and Redclift 2010, Buzinde, Manuel-Navarrete, Yoo and Morais 2010), water quality and transparency (Englebert et al. 2008, Barbier et al. 2011, Hendriks et al. 2014, Marbà et al. 2014) and jellyfish outbreaks (Purcell et al. 2007, Gössling et al. 2012) are important determinants of the satisfaction of sand-and-beach tourists. Second, because they demonstrate that CC effects on the provision of these environmental attributes will alter the attractiveness of the destination (Gössling et al. 2012).

In addition, the results of the mixed logit model estimated in this application have also found evidence of preference heterogeneity among individuals with different socioeconomic and travel characteristics. In line with previous works (see, for instance, Dolnicar 2004, Dolnicar et al. 2008), while older and higher-educated individuals are more concerned with CC impacts showing a stronger support to the adoption of adaptation measures, tourists visiting the destination for its provision of *accommodation infrastructure* will not be so concerned about climate-induced environmental changes on coastal ecosystems and, hence, will show a weaker support to CC adaptation.

Finally, the economic impact of the above-mentioned ecosystem changes has been inferred by measuring the MWTP, per tourist and day of stay, to introduce CC adaptation policies in the context of a CE application. Estimated results show that beach retreat will generate the worst marginal impact on sun-and-beach tourists (1.23 euros), followed by beach closure due to jellyfish outbreaks (0.90 euros) and loss of *Posidonia oceanica* meadows (0.31 euros). Although to the best of our knowledge this is one of the first attempts to measure the economic impact caused by climate-induced environmental changes on the wellbeing of tourists, the results obtained here are consistent with similar analysis performed outside the tourism field. In this setting, the most relevant example is the CE by Remoundou et al. (2015) eliciting the WTP of residents for mitigation measures against environmental changes caused by CC (affecting beach size, biodiversity and beach closure due to jellyfish blooms) on coastal and marine ecosystem in the Bay of Santander, Northern Spain.

Overall, there is no doubt that these findings are relevant for tourism planning as they can guide the design of adaptation policies reducing the negative impact of CC on the wellbeing of tourists and, in this way, minimizing the loss of attractiveness of the

destination. However, this paper is only a first step in fulfilling the existing gap in the literature on CC impacts on coastal tourism. Further research is needed to extend the investigation to other coastal destinations as well as to other potential climate-induced environmental changes to support decision-making processes oriented to reduce the vulnerabilities and/or to exploit the new opportunities of coastal destinations in the face of a changing climate.

Acknowledgments

This work is supported by the CLIMPACT project (CGL2014-54246-C2-1-R) funded by the Spanish Ministry of Economy. Alejandra R. Enríquez acknowledges an FPI grant associated with the CLIMPACT project.

Chapter 5

Summary and Conclusions.

Beach erosion and shoreline retreat in response to mean sea-level rise have important implications for coastal communities. Beaches represent a natural protection system against marine extremes caused by storm surges and waves and also, they are strongly linked to touristic economic activities which are, often, central to local economies. In this thesis, we have assessed the physical and economic impacts of climate change focusing on three beaches as site studies, one natural and two urban, located in the Balearic Islands (western Mediterranean). Because of their characteristics and morphology, these beaches can be taken as representative of a large part of the Mediterranean coasts.

One major development of the work has been the combination of different state-of-the-art numerical models to simulate two oceanic mechanisms acting at different time scales: mean sea-level rise and storm waves. The effects of these two forces on sandy coasts have been assessed under different assumptions. First, we have analysed the shoreline retreat in urban beaches, neglecting the sediment transport and the morphological evolution, since the beach shapes are highly dependent on human activities. This is a limiting premise that, nevertheless, has been found to be reasonable in this context; after the work developed, we can now conclude that neglecting the sediment transport could induce a bias in the rates of shoreline retreat. This is in fact confirmed when simulating the sediment transport in the natural beach case study. Here, the beach morphological features have proved to be a key point in the shoreline retreat and erosion processes as well as in their rates.

We have applied both hydro- and morphodynamic models distinctly. In particular, hydrodynamic models have been used to simulate the wave propagation from offshore to nearshore conditions and, in the urban beaches, also to obtain the shoreline retreat under mean sea-level rise. Our research has shown the good capabilities of the hydrodynamic models to reproduce wave propagation as well as to simulate changes in the shoreline position under present-day climate, when compared to observations. Therefore, we have applied the same models under projected mean sea-level rise and wave climate changes, using regionalized projections in the western Mediterranean Sea. In the case of the natural beach, the hydrodynamic simulation has been combined with

morphodynamic models to assess the sediment transport and the morphological changes caused by mean sea-level rise and waves.

We have found that both in natural and urban beaches in the Balearic Islands, mean sea-level rise is the major driver of the projected shoreline retreat. Waves play an important role under extreme conditions (i.e., storm events), mostly because they act onto higher mean sea-level. In the two urban beaches studied, Cala Millor and Playa de Palma (Mallorca Island), our results project that almost the entire aerial beach will be flooded during moderate extreme events by 2100; in addition, the permanent beach loss due to only mean sea-level rise reaches half of the present-day area.

In the natural beach of Son Bou (Menorca Island), we have quantified the role of the morphological changes, which have proved to be especially relevant to the magnitude of the shoreline retreat in this type of natural beaches. The shoreline retreat slows down when simulating the erosion of the berm caused by mean sea-level rise, highlighting the relevance of the beach features to the coastal protection. Importantly, we have found that the existence or disappearance of the berm controls the erosion and vulnerability of the backward features, as the case of the dunes in Son Bou. This and the above-mentioned results, outline the importance of simulating the sediment transport and the morphological changes of beaches, especially in cases with land sediment input and natural environment.

The coastal environmental degradation in the Mediterranean region in response to marine changing conditions is expected to derive in local economic damages because tourism, one of the most important economic activities in the region, is highly dependent on the provision of natural resources, which determine the attractiveness of the destination. In the present thesis, the economic impact of beach retreat, but also the loss of seagrass meadows and the beach closure, has been assessed through the measurement of the change in the tourist's wellbeing by applying a choice experiment. Our results confirm the tourist's support to implement policies aimed at reducing these three environmental changes. This support, as well as the respondent's utility changes, has shown to vary among individuals with different socioeconomic and travel characteristics: those older and higher-educated respondents presented a stronger support to the adoption of action policies. On the contrary, tourists visiting the destination for its accommodation features and those who had already found an environmental degradation during their visit, revealed weaker support to climate change adaptation. Interestingly, the higher WTP has been found to be associated to the reduction of the beach retreat, pointing at the loss of beach area as one of the most economically damaging consequences of climate change in coastal environments.

The main results and derived conclusions discussed above can be extrapolated to other beaches with similar tidal signal and wave climate conditions. This is the case

of the Mediterranean coastal region that, in addition, is exposed to a similar human pressure.

Chapter 6

Main findings.

- The hydrodynamic models used in the present thesis, namely SWAN and SWASH, have shown good capabilities in the simulation of wave propagation and shoreline changes in the three beaches in the Balearic Islands, representative of the coasts of the archipelago. The comparison to in-situ observations displays a high correlation and low RMSE for wave height and wave period, although with poorer results for wave direction.
- Mean sea-level rise is the main oceanic driving mechanism in the beach reduction and erosion processes, in comparison with wind-waves, for both urban and natural beaches in the Western Mediterranean Sea.
- Future projected changes in wave climate are negligible in Western Mediterranean Sea, especially regarding to wave direction, according to regional wave models.
- While mean sea-level rise will cause a permanent reduction of approximately half of the present beach size by 2100, storm wave events will produce temporal flooding of almost the complete present area in the urban beaches.
- The natural beach is not expected to disappear within the present century; it will move landward, in a natural process that involves dune erosion.
- The morphological beach features (berm, slope changes, dunes, etc.) have proved to be an efficient protection system that, in our natural beach case study, reduce the shoreline retreat process. When these structures are not taken into account, the beach erosion and shoreline retreat can be overestimated.
- The provision of coastal natural resources is important in the attractiveness of the sun-and-beach tourism in the Balearic Island.
- Environmental degradation derived from climate change will causes tourist's discomfort and, therefore, an economic impact. Overall, tourists support the implementation of adaptation policies aimed to reduce these impacts.

- Tourist's disutility derived from climate change impacts as well as their support to adaptation policies, varies among individuals: older and high-educated people showed higher climate change concern and support to the action policies. On the other hand, individuals who visited Mallorca for its provision of accommodation infrastructure and those who found an environmental degradation during their stay, exhibited lower concern of climate change effects and lower support to adaptation policies.
- The tourist's discomfort also varies with the three climate change impacts considered in this thesis: higher disutility is obtained for beach loss, following by beach closure and seagrass loss.

References

- Ahn, S., De Steiguer, J. E., Palmquist, R. B. and Holmes, T. P. (2000), 'Economic analysis of the potential impact of climate change on recreational trout fishing in the southern Appalachian Mountains: an application of a nested multinomial logit model', *Climatic Change* **45**(3-4), 493–509.
- Akter, S. and Bennett, J. (2011), 'Household perceptions of climate change and preferences for mitigation action: the case of the carbon pollution reduction scheme in australia', *Climatic change* **109**(3-4), 417–436.
- Alongi, D. M. (2008), 'Mangrove forests: resilience, protection from tsunamis, and responses to global climate change', *Estuarine, Coastal and Shelf Science* **76**(1), 1–13.
- Amelung, B. and Nicholls, S. (2014), 'Implications of climate change for tourism in Australia', *Tourism Management* **41**, 228–244.
- Amelung, B., Nicholls, S. and Viner, D. (2007), 'Implications of global climate change for tourism flows and seasonality', *Journal of Travel research* **45**(3), 285–296.
- Amelung, B. and Viner, D. (2006), 'Mediterranean tourism: exploring the future with the tourism climatic index', *Journal of sustainable tourism* **14**(4), 349–366.
- Andreopoulos, D., Damigos, D., Comiti, F. and Fischer, C. (2015), 'Estimating the non-market benefits of climate change adaptation of river ecosystem services: A choice experiment application in the Aaos basin, Greece', *Environmental Science and Policy* **45**, 92–103.
- Antonov, J. I., Levitus, S. and Boyer, T. P. (2002), 'Steric sea level variations during 1957-1994: Importance of salinity', *Journal of Geophysical Research: Oceans* **107**(C12), SRF 14–1–SRF 14–8.
- Arns, A., Dangendorf, S., Jensen, J., Talke, S. and Bender, J. (2017), 'Sea-level rise induced amplification of coastal protection design heights', *Nature Publishing Group* pp. 1–9.
URL: <http://dx.doi.org/10.1038/srep40171>
- Arriaga, J., Rutten, J., Ribas, F., Falqués, A. and Ruessink, G. (2017), 'Modeling the long-term diffusion and feeding capability of a mega-nourishment', *Coastal Engineering* **121**, 1–13.
- Attrill, M. J., Wright, J. and Edwards, M. (2007), 'Climate-related increases in jellyfish frequency suggest a more gelatinous future for the North Sea', *Limnology and Oceanography* **52**(1), 480–485.

Aznar, R., Padorno, M. E., Pérez, B., Gómez Lahoz, M., García Sotillos, M., Álvarez Fanjul, E., Pérez Jordán, G., Marcos, M., Martínez Asensio, A., Llasses, J. et al. (2016), 'Vulnerabilidad de los puertos españoles ante el cambio climático. vol. 1: Tendencias de variables físicas oceánicas y atmosféricas durante las últimas décadas y proyecciones para el siglo xxi'.

Baettig, M. B., Wild, M. and Imboden, D. M. (2007), 'A climate change index: Where climate change may be most prominent in the 21st century', *Geophysical Research Letters* **34**(1).

Barbier, E. B., Hacker, S. D., Kennedy, C., Koch, E. W., Stier, A. C. and Silliman, B. R. (2011), 'The value of estuarine and coastal ecosystem services', *Ecological monographs* **81**(2), 169–193.

Becken, S. (2013), 'A review of tourism and climate change as an evolving knowledge domain', *Tourism Management Perspectives* **6**, 53–62.

Beiser-McGrath, L. and Huber, R. (2018), 'Assessing the relative importance of psychological and demographic factors for predicting climate and environmental attitudes.', *Climatic Change* **149**, 335–347.

Birol, E. and Koundouri, P. (2008), *Choice experiments informing environmental policy: a European perspective*, Edward Elgar Publishing.

Bobba, A. G., Singh, V. P., Berndtsson, R. and Bengtsson, L. (2000), 'Numerical simulation of saltwater intrusion into Laccadive Island aquifers due to climate change', *J. Geol. Soc. India* **55**, 589.

Booij, N., Ris, R. C. and Holthuijsen, L. H. (1999), 'A third-generation wave model for coastal regions: 1. model description and validation', *Journal of geophysical research: Oceans* **104**(C4), 7649–7666.

Brotz, L., Cheung, W. W. L., Kleisner, K., Pakhomov, E. and Pauly, D. (2012), 'Increasing jellyfish populations: Trends in Large Marine Ecosystems', *Hydrobiologia* **690**, 3–20.

Brotz, L. and Pauly, D. (2012), 'Jellyfish populations in the Mediterranean Sea', *Acta Adriat* **53**(2), 213–231.

Brouwer, R. and Schaafsma, M. (2013), 'Modelling risk adaptation and mitigation behaviour under different climate change scenarios', *Climatic Change* **117**(1-2), 11–29.

Brunel, C. and Sabatier, F. (2009), 'Potential influence of sea-level rise in controlling shoreline position on the french mediterranean coast', *Geomorphology* **107**(1-2), 47–57.

Bruun, P. (1962), 'Sea-level rise as a cause of shore erosion', *Journal of the Waterways and Harbors division* **88**(1), 117–132.

Bugajny, N., Furmańczyk, K., Dudzińska-Nowak, J. and Paplińska-Swerpel, B. (2013), 'Modelling morphological changes of beach and dune induced by storm on the southern baltic coast using xbeach (case study: Dziwnow spit)', *Journal of Coastal Research* **65**(sp1), 672–677.

Bujosa, A. B. (2014), 'Substitution patterns across alternatives as a source of preference heterogeneity in recreation demand models', *Journal of environmental management* **144**, 212–217.

Bujosa, A. and Rosselló, J. (2013), 'Climate change and summer mass tourism: the case of spanish domestic tourism', *Climatic Change* **117**(1-2), 363–375.

Bujosa, A., Torres, C. and Riera, A. (2018), 'Framing Decisions in Uncertain Scenarios: An Analysis of Tourist Preferences in the Face of Global Warming', *Ecological economics* **148**, 36–42.

Buzinde, C. N., Manuel-Navarrete, D., Kerstetter, D. and Redclift, M. (2010), 'Representations and adaptation to climate change', *Annals of tourism research* **37**(3), 581–603.

Buzinde, C. N., Manuel-Navarrete, D., Yoo, E. E. and Morais, D. (2010), 'Tourists' perceptions in a climate change: Eroding Destinations', *Annals of Tourism Research* **37**(2), 333–354.

Cabrini, L., Simpson, M. and Scott, D. (2009), From Davos to Copenhagen and beyond: Advancing tourism's response to climate change, in 'UN Copenhagen Climate Change Conference, Madrid, Spain: UNWTO'.

Camus, P., Mendez, F. J. and Medina, R. (2011), 'A hybrid efficient method to down-scale wave climate to coastal areas', *Coastal Engineering* **58**(9), 851–862.

Camus, P., Mendez, F. J., Medina, R. and Cofiño, A. S. (2011), 'Analysis of clustering and selection algorithms for the study of multivariate wave climate', *Coastal Engineering* **58**(6), 453–462.

Carson, R. T. and Louviere, J. J. (2011), 'A common nomenclature for stated preference elicitation approaches', *Environmental and Resource Economics* **49**(4), 539–559.

Carter, R. W. G. (2013), *Coastal environments: an introduction to the physical, ecological, and cultural systems of coastlines*, Elsevier.

Cazenave, A., Dominh, K., Soudarin, L., Ponchaut, F., Cretaux, J. F. and Le Provost, C. (1999), 'Sea level changes from Topex-Poseidon altimetry and tide gauges, and vertical crustal motions from DORIS', *Geophysical Research Letters* **26**(14), 2077–2080.

Cazenave, A. and Le Cozannet, G. (2014), 'Sea level rise and its coastal impacts', *Earth's Future* **2**(2), 15–34.

Chaikaew, P., Hodges, A. W. and Grunwald, S. (2017), 'Estimating the value of ecosystem services in a mixed-use watershed: a choice experiment approach', *Ecosystem services* **23**, 228–237.

Church, J. A. and White, N. J. (2011), 'Sea-level rise from the late 19th to the early 21st century', *Surveys in geophysics* **32**(4-5), 585–602.

Church, J., Clark, P., Cazenave, A., Gregory, J., Jevrejeva, S., Levermann, A., Merrifield, M., Milne, G., Nerem, R., Nunn, P. et al. (2013), 'Sea level change. climate change 2013: the physical science basis. contribution of working group i to the fifth assessment report of the intergovernmental panel on climate change', *Cambridge University Press, Cambridge, United Kingdom and New York, NY, USA* pp. 1137–1216.

Dangendorf, S., Marcos, M., Wöppelmann, G., Conrad, C. P., Frederikse, T. and Riva, R. (2017), 'Reassessment of 20th century global mean sea level rise', **114**(23), 1–6.

Dasgupta, S., Laplante, B., Meisner, C., Wheeler, D. and Yan, J. (2007), *The impact of sea level rise on developing countries: a comparative analysis*, The World Bank.

Davidson-Arnott, R. G., Van Proosdij, D., Ollerhead, J. and Schostak, L. (2002), 'Hydrodynamics and sedimentation in salt marshes: examples from a macrotidal marsh, bay of fundy', *Geomorphology* **48**(1-3), 209–231.

De Winter, R., Gongriep, F. and Ruessink, B. (2015), 'Observations and modeling of alongshore variability in dune erosion at egmond aan zee, the netherlands', *Coastal Engineering* **99**, 167–175.

De Winter, R. and Ruessink, B. (2017), 'Sensitivity analysis of climate change impacts on dune erosion: case study for the dutch holland coast', *Climatic Change* **141**(4), 685–701.

Deng, J., Harff, J., Schimanke, S. and Meier, H. M. (2015), 'A method for assessing the coastline recession due to the sea level rise by assuming stationary wind-wave climate', *Oceanological and Hydrobiological Studies* **44**(3), 362–380.

Dolnicar, S. (2004), 'Insights into sustainable tourists in Austria: A data-based a priori segmentation approach.', *Journal of Sustainable Tourism* **12**(3), 209–218.

- Dolnicar, S., Crouch, G. and Long, P. (2008), 'Environment-friendly tourists: What do we really know about them?', *Journal of Sustainable Tourism* **16**(3), 197–210.
- Ehmer, P., Heymann, E., Just, T., Fuchs-Sobolew, G. and Walter, N. (2008), 'Climate change and tourism: Where will the journey lead', *Frankfurt am Main* .
- Englebert, E. T., McDermott, C. and Kleinheinz, G. T. (2008), 'Effects of the nuisance algae, *Cladophora*, on *Escherichia coli* at recreational beaches in Wisconsin', *Science of the Total Environment* **404**(1), 10–17.
- Enríquez, A. R., Marcos, M., Álvarez-Ellacuría, A., Orfila, A. and Gomis, D. (2017), 'Changes in beach shoreline due to sea level rise and waves under climate change scenarios: application to the balearic islands (western mediterranean)', *Natural Hazards and Earth System Sciences* **17**(7), 1075–1089.
- Esteves, L., Williams, J., Nock, A. and Lymbery, G. (2009), 'Quantifying shoreline changes along the sefton coast (uk) and the implications for research-informed coastal management', *Journal of Coastal Research* pp. 602–606.
- Eurostat (2011), 'The mediterranean and black sea basins, available at: <http://ec.europa.eu/eurostat/en/web/products-statistics-in-focus/-/ks-sf-11-014> last access: 23 march 2011'.
- Faccioli, M., Font, A. R. and Figuerola, C. M. T. (2015), 'Valuing the recreational benefits of wetland adaptation to climate change: a trade-off between species' abundance and diversity', *Environmental management* **55**(3), 550–563.
- Faccioli, M., Kuhfuss, L. and Czajkowski, M. (2019), 'Stated preferences for conservation policies under uncertainty: insights on the effect of individuals' risk attitudes in the environmental domain', *Environmental and Resource Economics* **73**(2), 627–659.
- Falqués, A., Garnier, R., Ojeda, E., R. F. and Guillen, J. (2007), 'Q2d-morfo: a medium to long term model for beach morphodynamics', *River, Coastal and Estuarine Morphodynamics: RCEM* **1**, 71–78.
- Feagin, R. A., Sherman, D. J. and Grant, W. E. (2005), 'Coastal erosion, global sea-level rise, and the loss of sand dune plant habitats', *Frontiers in Ecology and the Environment* **3**(7), 359–364.
- Fenner, P. J., Lippmann, J. and Gershwin, L. (2010), 'Fatal and nonfatal severe jellyfish stings in Thai waters', *Journal of travel medicine* **17**(2), 133–138.
- Ferreira, Ó. (2005), 'Storm groups versus extreme single storms: predicted erosion and management consequences', *Journal of Coastal Research* pp. 221–227.

FitzGerald, D. M., Fenster, M. S., Argow, B. A. and Buynevich, I. V. (2008), 'Coastal impacts due to sea-level rise', *Annual Review of Earth and Planetary Sciences* **36**.

Fowler, H. J., Ekström, M., Blenkinsop, S. and Smith, A. P. (2007), 'Estimating change in extreme European precipitation using a multimodel ensemble', *Journal of Geophysical Research: Atmospheres* **112**(D18).

Franzen, A. and Vogl, D. (2013), 'Two decades of measuring environmental attitudes: A comparative analysis of 33 countries', *Global Environmental Change* **23**(5), 1001–1008.

Fredsoe, J. and Deigaard, R. (1992), *Mechanics of coastal sediment transport*.

Giorgi, F. (2006), 'Climate change hot-spots', *Geophysical Research Letters* .

Giorgi, F. and Lionello, P. (2008), 'Climate change projections for the Mediterranean region', *Global and planetary change* **63**(2-3), 90–104.

Goh, C. (2012), 'Exploring impact of climate on tourism demand', *Annals of Tourism Research* **39**(4), 1859–1883.

González, M., Medina, R., González-Ondina, J., Osorio, A., Méndez, F. and García, E. (2007), 'An integrated coastal modeling system for analyzing beach processes and beach restoration projects, smc', *Computers and geosciences* **33**(7), 916–931.

Gornitz, V. (1995), 'Monitoring sea level changes', *Climatic Change* **31**, 515–544.

URL: <https://link.springer.com/content/pdf/10.1007%2F01095160.pdf>

Gössling, S. and Hall, C. M. (2006), 'Uncertainties in predicting tourist flows under scenarios of climate change', *Climatic change* **79**(3-4), 163–173.

Gössling, S., Scott, D., Hall, C. M., Ceron, J.-P. and Dubois, G. (2012), 'Consumer behaviour and demand response of tourists to climate change', *Annals of tourism research* **39**(1), 36–58.

Greene, W. H. and Hensher, D. A. (2010), 'Ordered choices and heterogeneity in attribute processing', *Journal of Transport Economics and Policy (JTEP)* **44**(3), 331–364.

Greene, W. H., Hensher, D. A. and Rose, J. (2006), 'Accounting for heterogeneity in the variance of unobserved effects in mixed logit models', *Transportation Research Part B: Methodological* **40**, 75–92.

Guimarães, P. V., Farina, L., Toldo Jr, E., Diaz-Hernandez, G. and Akhmatkaya, E. (2015), 'Numerical simulation of extreme wave runup during storm events in tramandaí beach, rio grande do sul, brazil', *Coastal Engineering* **95**, 171–180.

- Gulev, S. K. and Grigorieva, V. (2004), 'Last century changes in ocean wind wave height from global visual wave data', *Geophysical Research Letters* **31**(24), 1–4.
- Gutierrez, B. T., Plant, N. G. and Thieler, E. R. (2011), 'A bayesian network to predict coastal vulnerability to sea level rise', *Journal of Geophysical Research: Earth Surface* **116**(F2).
- Hamilton, J. M., Maddison, D. J. and Tol, R. S. J. (2005), 'Effects of climate change on international tourism', *Climate research* **29**(3), 245–254.
- Hanemann, W. M. (1984), 'Welfare evaluations in contingent valuation experiments with discrete responses', *American journal of agricultural economics* **66**(3), 332–341.
- Hanley, N., Wright, R. E. and Adamowicz, V. (1998), 'Using choice experiments to value the environment', *Environmental and resource economics* **11**(3-4), 413–428.
- Hanson, S., Nicholls, R., Ranger, N., Hallegatte, S., Corfee-Morlot, J., Herweijer, C. and Chateau, J. (2011), 'A global ranking of port cities with high exposure to climate extremes', *Climatic change* **104**(1), 89–111.
- Harley, M., Armaroli, C. and Ciavola, P. (2011), 'Evaluation of xbeach predictions for a real-time warning system in emilia-romagna, northern italy', *Journal of Coastal Research* pp. 1861–1865.
- Harley, M. D., Valentini, A., Armaroli, C., Perini, L., Calabrese, L. and Ciavola, P. (2016), 'Can an early-warning system help minimize the impacts of coastal storms? a case study of the 2012 halloween storm, northern italy', *Natural Hazards and Earth System Sciences* **16**(1), 209–222.
- Hay, C. C., Morrow, E., Kopp, R. E. and Mitrovica, J. X. (2015), 'Probabilistic reanalysis of twentieth-century sea-level rise', *Nature* **517**(7535), 481–484.
URL: <http://dx.doi.org/10.1038/nature14093>
- Hemer, M. A., Fan, Y., Mori, N., Semedo, A. and Wang, X. L. (2013), 'Projected changes in wave climate from a multi-model ensemble', *Nature Climate Change* **3**(5), 471–476.
URL: <http://dx.doi.org/10.1038/nclimate1791>
- Hendriks, I. E., Olsen, Y. S., Ramajo, L., Basso, L., Moore, T. S., Howard, J. and Duarte, C. M. (2014), 'Photosynthetic activity buffers ocean acidification in seagrass meadows', *Biogeosciences* **11**, 333–346.
- Hensher, D. A. and Greene, W. H. (2003), 'The mixed logit model: the state of practice', *Transportation* **30**(2), 133–176.

Hensher, D. A., Rose, J. and Greene, W. H. (2005), 'The implications on willingness to pay of respondents ignoring specific attributes', *Transportation* **32**(3), 203–222.

Hess, S. and Rose, J. M. (2009), 'Allowing for intra-respondent variations in coefficients estimated on repeated choice data', *Transportation Research Part B: Methodological* **43**(6), 708–719.

Hinkel, J., Lincke, D., Vafeidis, A. T., Perrette, M., Nicholls, R. J., Tol, R. S. J., Marzeion, B., Fettweis, X., Ionescu, C. and Levermann, A. (2014), 'Coastal flood damage and adaptation costs under 21st century sea-level rise', *Proceedings of the National Academy of Sciences* **111**(9), 3292–3297.

URL: <http://www.pnas.org/lookup/doi/10.1073/pnas.1222469111>

Idier, D., Rohmer, J., Bulteau, T. and Delvallée, E. (2013), 'Development of an inverse method for coastal risk management', *Natural Hazards and Earth System Sciences* **13**(4), 999–1013.

IPCC (2000), 'Special report on emissions scenarios', *IPCC SRES, Geneva* .

IPCC (2007a), *Climate Change 2007: Impacts, Adaptation and Vulnerability. Contribution of Working Group II to the Fourth Assessment Report of the Intergovernmental Panel on Climate Change*, Technical report, Cambridge, UK.

IPCC (2007b), *Climate Change 2007: Synthesis Report. Contribution of Working Groups I, II and III to the Fourth Assessment Report of the Intergovernmental Panel on Climate Change*, Technical report, Geneva, Switzerland.

URL: https://www.ipcc.ch/site/assets/uploads/2018/02/ar4_syr.pdf

IPCC (2007c), *Contribution of Working Group I to the Fourth Assessment Report of the Intergovernmental Panel on Climate Change*, Technical report, Cambridge University Press, Cambridge, United Kingdom and New York, NY, USA.

IPCC (2013), *Climate Change 2013: The Physical Science Basis, Contribution of Working Group I to the Fifth Assessment Report of the Intergovernmental Panel on Climate Change*, Technical report, Cambridge, United Kingdom and New York, NY, USA., Cambridge University Press.

URL: <http://www.climatechange2013.org/report/full-report/>

Jevrejeva, S., Moore, J., Grinsted, A., Matthews, A. and Spada, G. (2014), 'Trends and acceleration in global and regional sea levels since 1807', *Global and Planetary Change* **113**, 11–22.

Jordà, G., Marbà, N. and Duarte, C. M. (2012), 'Mediterranean seagrass vulnerable to regional climate warming', *Nature Climate Change* **2**(11), 821.

- Karunaratna, H., Brown, J., Chatzirodou, A., Dissanayake, P. and Wisse, P. (2018), ‘Multi-timescale morphological modelling of a dune-fronted sandy beach’, *Coastal Engineering* **136**, 161–171.
- Knutson, T., Kossin, J., Mears, C., Perlwitz, J. and Wehner, M. (2017), ‘Detection and attribution of climate change. In: Climate Science Special Report: Fourth National Climate Assessment, Volume I [Wuebbles, D.J., D.W. Fahey, K.A. Hibbard, D.J. Dokken, B.C. Stewart, and T.K. Maycock (eds.)]’, *U.S. Global Change Research Program, Washington, DC, USA* pp. 114–132.
- Kogovšek, T., Bogunović, B. and Malej, A. (2010), Recurrence of bloom-forming scyphomedusae: wavelet analysis of a 200-year time series, in ‘Jellyfish Blooms: New Problems and Solutions’, Springer, pp. 81–96.
- Kopp, R. E., Kemp, A. C., Bittermann, K., Horton, B. P., Donnelly, J. P., Gehrels, W. R., Hay, C. C., Mitrovica, J. X., Morrow, E. D. and Rahmstorf, S. (2016), ‘Temperature-driven global sea-level variability in the common era’, *Proceedings of the National Academy of Sciences* **113**(11), E1434–E1441.
- Kragt, M. E. and Bennett, J. W. (2012), ‘Attribute framing in choice experiments: how do attribute level descriptions affect value estimates?’, *Environmental and Resource Economics* **51**(1), 43–59.
- Krinsky, I. and Robb, A. (1986), ‘Approximating the Statistical Properties of Elasticities’, *Review of Economics and Statistics* **68**, 715–19.
- Lancaster, K. J. (1966), ‘A new approach to consumer theory’, *Journal of political economy* **74**(2), 132–157.
- Landauer, M., Pröbstl, U. and Haider, W. (2012), ‘Managing cross-country skiing destinations under the conditions of climate change—Scenarios for destinations in Austria and Finland’, *Tourism Management* **33**(4), 741–751.
- Landry, C. E., Keeler, A. G. and Kriesel, W. (2003), ‘An economic evaluation of beach erosion management alternatives’, *Marine Resource Economics* **18**(2), 105–127.
- Le Cozannet, G., Bulteau, T., Castelle, B., Ranasinghe, R., Wöppelmann, G., Rohmer, J., Bernon, N., Idier, D., Louisor, J. and Salas-y Mélia, D. (2019), ‘Quantifying uncertainties of sandy shoreline change projections as sea level rises’, *Scientific reports* **9**(1), 42.
- Le Cozannet, G., Garcin, M., Yates, M., Idier, D. and Meyssignac, B. (2014), ‘Approaches to evaluate the recent impacts of sea-level rise on shoreline changes’, *Earth-science reviews* **138**, 47–60.

Lee, E. M. (2008), 'Coastal cliff behaviour: Observations on the relationship between beach levels and recession rates', *Geomorphology* **101**(4), 558–571.

Lee, T., Markowitz, E., Howe, P., Ko, C. and Leiserowitz, A. (2015), 'Predictors of public climate change awareness and risk perception around the world.', *Nature Climate Change* **5**.

Lionello, P. (2012), *The climate of the Mediterranean region: From the past to the future*, Elsevier.

Lionello, P., Malanotte-Rizzoli, P., Boscolo, R., Alpert, P., Artale, V., Li, L., Luterbacher, J., May, W., Trigo, R., Tsimplis, M., Ulbrich, W. and Xoplacki, E. (2006), 'The Mediterranean climate: An overview of the main characteristics and issues', *Developments in Earth and Environmental Sciences* **4**, 1–26.

Luijendijk, A., Hagenaars, G., Ranasinghe, R., Baart, F., Donchyts, G. and Aarninkhof, S. (2018), 'The state of the world's beaches', *Scientific reports* **8**(1), 6641.

Lundhede, T., Jacobsen, J. B., Hanley, N., Strange, N. and Thorsen, B. J. (2015), 'Incorporating outcome uncertainty and prior outcome beliefs in stated preferences', *Land Economics* **91**(2), 296–316.

Maddison, D. (2001), 'In search of warmer climates? The impact of climate change on flows of British tourists', *Climatic change* **49**(1-2), 193–208.

Manski, C. F. (1977), 'The structure of random utility models', *Theory and decision* **8**(3), 229–254.

Marbà, N., Díaz-Almela, E. and Duarte, C. M. (2014), 'Mediterranean seagrass (*Posidonia oceanica*) loss between 1842 and 2009', *Biological Conservation* **176**, 183–190.

Marbà, N. and Duarte, C. M. (2010), 'Mediterranean warming triggers seagrass (*Posidonia oceanica*) shoot mortality', *Global Change Biology* **16**(8), 2366–2375.

Marcos, M., Jordà, G. and Le Cozannet, G. (2016), 'Sea level rise and its impacts on the mediterranean', *The Mediterranean Region under Climate Change* p. 265.

Marcos, M. and Tsimplis, M. N. (2008), 'Coastal sea level trends in southern europe', *Geophysical Journal International* **175**(1), 70–82.

Marcos, M. and Woodworth, P. L. (2017), 'Spatiotemporal changes in extreme sea levels along the coasts of the north atlantic and the gulf of mexico', *Journal of Geophysical Research: Oceans* **122**(9), 7031–7048.

- Mariotti, A., Zeng, N., Yoon, J.-H., Artale, V., Navarra, A., Alpert, P. and Li, L. Z. X. (2008), 'Mediterranean water cycle changes: transition to drier 21st century conditions in observations and CMIP3 simulations', *Environmental Research Letters* **3**(4), 44001.
- Marsh, D., Mkwara, L. and Scarpa, R. (2011), 'Do respondents' perceptions of the status quo matter in non-market valuation with choice experiments? An application to New Zealand freshwater streams', *Sustainability* **3**(9), 1593–1615.
- Martínez-Asensio, A., Marcos, M., Jordà, G. and Gomis, D. (2013), 'Calibration of a new wind-wave hindcast in the western mediterranean', *Journal of Marine Systems* **121**, 1–10.
- Martínez-Asensio, A., Tsimplis, M. N., Marcos, M., Feng, X., Gomis, D., Jordà, G. and Josey, S. A. (2016), 'Response of the north atlantic wave climate to atmospheric modes of variability', *International Journal of Climatology* **36**(3), 1210–1225.
- Mawdsley, R. J., Haigh, I. D. and Wells, N. C. (2015), 'Global secular changes in different tidal high water, low water and range levels', *Earth's Future* **3**(2), 66–81.
- Mazas, F. and Hamm, L. (2017), 'An event-based approach for extreme joint probabilities of waves and sea levels', *Coastal Engineering* **122**, 44–59.
- McCall, R. T., De Vries, J. V. T., Plant, N., Van Dongeren, A., Roelvink, J., Thompson, D. and Reniers, A. (2010), 'Two-dimensional time dependent hurricane overwash and erosion modeling at santa rosa island', *Coastal Engineering* **57**(7), 668–683.
- McFadden, D. (1973), 'Conditional logit analysis of qualitative choice behavior'.
- McFadden, D. and Train, K. (2000), 'Mixed MNL models for discrete response', *Journal of applied Econometrics* **15**(5), 447–470.
- Medellín, G., Brinkkemper, J., Torres-Freyermuth, A., Appendini, C., Mendoza, E. and Salles, P. (2016), 'Run-up parameterization and beach vulnerability assessment on a barrier island: a downscaling approach', *Natural Hazards and Earth System Sciences* **16**(1), 167–180.
- Menéndez, M. and Woodworth, P. L. (2010), 'Changes in extreme high water levels based on a quasi-global tide-gauge data set', *Journal of Geophysical Research: Oceans* **115**(C10).
- Mentaschi, L., Vousdoukas, M. I., Voukouvalas, E., Dosio, A. and Feyen, L. (2017), 'Global changes of extreme coastal wave energy fluxes triggered by intensified teleconnection patterns', *Geophysical Research Letters* **44**(5), 2416–2426.

Meyssignac, B., Piecuch, C. G., Merchant, C. J., Racault, M., Palanisamy, H., Macintosh, C., Sathyendranath, S. and Brewin, R. (2017), 'Causes of the Regional Variability in Observed Sea Level , Sea Surface Temperature and Ocean Colour Over the Period 1993 – 2011', *Surveys in Geophysics* **38**(1), 187–215.

Mieczkowski, Z. (1985), 'The tourism climatic index: a method of evaluating world climates for tourism', *Canadian Geographer/Le Géographe Canadien* **29**(3), 220–233.

Mitrovica, J. X., Tamisiea, M. E., Davis, J. L. and Milne, G. A. (2001), 'Recent mass balance of polar ice sheets inferred from patterns of global sea-level change', *Nature* **409**(6823), 1026–1029.

URL: <https://doi.org/10.1038/35059054>

Morales-Márquez, V., Orfila, A., Gómez-Pujol, L., Conti, D., Simarro, G., Álvarez Ellacuría, A., Osorio, A. F., Marcos, M. and Galán, A. (2017), 'Numerical and observational data for addressing the beach dynamics and recovery associated to a storm group impact', *Marine Geology in review*.

Moreno, A. and Amelung, B. (2009), 'Climate change and tourist comfort on Europe's beaches in summer: A reassessment', *Coastal management* **37**(6), 550–568.

Moss, R. H., Edmonds, J. A., Hibbard, K. A., Manning, M. R., Rose, S. K., Vuuren, D. P. V., Carter, T. R., Emori, S., Kainuma, M., Kram, T., Meehl, G. A., Mitchell, J. F. B., Nakicenovic, N., Riahi, K., Smith, S. J., Stouffer, R. J., Thomson, A. M., Weyant, J. P. and Wilbanks, T. J. (2010), 'The next generation of scenarios for climate change research and assessment', *Nature* **463**(7282), 747–756.

URL: <http://dx.doi.org/10.1038/nature08823>

Muñoz-Perez, J. and Medina, R. (2010), 'Comparison of long-, medium-and short-term variations of beach profiles with and without submerged geological control', *Coastal Engineering* **57**(3), 241–251.

Nahuelhual, L., Loureiro, M. L. and Loomis, J. (2004), 'Using random parameters to account for heterogeneous preferences in contingent valuation of public open space', *Journal of Agricultural and Resource Economics* pp. 537–552.

Naylor, L. A., Stephenson, W. J. and Trenhaile, A. S. (2010), 'Rock coast geomorphology: recent advances and future research directions', *Geomorphology* **114**(1-2), 3–11.

Ngazy, Z., Jiddawi, N. and Cesar, H. (2004), 'Coral bleaching and the demand for coral reefs: A marine recreation case in Zanzibar', *Economic valuation and policy priorities for sustainable management of coral reefs* pp. 118–125.

- Nicholls, R. J. (2002), 'Analysis of global impacts of sea-level rise: a case study of flooding', *Physics and Chemistry of the Earth, Parts A/B/C* **27**(32-34), 1455–1466.
- Nicholls, R. J. and Cazenave, A. (2010), 'Sea-Level Rise and Its Impact on Coastal Zones', *Science* **328**(5985), 1517 LP – 1520.
URL: <http://science.sciencemag.org/content/328/5985/1517.abstract>
- Nieto, M. A., Garau, B., Balle, S., Simarro, G., Zarruk, G. A., Ortiz, A., Tintoré, J., Álvarez-Ellacuría, A., Gómez-Pujol, L. and Orfila, A. (2010), 'An open source, low cost video-based coastal monitoring system', *Earth Surface Processes and Landforms* **35**(14), 1712–1719.
- Parsons, G. R., Chen, Z., Hidrue, M. K., Standing, N. and Lilley, J. (2013), 'Valuing beach width for recreational use: Combining revealed and stated preference data', *Marine Resource Economics* **28**(3), 221–241.
- Passeri, D. L., Hagen, S. C., Medeiros, S. C., Bilskie, M. V., Alizad, K. and Wang, D. (2015), 'The dynamic effects of sea level rise on low-gradient coastal landscapes: A review', *Earth's Future* **3**(6), 159–181.
- Peltier, W. (2004), 'Global glacial isostasy and the surface of the ice-age earth: the ice-5g (vm2) model and grace', *Annu. Rev. Earth Planet. Sci.* **32**, 111–149.
- Perch-Nielsen, S. L. (2010), 'The vulnerability of beach tourism to climate change-an index approach', *Climatic Change* **100**(3), 579–606.
- Perch-Nielsen, S. L., Amelung, B. and Knutti, R. (2010), 'Future climate resources for tourism in Europe based on the daily Tourism Climatic Index', *Climatic Change* **103**(3), 363–381.
URL: <https://doi.org/10.1007/s10584-009-9772-2>
- Pilar, P., Soares, C. G. and Carretero, J. (2008), '44-year wave hindcast for the north east atlantic european coast', *Coastal Engineering* **55**(11), 861–871.
- Plant, N. G., Robert Thieler, E. and Passeri, D. L. (2016), 'Coupling centennial-scale shoreline change to sea-level rise and coastal morphology in the gulf of mexico using a bayesian network', *Earth's Future* **4**(5), 143–158.
- Pongkijvorasin, S. and Chotiyaputta, V. (2013), 'Climate change and tourism: Impacts and responses. a case study of khaoyai national park', *Tourism Management Perspectives* **5**, 10–17.
- Poulter, B. and Halpin, P. N. (2008), 'Raster modelling of coastal flooding from sea-level rise', *International Journal of Geographical Information Science* **22**(2), 167–182.

- Pröbstl-Haider, U., Haider, W., Wirth, V. and Beardmore, B. (2015), 'Will climate change increase the attractiveness of summer destinations in the European Alps? A survey of German tourists', *Journal of outdoor recreation and tourism* **11**, 44–57.
- Purcell, J. E. (2012), 'Jellyfish and Ctenophore Blooms Coincide with Human Proliferations and Environmental Perturbations', *Annual Review of Marine Science* **4**, 209–235.
- Purcell, J. E., Uye, S.-i. and Lo, W.-t. (2007), 'Anthropogenic causes of jellyfish blooms and their direct consequences for humans : a review', *Marine Ecology Progress Series* **350**, 153–174.
- Purvis, M. J., Bates, P. D. and Hayes, C. M. (2008), 'A probabilistic methodology to estimate future coastal flood risk due to sea level rise', *Coastal engineering* **55**(12), 1062–1073.
- Ranasinghe, R. (2016), 'Assessing climate change impacts on open sandy coasts: A review', *Earth-science reviews* **160**, 320–332.
- Ranasinghe, R., Callaghan, D. and Stive, M. J. (2012), 'Estimating coastal recession due to sea level rise: beyond the bruun rule', *Climatic Change* **110**(3-4), 561–574.
- Remoundou, K., Diaz-Simal, P., Koundouri, P. and Rulleau, B. (2015), 'Valuing climate change mitigation: A choice experiment on a coastal and marine ecosystem', *Ecosystem services* **11**, 87–94.
- Revell, D. L., Battalio, R., Spear, B., Ruggiero, P. and Vandever, J. (2011), 'A methodology for predicting future coastal hazards due to sea-level rise on the california coast', *Climatic Change* **109**(1), 251–276.
- Revelt, D. and Train, K. (1998), 'Mixed logit with repeated choices: households' choices of appliance efficiency level', *Review of economics and statistics* **80**(4), 647–657.
- Richardson, A. J., Bakun, A., Hays, G. C. and Gibbons, M. J. (2009), 'The jellyfish joyride: causes, consequences and management responses to a more gelatinous future', *Trends in ecology and evolution* **24**(6), 312–322.
- Rodrigues, L. C., van den Bergh, J. C. J. M., Loureiro, M. L., Nunes, P. A. L. D. and Rossi, S. (2016), 'The cost of Mediterranean Sea warming and acidification: a choice experiment among scuba divers at Medes Islands, Spain', *Environmental and resource economics* **63**(2), 289–311.
- Roelvink, D., Reniers, A., Van Dongeren, A., de Vries, J. v. T., McCall, R. and Lescinski, J. (2009), 'Modelling storm impacts on beaches, dunes and barrier islands', *Coastal engineering* **56**(11-12), 1133–1152.

- Roland, A. and Ardhuin, F. (2014), 'On the developments of spectral wave models: Numerics and parameterizations for the coastal ocean Topical Collection on the 7th International Conference on Coastal Dynamics in Arcachon, France 24-28 June 2013', *Ocean Dynamics* **64**(6), 833–846.
- Roman, G. S., Dearden, P. and Rollins, R. (2007), 'Application of zoning and "limits of acceptable change" to manage snorkelling tourism', *Environmental Management* **39**(June), 819–830.
- Rosati, J. D., Dean, R. G. and Walton, T. L. (2013), 'The modified bruun rule extended for landward transport', *Marine Geology* **340**, 71–81.
- Rosselló-Nadal, J. (2014), 'How to evaluate the effects of climate change on tourism', *Tourism Management* **42**, 334–340.
- Rosselló-Nadal, J., Riera-Font, A. and Cárdenas, V. (2011), 'The impact of weather variability on British outbound flows', *Climatic change* **105**(1-2), 281–292.
- Ruggiero, P., Komar, P. D., McDougal, W. G., Marra, J. J. and Beach, R. A. (2013), 'Wave runup, extreme water levels and the erosion of properties backing beaches', *Journal of Coastal Research* **17**(2).
- Ruju, A., Lara, J. L. and Losada, I. J. (2014), 'Numerical analysis of run-up oscillations under dissipative conditions', *Coastal Engineering* **86**, 45–56.
- Ruti, P. M., Somot, S., Giorgi, F., Dubois, C., Flaounas, E., Obermann, A., Dell'Aquila, A., Pisacane, G., Harzallah, A. and Lombardi, E. (2016), 'MED-CORDEX initiative for Mediterranean climate studies', *Bulletin of the American Meteorological Society* **97**(7), 1187–1208.
- Sayol, J. and Marcos, M. (2018), 'Assessing flood risk under sea level rise and extreme sea levels scenarios: application to the ebro delta (spain)', *Journal of Geophysical Research: Oceans* **123**(2), 794–811.
- Scarpa, R. and Rose, J. M. (2008), 'Design efficiency for non-market valuation with choice modelling: how to measure it, what to report and why', *Australian journal of agricultural and resource economics* **52**(3), 253–282.
- Scarpa, R. and Thiene, M. (2005), 'Destination choice models for rock climbing in the Northeastern Alps: a latent-class approach based on intensity of preferences', *Land economics* **81**(3), 426–444.
- Scarpa, R., Willis, K. G. and Acutt, M. (2007), 'Valuing externalities from water supply: Status quo, choice complexity and individual random effects in panel kernel logit

analysis of choice experiments', *Journal of Environmental Planning and Management* **50**(4), 449–466.

Scott, D., de Freitas, C. and Matzarakis, A. (2009), Adaptation in the tourism and recreation sector, in 'Biometeorology for adaptation to climate variability and change', Springer, pp. 171–194.

Scott, D., Gössling, S. and de Freitas, C. R. (2008), 'Preferred climates for tourism: case studies from Canada, New Zealand and Sweden', *Climate Research* **38**(1), 61–73.

Scott, D. and Hall, C. M. (2012), 'Consumer behaviour and demand response of tourists', *Annals of Tourism Research* **39**(1), 36–58.

URL: <http://dx.doi.org/10.1016/j.annals.2011.11.002>

Scott, D., McBoyle, G. and Schwartzentruber, M. (2004), 'Climate change and the distribution of climatic resources for tourism in North America', *Climate research* **27**(2), 105–117.

Short, A. D. (1996), 'The role of wave height, period, slope, tide range and embayment-institution in beach classifications: a review', *Revista chilena de historia natural* **69**(4), 589–604.

Shoyama, K., Managi, S. and Yamagata, Y. (2013), 'Public preferences for biodiversity conservation and climate-change mitigation: A choice experiment using ecosystem services indicators', *Land Use Policy* **34**, 282–293.

Simarro, G., Ribas, F., Álvarez, A., Guillén, J., Chic, Ò. and Orfila, A. (2017), 'Ulises: An open source code for extrinsic calibrations and planview generations in coastal video monitoring systems', *Journal of Coastal Research* **33**(5), 1217–1227.

Simeone, S., De Falco, G., Quattrocchi, G. and Cucco, A. (2014), 'Morphological changes of a mediterranean beach over one year (san giovanni sinis, western mediterranean)', *Journal of Coastal Research* **70**(sp1), 217–223.

Slangen, A. B. A., Carson, M., Katsman, C. A., van de Wal, R. S. W., Köhl, A., Vermeersen, L. L. A. and Stammer, D. (2014), 'Projecting twenty-first century regional sea-level changes', *Climatic Change* **124**, 317–332.

Small, C., Nicholls, R. J., Smallt, C. and Nichollst, R. J. (2003), 'A Global Analysis of Human Settlement in Coastal Zones', *Source: Journal of Coastal Research Journal of Coastal Research* **19**(19), 584–599.

Smallegan, S. M., Irish, J. L., Van Dongeren, A. R. and Den Bieman, J. P. (2016), 'Morphological response of a sandy barrier island with a buried seawall during hurricane sandy', *Coastal Engineering* **110**, 102–110.

- Smith, E. R., Wang, P. and Zhang, J. (2003), 'Evaluation of the CERC formula using large-scale laboratory data'.
- Stammer, D., Van de Wal, R., Nicholls, R., Church, J., Le Cozannet, G., Lowe, J., Horton, B., White, K., Behar, D. and Hinkel, J. (2019), 'Framework for high-end estimates of sea level rise for stakeholder applications', *Earth's Future* **7**(8), 923–938.
- Stive, M. J. (2004), 'How important is global warming for coastal erosion?', *Climatic Change* **64**(1), 27–39.
- Stockdon, H. F., Holman, R. A., Howd, P. A. and Sallenger, A. H. (2006), 'Empirical parameterization of setup, swash, and runup', *Coastal Engineering* .
- Tamisiea, M. and Mitrovica, J. (2011), 'The moving boundaries of sea level change: Understanding the origins of geographic variability', *Oceanography* **24**(2), 24–39.
- Tintoré, J., Vizoso, G., Casas, B., Heslop, E., Pascual, A., Orfila, A., Ruiz, S., Martínez-Ledesma, M., Torner, M. and Cusí, S. (2013), 'SOCIB: the Balearic Islands coastal ocean observing and forecasting system responding to science, technology and society needs', *Marine Technology Society Journal* **47**(1), 101–117.
- Tol, R. S. J. (2002), 'Estimates of the damage costs of climate change. Part 1: Benchmark estimates', *Environmental and resource Economics* **21**(1), 47–73.
- Tol, R. S. J. (2018), 'The economic impacts of climate change', *Review of Environmental Economics and Policy* **12**(1), 4–25.
- Tol, R. S. J. and Walsh, S. (2012), The impact of climate on tourist destination choice, Technical report.
- Torres, C., Faccioli, M. and Font, A. R. (2017), 'Waiting or acting now? The effect on willingness-to-pay of delivering inherent uncertainty information in choice experiments', *Ecological economics* **131**, 231–240.
- Tseng, W.-C., Chen, C.-C., Chang, C.-C., Chu, Y.-H., Tseng, W.-C., Chen, . C.-C., Chu, Y.-H. and Chang, C.-C. (2009), 'Estimating the economic impacts of climate change on infectious diseases: a case study on dengue fever in Taiwan', *Climatic Change* **92**, 123–140.
- Tsimplis, M., Marcos, M., Somot, S. and Barnier, B. (2008), 'Sea level forcing in the Mediterranean Sea between 1960 and 2000', *Global and Planetary Change* **63**(4), 325–332.
- Tsimplis, M., Proctor, R. and Flather, R. (1995), 'A two-dimensional tidal model for the mediterranean sea', *Journal of Geophysical Research: Oceans* **100**(C8), 16223–16239.

- Unbehaun, W., Pröbstl, U. and Haider, W. (2008), 'Trends in winter sport tourism: challenges for the future', *Tourism Review* **63**(1), 36–47.
- UNWTO (2018), '2018 Edition UNWTO International Tourism Trends 2017', pp. 1–20.
- Uyarra, M. C., Cote, I. M., Gill, J. A., Tinch, R. R., Viner, D. and Watkinson, A. R. (2005), 'Island-specific preferences of tourists for environmental features: implications of climate change for tourism-dependent states', *Environmental conservation* **32**(1), 11–19.
- Van den Berg, N., Falqués, A. and Ribas, F. (2011), 'Long-term evolution of nourished beaches under high angle wave conditions', *Journal of Marine Systems* **88**(1), 102–112.
- Van den Berg, N., Falqués, A. and Ribas, F. (2012), 'Modeling large scale shoreline sand waves under oblique wave incidence', *Journal of Geophysical Research: Earth Surface* **117**(F3).
- Van Dongeren, A., Bolle, A., Voudoukas, M. I., Plomaritis, T., Eftimova, P., Williams, J., Armaroli, C., Idier, D., Van Geer, P., Van Thiel de Vries, J. et al. (2009), Micore: dune erosion and overwash model validation with data from nine european field sites, in 'Proceedings Of Coastal Dynamics 2009: Impacts of Human Activities on Dynamic Coastal Processes (With CD-ROM)', World Scientific, pp. 1–15.
- Vander Naald, B. (2019), 'Examining tourist preferences to slow glacier loss: evidence from alaska', *Tourism Recreation Research* pp. 1–11.
- Vargas-Yáñez, M. and Salat, J. (2007), 'Cambio climático en el Mediterráneo español'. **URL:** http://www.ma.ieo.es/gcc/cambio_climatico_reedicion.pdf
- Veronesi, M., Chawla, F., Maurer, M. and Lienert, J. (2014), 'Climate change and the willingness to pay to reduce ecological and health risks from wastewater flooding in urban centers and the environment', *Ecological Economics* **98**, 1–10.
- Villatoro, M., Silva, R., Méndez, F., Zanuttigh, B., Pan, S., Trifonova, E., Losada, I., Izaguirre, C., Simmonds, D., Reeve, D. et al. (2014), 'An approach to assess flooding and erosion risk for open beaches in a changing climate', *Coastal Engineering* **87**, 50–76.
- Vitousek, S., Barnard, P. L. and Limber, P. (2017), 'Can beaches survive climate change?', *Journal of Geophysical Research: Earth Surface* **122**(4), 1060–1067.
- Voudoukas, M. I., Ferreira, Ó., Almeida, L. P. and Pacheco, A. (2012), 'Toward reliable storm-hazard forecasts: XBeach calibration and its potential application in an operational early-warning system', *Ocean Dynamics* **62**(7), 1001–1015.

- Vousdoukas, M. I., Mentaschi, L., Voukouvalas, E., Verlaan, M. and Feyen, L. (2017), 'Extreme sea levels on the rise along Europe's coasts', *Earth's Future* **5**(3), 304–323.
- Vousdoukas, M. I., Mentaschi, L., Voukouvalas, E., Verlaan, M., Jevrejeva, S., Jackson, L. P. and Feyen, L. (2018), 'Global probabilistic projections of extreme sea levels show intensification of coastal flood hazard', *Nature Communications* **9**(1), 1–12.
- Vousdoukas, M. I., Voukouvalas, E., Annunziato, A., Giardino, A. and Feyen, L. (2016), 'Projections of extreme storm surge levels along Europe', *Climate Dynamics* **47**(9–10), 3171–3190.
- Wahl, T., Plant, N. G. and Long, J. W. (2016), 'Probabilistic assessment of erosion and flooding risk in the northern Gulf of Mexico', *Journal of Geophysical Research: Oceans* **121**(5), 3029–3043.
- WAMDI Group, T. (1988), 'The WAM model - A third generation ocean wave prediction model'.
- Whitehead, J. C., Dumas, C. F., Herstine, J., Hill, J. and Buerger, B. (2008), 'Valuing beach access and width with revealed and stated preference data', *Marine Resource Economics* **23**(2), 119–135.
- Whitehead, J. C., Haab, T. C. and Huang, J.-C. (2000), 'Measuring recreation benefits of quality improvements with revealed and stated behavior data', *Resource and energy economics* **22**(4), 339–354.
- Wong, P., Losada, I., Gattuso, J., Hinkel, J., Khattabi, A., McInnes, K., Saito, Y. and Sallenger, A. (2014), 'Coastal systems and low-lying areas. climate change 2014: Impacts, adaptation, and vulnerability. part a: Global and sectoral aspects. contribution of working group ii to the fifth assessment report of the intergovernmental panel on climate change'.
- Wöppelmann, G. and Marcos, M. (2016), 'Vertical land motion as a key to understanding sea level change and variability', *Reviews of Geophysics* **54**(1), 64–92.
- WTTC (2018), *World Travel and Tourism Council (2018) Travel and Tourism: Global Economic Impact and Issues 2018*, wtcc edn, London.
- Wu, S.-Y., Yarnal, B. and Fisher, A. (2002), 'Vulnerability of coastal communities to sea-level rise: a case study of cape may county, new jersey, usa', *Climate Research* **22**(3), 255–270.
- Young, I. R. (1999), 'Seasonal variability of the global ocean wind and wave climate', *International Journal of Climatology* **19**(9), 931–950.

Zeppel, H. (2012), 'Climate change and tourism in the Great Barrier Reef Marine Park', *Current Issues in Tourism* **15**(3), 287–292.

Zhang, K., Douglas, B. C. and Leatherman, S. P. (2004), 'Global warming and coastal erosion', *Climatic change* **64**(1-2), 41.

Zijlema, M., Stelling, G. and Smit, P. (2011), 'SWASH: An operational public domain code for simulating wave fields and rapidly varied flows in coastal waters', *Coastal Engineering* **58**(10), 992–1012.

List of Figures

2.1	Mallorca island with Cala Millor and Playa de Palma beaches marked with yellow squares. SIMAR grid points used to characterize the off-shore wave climate and the Capdepera wave buoy are also marked. The inset map represents the western Mediterranean basin.	18
2.2	Playa de Palma and Cala Millor self-organizing maps (SOMs). SIMAR databases are shown in 100 cells displaying the more representative deep water sea conditions at the Playa de Palma (a) and Cala Millor (b) beaches. The blue colour illustrates the frequency of the sea states, together with the Hs in metres (yellow to red), the period in seconds (white to black) and the direction in arrows. It can be seen that the more energetic conditions come from the SW in Playa de Palma and from the NE in Cala Millor, the higher frequency waves are also low-energy at both sites.	19
2.3	SWAN coarse (a) and fine (b) grids and SWASH (c) computational domains for the Cala Millor beach. Yellow line indicates the sector where the three ADCPs are located.	21
2.4	SWAN coarse (a) and fine (b) grids and SWASH (c) computational domains for Playa de Palma. Yellow dots indicate the locations of the shallow water wave buoy and ADCP.	22
2.5	Return periods in the A2 scenario for future projections (blue dashed line), control simulation (black dotted line) and hindcast (red line). Note that there are different time periods for the series as well as the overlapping of hindcast and control scenarios. The red line indicates the 1st day of hindcast time series.	25

2.6	Capdepera buoy observations (blue) and hindcasted SIMAR (black) time series of Hs, Tp and wave direction. RMSE and correlation are quoted for the wave direction.	26
2.7	Scatter plots of buoy observations vs. SIMAR hindcast for Hs (a) and Tp (b). RMSE and correlation are quoted in each figure.	26
2.8	Hs, Tp and wave direction as modelled by SWAN and observed at the ADCP deployed at 12 m depth in the Cala Millor beach.	27
2.9	SWAN vs. ADCP scatter plots of Hs (a) and Tp (b) in Cala Millor. . . .	28
2.10	Hs, Tp and wave direction as modelled by the SWAN model and observed at the buoy deployed at 23 m depth in Playa de Palma.	29
2.11	. SWAN vs. ADCP scatter plots of Hs (a) and Tp (b) in Playa de Palma.	29
2.12	Observed (black) and modelled by SWASH (red) shoreline positions in Cala Millor.	31
2.13	Observed (black) and modelled by SWASH (red) shoreline positions in Playa de Palma.	32
2.14	Modelled (red) and observed (blue) shorelines positions in Cala Millor with mean shoreline position (black line) and its standard deviation (grey shadow) zoomed in to the central sector.	33
2.15	Modelled (red) and observed (blue) shorelines positions in Playa de Palma with mean shoreline position (black line), its standard deviation (grey shadow) and the resolution of the pixels of the cameras (orange shadow).	34
2.16	Changes in the cross profile in Cala Millor (a) and Playa de Palma (b) in the nearshore area under different sea levels.	34
2.17	Present-day shoreline position (in black) and landward migration (in red) in the worst case scenario (mean sea-level rise under RCP8.5 and extreme wave conditions) by the end of the 21 st century in the Cala Millor beach.	36
2.18	Present-day shoreline position (in black) and landward migration (in red) in the worst case scenario (mean sea-level rise under RCP8.5 and extreme wave conditions) by the end of the 21 st century in Playa de Palma.	36

3.1 Left panel: (a) location map of Son Bou beach, Menorca Island, Western Mediterranean and the offshore wave data point. The buoy location and the location of the beach profile transects are shown in (b). Right panel; directional distributions of Hs at (c) offshore conditions and at (d) the coastal wave buoy. 43

3.2 Projected sea level rise scenarios used in the present study. 5–95% refer to the uncertainties derived from the multi-model ensemble spread of each of the two scenarios. The vertical lines indicate the time lapses when the erosion volume is estimated (see Section 3.3.3). 48

3.3 Shoreline retreat comparison using Q2D-morfo model (dashed lines) and Bruun Rule (solid lines) under (a) RCP8.5 (red colour) and (b) RCP4.5 (blue colour) scenarios. The light colours represent the uncertainties of the two scenarios and the shadow areas represent the intra-model uncertainties. 51

3.4 Shoreline retreats derived from maximum annual storms and sea level rise under two scenarios with respect to the annual mean position. Red and blue solid lines represent shoreline retreats on average, under RCP8.5 and RCP4.5 mean sea-level rise scenarios, respectively. Shadow areas represent the variability of shoreline retreat along the beach and the dashed lines are the trends. 52

3.5 Number of events reaching the dune toe under RCP8.5 mean sea-level rise using the beach retreat obtained by Q2D-morfo model (solid red line) and Bruun Rule (dashed green line) results. Shaded areas represent the standard deviation derived from the of 10,000 wave time series simulations performed. Horizontal lines after late 2060s indicate that all the events considered (that represent the top 10% of highest waves) reach the dune toe. 53

3.6 Dune-beach erosion volume taking into account the sea-level rise and the 10-year RP (dark blue line, left axis) and 100-year RP (orange line, right axis) under RCP8.5 scenario. The shadowed areas indicate the standard deviation based on the equilibrium profile used in the Q2D-morfo model simulations. 54

4.1 Example choice card. 63

List of Tables

2.1	Input condition of the model set-up under climate change scenarios for the two beaches. See the text for details on their computation.	24
2.2	Comparison between SWAN results and nearshore wave observations in the Cala Millor beach. The period spanned by the series is from 14 March to 14 April 2014.	27
2.3	Comparison between SWAN results and nearshore wave observations in Playa de Palma. The period spanned by the series is from 1 to 30 September 2015.	28
2.4	Dates and forcing conditions of the SWASH simulations and results of the validation against observed shoreline position in the Cala Millor beach.	30
2.5	Dates and forcing conditions of the SWASH simulations and results of the validation against observed shoreline position in Playa de Palma. . .	30
2.6	Loss of aerial beach (defined here as the landward migration of the shoreline averaged over the entire beach) for both the mean and extreme conditions expected under climate change scenarios in Cala Millor (in m). For the extreme conditions, the maximum loss is also quoted.	35
2.7	Loss of aerial beach (defined here as the landward migration of the shoreline averaged over the entire beach) for both the mean and extreme conditions expected under climate change scenarios in Playa de Palma (in m). For the extreme conditions, the maximum loss is also quoted. . .	35
4.1	Attributes and their levels	62
4.2	Socioeconomic characteristics of the sample.	64
4.3	Trip characteristics if the sample.	65
4.4	Mixed logit model results.	69

4.5 MWTP estimates: WTP per individual and day of stay, in euros. 95% confidence intervals based on the 2.5 th and 97.5 th percentile of the simulated MWTP distribution	70
--	----

List of Terms and Abbreviations

ADCP	Acoustic Doppler Current Profiler
AOGCM	Atmospheric-Ocean General Circulation Models
ASC	Alternative Specific Constant
AWAC	AcousticWaves and Currents
BAU	Business As Usual
CC	Climate Change
CE	Choice Experiment
CMIP5	Coupled Model Intercomparison Project Phase 5
DH	Horizontal Dimension
EU	European Union
GDP	Gross Domestic Product
GHG	Greenhouse Gases
GIA	Glacial Isostatic Adjustment
GMSL	Global Mean Sea Level
GNSS	Global Navigation Satellite System
GPD	Generalized Pareto Distribution
GPS	Global Positioning System
Hs	Significant wave height

IMEDEA Mediterranean Institute of Advanced Studies

IPCC Intergovernmental Panel on Climate Change

MDA Maximum Dissimilarity Algorithm

MWTP Marginal Willingness-To-Pay

RBF Radial Basis Functions

RCP Representative Concentration Pathways

RMSE Root Mean Square Error

RP Return Period

RTK-GPS Real Time Kinematic Global Position System

SOCIB Balearic Islands Coastal Observing and Forecasting System

SOM Self-Organizing Maps

SWAN Simulating WAVes Nearshore

SWASH Simulating WAVes till SHore

T_p Peak period

WTP Willingness-To-Pay

WTTC World Travel Tourism Council